DEVELOPMENT OF AN *IN VITRO* 3D CO-CULTURE SYSTEM AS AN AMELOBLASTOMA DISEASE MODEL

LEE SOO LENG

DEPARTMENT OF ORAL AND MAXILLOFACIAL CLINICAL SCIENCESFACULTY OF DENTISTRY
UNIVERSITY OF MALAYA
KUALA LUMPUR

2018

DEVELOPMENT OF AN *IN VITRO* 3D CO-CULTURE SYSTEM AS AN AMELOBLASTOMA DISEASE MODEL

LEE SOO LENG

DISSERTATION SUBMITTED IN FULFILMENT OF THE REQUIREMENTS FOR THE DEGREE OF MASTER OF DENTAL SCIENCE

DEPARTMENT OF ORAL AND MAXILLOFACIAL CLINICAL SCIENCESFACULTY OF DENTISTRY
UNIVERSITY OF MALAYA
KUALA LUMPUR

2018

UNIVERSITY OF MALAYA

ORIGINAL LITERARY WORK DECLARATION

Name of Candidate: Lee Soo Leng

Matric No: DGC 150007

Name of Degree: Master of Dental Science

Title of Project Paper/Research Report/Dissertation/Thesis ("this Work"):

Development of an *in vitro* 3D co-culture system as an ameloblastoma disease model

Field of Study: Odontogenic tumour

I do solemnly and sincerely declare that:

(1) I am the sole author/writer of this Work;
(2) This Work is original;
(3) Any use of any work in which copyright exists was done by way of fair dealing and for permitted purposes and any excerpt or extract from, or reference to or reproduction of any copyright work has been disclosed expressly and sufficiently and the title of the Work and its authorship have been acknowledged in this Work;
(4) I do not have any actual knowledge nor do I ought reasonably to know that the making of this work constitutes an infringement of any copyright work;
(5) I hereby assign all and every rights in the copyright to this Work to the University of Malaya ("UM"), who henceforth shall be owner of the copyright in this Work and that any reproduction or use in any form or by any means whatsoever is prohibited without the written consent of UM having been first had and obtained;
(6) I am fully aware that if in the course of making this Work I have infringed any copyright whether intentionally or otherwise, I may be subject to legal action or any other action as may be determined by UM.

Candidate's Signature Date: 20 Feb 2018

Subscribed and solemnly declared before,

Witness's Signature Date: 20/2/2018

Name: Siar Chong Huat

Designation: Former Professor

ABSTRACT

Ameloblastoma, the most clinically significant odontogenic epithelial tumour, is a locally-invasive and destructive lesion in the jawbones. Stromal cells as key contributors to the tumour microenvironment have a prominent role in tumour growth, progression and the spread of tumours. Therefore, the reciprocal parenchymal-stromal interactions in the milieu of the tumour microenvironment are inevitably capable of addressing the ill-understood nature of the infiltrativeness and destructive behaviour of ameloblastoma. **Objective:** An *in vitro* three-dimensional (3D) ameloblastoma tumour-osteoblast co-culture model was established to elucidate the effect of heterotypic cell interactions on tumour growth and morphological characteristics of tumour cell. **Materials and Methods:** Stromal cell line, ST2 cells, pre-osteoblastic cell line, KUSA/A1 cells and osteoblastic cell line, MC3T3-E1 cells were separately co-seeded with the ameloblastoma tumour cell line, AM-1 in collagen gel incubated with mineralization medium. **Results:** AM-1/KUSA-A1 co-culture showed a heterogeneous cell population with two distinct morphologies: elongated spindle-shaped vimentin-positive cells with long anastomosing cytoplasmic processes interspersed and encircled cytokeratin-positive round cell which organized into nest-like aggregates. Both round cell with nest-like structures and elongated spindle-shaped cells in co-culture strongly expressed RANK, mildly for RANKL and OPG. 14-day-old KUSA/A1 monocultures shown evidence of intense extracellular matrix mineralization as confirmed by intense Alizarin Red S staining. In contrast, KUSA/A1 cells in the AM co-culture shown reduced Alizarin Red S staining revealed diminished calcification. Furthermore, 3D AM co-cultures showed a significant increase in AM-1 cell count compared to their monoculture counterparts, and formation of visible AM-1 epithelial nest-like structures resembling ameloblastoma cells in their native state. **Conclusion:** The *in vitro* 3D co-culture system as established in the present study provided some insights into the biological behaviour of enigmatic amelobastoma

disease. Present *in vitro* findings suggest that, bidirectional ameloblastoma-osteoblastic interactions might play an important role in modulating tumour growth and local bone metabolism.

Keywords: co-culture system, ameloblast, pre-osteoblast, ameloblastoma modelling

ABSTRAK

Ameloblastoma, tumor epitelium odontogenik yang paling umum secara klinikal, merupakan lesi invasif setempat dan lesi destruktif yang didapati di tulang rahang. Sel stromal sebagai penyumbang penting kepada mikroalam sekitar tumor mempunyai peranan yang penting dalam pertumbuhan tumor, perkembangan dan penyebaran tumor. Oleh itu, interaksi antara parenkima-stromal dalam mikroalam sekitar diyakini untuk menangani sifat menyusup dan kelakuan pemusnah penyakit ameloblastoma. **Objektif:** Model *in vitro* tiga-dimensi (3D) tumor ameloblastoma-osteoblast yang ditubuhkan untuk menjelaskan kesan interaksi sel heterotip pada pertumbuhan tumor dan ciri-ciri morfologi sel tumor. **Bahan dan Kaedah**: Sel stromal, sel ST2, sel pra-osteoblastik, sel KUSA/A1, dan sel osteoblastik, sel MC3T3-E1 bersandarkan dengan sel-sel tumor ameloblastoma, AM-1 secara berasingan dalam gel kolagen dan diinkubasi dengan medium mineralisasi. **Keputusan**: Ko-kultivar AM-1/KUSA-A1 menunjukkan kemunculan satu populasi sel yang heterogen dengan dua morfologi yang berbeza: sel-sel vimentin-positif yang berbentuk gelendong memanjang dengan proses sitoplasmik anastomosis yang panjang, didapati berselerak dan mengelilingi sekitar sel-sel cytokeratin-positif yang berbentuk bulat telah diorganisasikan menjadi agregat yang seperti sarang. Kedua-dua sel yang berbentuk bulat dan menpunyai struktur seperti sarang serta sel yang berbentuk gelendong memanjang dalam ko-kultivar mengungkapkan RANK secara kuat, tetapi mengungkapkan RANKL and OPG secara sedikit. Sel-sel KUSA/A1 dalam mono-kultivar selama 14 hari menunjukkan bukti pemineralan matriks ekstrasel yang beramatan, seperti yang disahkan oleh pewarnaan Alizarin Red S yang beramatan. Sebaliknya, sel-sel KUSA/A1 dalam ko-kultivar AM-1/KUSA/A1 ditunjukkan pengurangan pewarnaan Alizarin Red S mendedahkan kekurangan pengkalsiuman. Tambahan pula, kultivar 3D AM menunjukkan peningkatan ketara dalam jumlah bilangan sel AM-1 berbanding dengan sel AM-1 dalam monokultur, disertai

pembentukan struktur seperti sarang epithelium AM-1 yang kelihatan menyerupai sel ameloblastoma dalam keadaan asalnya. **Kesimpulan**: Sistem ko-kultur *in vitro* 3D seperti yang ditubuhkan dalam kajian ini memberikan pemahaman tentang sifat dan kelakuan biologi penyakit amelobastoma. Penemuan dalam *in vitro* kajian ini mencadangkan bahawa, interaksi dua hala ameloblastoma-osteoblastik mungkin memainkan peranan yang penting dalam memodulasi pertumbuhan tumor dan metabolisme tulang setempat.

Kata kunci: system ko-kultur, ameloblas, pra-osteoblas, pemodelan ameloblastoma

ACKNOWLEDGEMENTS

First and foremost, I am so grateful to the Graduate Research Assistantship Scheme and the University of Malaya for making this research study possible. My special heartily and thanks to my supervisors, Prof. Dr. Siar Chong Huat and Dato' Zainal, for not only accepting me into their group but also being a great mentor that constantly encourage and direct me along the way. Further thanks to Prof. Siar for rewarding me a graduate school experience, giving me intellectual freedom in my work, supporting my research work in Japan and attendance at both local and international conferences, guiding and giving me valuable ideas in my scientific and dissertation writing, in the meantime demanding a high quality of work in all my endeavours.

Additionally, I would like to thank Prof. Hitoshi Nagatsuka and Prof. Hidetsugu Tsujigiwa from Okayama University, Japan for their valuable contributions. It is with the help and support of them and the fellow labmates that this work came into existence, and without their efforts, my research would have undoubtedly been more difficult. I was fortunate to have the chance to work with them in Japan. They provided a friendly and cooperative atmosphere at my work place and useful feedback and insightful comments on my work.

Finally, I would like to acknowledge my family and my friends who supported and encouraged me throughout the time of my research work. I faced drastic changes and conflicts between my family members within these two years, but I am lucky to have my family who loved me and constantly giving their unyielding support to enable me to go through these hardships during the time of my research.

I am truly appreciated all who in one way or another contributed to the completion of this thesis. This thesis is heartily dedicated to all of them. May the Almighty God richly bless all of you.

TABLE OF CONTENTS

LIST OF FIGURES

LIST OF TABLES

LIST OF SYMBOLS AND ABBREVIATIONS

3D	:	Three-dimensional
2D	:	Two-dimensional
AM	:	Ameloblastoma
OTs	:	Odontogenic tumours
DNA	:	Deoxyribonucleic acid
CT	:	Computerized Tomography
MRI	:	Magnetic Resonance Imaging
MAPK	:	Mitogen-activated protein kinase
FGFR2	:	Fibroblast growth factor receptor 2
MDM2	:	Murine double minute 2
HPV	:	Human papillomavirus
EBV	:	Epstein-Barr virus
UAM	:	Unicystic ameloblastoma
BMPs	:	Bone morphogenetic proteins
PTH	:	Parathyroid Hormone
M-CSF	:	Macrophage colony-stimulating factor
NF-κB	:	Nuclear factor-κB
RANK	:	Receptor activator of NF-κB
RANKL	:	Receptor activator of NF-κB ligand
OPG	:	Osteoprotegerin
PTHrP	:	Parathyroid hormone-related protein
IL-1	:	Interleukin-1
TNF	:	Tumor necrosis factor
PGE2	:	Prostaglandin E2
ECM	:	Extracellular matrix

AAFs	:	Ameloblastoma-associated fibroblasts
GFs	:	Gingival fibroblasts
TGF-β	:	Transforming growth factor beta
HOS	:	Human osteosarcoma
OSCC	:	Oral squamous carcinoma cells
ALP	:	Alkaline phosphatase
CK	:	Cytokeratin
IF	:	Intermediate filament
EMT	:	Epithelial-mesenchymal transition
OC	:	Osteocalcin
OPN	:	Osteopontin
BSP	:	Bone sialoprotein
H&E	:	Hematoxylin and Eosin
ARAS	:	Alizarin Red S staining
IHC	:	Immunohistochemistry
PAP	:	Peroxidase anti-peroxidase
ABC	:	Avidin-biotin complexs
HRP	:	Horseradish peroxidase
PBS	:	Phosphate buffered saline
α-MEM	:	Minimal Essential Alpha medium
K-SFM	:	Keratinocyte-Serum Free medium
EGF	:	Epidermal growth factor
EDTA	:	Ethylenediaminetetraacetic acid
DAPI	:	4',6-diamidino-2-phenylindole
IL-6	:	Interleukin-6
sFRP-2	:	Secreted frizzled-related protein 2

LIST OF APPENDICES

CHAPTER 1: INTRODUCTION

1.1 General Introduction

Ameloblastoma, the most clinically significant odontogenic neoplasm arising from the odontogenic epithelium of putative enamel organ origin. Although clinically benign, it is characterized by slow but persistent growth, locally invasive and infiltrative lesion with a high risk of recurrence in the jawbones. It accounts for 11% to 18% of all odontogenic tumours and with a marked predilection for the posterior mandible. Ameloblastoma exhibits an almost equal gender predilection and occurs over a wide age range, with a peak incidence in young adults in their 30s and 40s. It typically causes no symptoms until a visible painless swelling or expansion of the jaw emerges, causing facial asymmetry. They are classified into four clinicopathologic subtypes: ameloblastoma, unicystic ameloblastoma and extraosseous/peripheral ameloblastoma according to the 2017 World Health Organization Classification of Head and Neck Tumours.

Given the relative rarity of this disease, to date, little is known about the aetiology and molecular underpinnings the infiltrativeness and osseo-destructive behavior of ameloblastoma, and its subsequent progression. This hinders the development of widely accepted novel non-invasive therapies for the management of ameloblastoma. Moreover, the molecular pathogenesis in ameloblastoma, including those involved in tumour growth, and its interactions with stromal cells in the tumour microenvironment for the subsequent bone invasion remains ill-understood. has seen the accelerating implementation of 3D cell cultures.

The *in vitro* three-dimensional (3D) cell culture model has gained significant popularity in the last ten years and has seen the accelerating implementation of this model in cancer research to model the hallmark behaviour of tumour cells in promoting tumour growth and the subsequent metastasis. Cells propagated in 3D model bridges the gap

between cellular physiology and the *in vitro* cell culture system. Consequently, an *in vitro* model that better represents ameloblastoma and its microenvironment is vital in elucidating the molecular signalling and mechanisms mediating the growth and invasiveness of ameloblastoma within the bone.

It has become widely recognized that the stroma plays a prominent role in tumour growth and progression. In addition, the tumour-stroma interactions have a significant impact on prognosis and therapeutic responses. In ameloblastomas, the stroma-tumour interaction is achieved through the interplay of biological molecules that acting in both autocrine and paracrine manner not only responsible for the AM tumour growth and invasion, but also enhanced bone resorption and suppression of new bone formation in the jaw. Emerging evidence has suggested the direct role of fibroblastic cells on tumour growth in bone-invasive lesions. The tumour-fibroblast interaction has been shown to play an important role in providing a favourable microenvironment for tumour-induced osteoclast formation at the tumour-bone interface, and the subsequent tumour-associated bone destruction. However, tumour-fibroblast interactions and their subsequent role in the infiltrativeness and invasiveness nature of ameloblastoma, resulting in the dysregulation of bone remodelling have not yet been reported.

1.2 General Aims

Ameloblastoma is a benign odontogenic epithelial tumour of the jawbones. However, it demonstrated a propensity for local invasion with high risk of recurrence. Therefore, further refine the understanding of the disease both clinically and molecularly is imperative to address the challenging survival prognosis of ameloblastoma, particularly of those with ill-defined radiographic boundary.

Stroma is widely recognized as a key contributor which can profoundly enhance tumour progression and metastasis, and impacting on the therapeutic responses (Celli, 2012). In recent cancer research, efforts have increasingly focussed on *in vitro* 3D models including metastatic bone models to better understand tumour-stromal interactions (Luis-Ravelo *et al.*, 2011; Kim & Othmer, 2013; Fong *et al.*, 2016; Liu *et al.*, 2016; Wendler *et al.*, 2016). However, parenchyma-osteoblast interactions and their potential role in regulating tumoral growth and local invasiveness in ameloblastoma are less appreciated, with fewer *in vitro* studies have investigated on the role of tumour-stromal interactions on tumour properties and its dynamics in ameloblastoma.

Consequently, an *in vitro* 3D model that better represents ameloblastoma and the jaw microenvironment in ameloblastoma disease plays a prominent role in elucidating the molecular signalling and mechanisms mediating the infiltrative nature and destructive behaviour of ameloblastoma. Therefore, the aim of the present study was to explore a potential *in vitro* 3D co-culture system to stimulate an ameloblastoma disease model to investigate the effects of heterotypic cell-cell interactions on tumoral growth and bone turnover interactions. The rationale was to gain some insights into the cellular dynamics of this enigmatic neoplasm.

1.3 Objectives

The objectives of this study were as follows:

i) To investigate the heterotypic interactions between two distinct cell populations in the *in vitro* 3D co-culture system for ameloblastoma disease

ii) To identify *in vitro* 3D co-culture model that best reflects the tumour-stromal interactions in ameloblastoma

iii) To assess the biological significance of the heterotypic cell-cell interactions on the biological behaviour of cultured cells

CHAPTER 2: LITERATURE REVIEW

2.1 Odontogenic tumours

Odontogenic tumours (OTs) as coined by Broca in 1869, represent a spectrum of lesions ranging from jaw cysts and benign neoplasms to malignant tumours with metastatic potential and high risk of recurrence; derived from the dental remnants such as epithelium and/or mesenchymal elements of the tooth-forming apparatus (Vered *et al.*, 2017). These tumours, are therefore found within the maxillofacial skeleton or soft tissue overlying the tooth-bearing areas or alveolar mucosa in edentulous regions. OTs are uncommon and rare tumours that may generate at any stage in the life of an individual, but it can pose a significant diagnostic, and therapeutic challenge due to the lack of distinct phenotypic and molecular features, and an unclear pathogenesis of the tumours. In general, OTs derived from the more primitive dental structures are thought to be more aggressive and vice versa (Pogrel *et al.*, 2006). The biological behaviour and the histological pattern of the lesions are essential in the classification, diagnosis and prognosis of these lesions (Philipsen *et al.*, 2005). Basically, OTs are classified based on their behaviour dividing into: benign, malignant and non-neoplastic. Benign tumours are then subdivided based on the types of odontogenic tissues involved: lesions composed mainly of epithelium, mesenchyme and those composed of mixed epithelium and mesenchyme.

Table 2.1: WHO classification 2017 of odontogenic tumours.

Malignant odontogenic tumours	Benign odontogenic tumours		Odontogenic cysts
Odontogenic carcinomas: • Ameloblastic carcinoma • Primary intraosseous carcinoma • Sclerosing odontogenic carcinoma • Clear cell odontogenic carcinoma • Ghost cell odontogenic carcinoma *Odontogenic sarcomas*: • Odontogenic carcinosarcoma • Odontogenic sarcomas	*Epithelial odontogenic tumours*: • Ameloblastoma ➢ Ameloblastoma, unicystic type ➢ Ameloblastoma, extraosseous/ peripheral type ➢ Metastasizing ameloblastoma* • Squamous odontogenic tumour • Calcifying epithelial odontogenic tumour • Adenomatoid odontogenic tumour	*Mesenchymal odontogenic tumours*: • Odontogenic fibroma • Odontogenic myxoma/myxofibroma • Cementoblastoma • Cemento-ossifying fibroma *Mixed epithelial and mesenchymal odontogenic tumours*: • Ameloblastic fibroma • Primordial odontogenic tumour • Odontoma ➢ Odontoma, compound type ➢ Odontoma, complex type • Dentinogenic ghost cell tumour	*Inflammatory origin*: • Radicular cyst • Inflammatory collateral cysts *Developmental origin*: • Dentigerous cyst • Odontogenic keratocyst • Lateral periodontal and botryoid odontogenic cyst • Gingival cyst • Glandular odontogenic cyst • Calcifying odontogenic cyst • Orthokeratinised odontogenic cyst

* Metastasizing ameloblastoma is an ameloblastoma that metastasize despite its benign histological appearance.

2.1.1 Epidemiology

The relative frequency of odontogenic tumours diverges in different countries due to the geographic and ethnic diversity. Many studies in different region of the world have shown distinct frequency in the relative prevalence of these tumours. Among the studies reported, ameloblastoma was the most frequent odontogenic tumours as reported by Luo and Li (2009) (37%) in Chinese, Adebayo *et al.* (2005) (48%) in Nigerian, Nalabolu *et al.* (2017) (49%) in Indian and highest in African region (80%) (Johnson *et al.*, 2014). Most of the reports agreed that benign OTs are the most frequently seen OT compared to malignant OTs (Ladeinde *et al.,* 2005). Notably, males were commonly inflicted than females, with no significant association between different types of OT (Nalabolu *et al.*, 2017). The discrepancy of the peak age incidences of these lesions was observed and OTs are generally shown a predilection for the mandible, specifically posterior mandible (Santos Tde *et al.*, 2014; Nalabolu *et al.*, 2017). In Malaysia, the epidemiological studies on OTs are scarce. However, the retrospective studies conducted by Nurhayu Ab Rahman (2014) revealed that 13% of the oral cavity lesions among Malaysian were odontogenic origin and ameloblastoma is the most prevalent lesion reported within the 12-year period.

2.1.2 Aetiopathogenesis

The exact aetiopathogenesis of odontogenic tumours is unfamiliar with no known specific predisposing factors, although several studies have reported the existence of molecular alterations in the induction of growth and development of odontogenic tumours (Sandros *et al.*, 1991; Fukumoto *et al.*, 2004; Kumamoto & Ooya, 2005). The majority of the odontogenic tumours are seemingly to arise de novo or from the pre-existing lesions without an apparent causative factor. However, the dysregulation of several genes involved in normal tooth development and key genes such as oncogenes, tumour suppressor genes, genes repair DNA, cell cycle regulator genes and apoptotic genes,

might perform an important part in the development and continued growth of the tumours of the tooth-forming apparatus.

2.1.3 Management: Diagnosis and treatment

The pre-operative differential diagnosis of odontogenic lesions highly aids in the treatment plan and thus survival outcome. Most cases of the odontogenic lesions are asymptomatic, and the diagnosis of odontogenic lesions is achieved by imaging modalities, including intraoral and extraoral imaging. The radiograms of the lesions often appeared radiolucent to radiopaque because it generally composed of soft and hard tissues. The intraoral imaging is usually the first means to identify the presence of an intrabony lesion, with panoramic imaging as the diagnostic protocol; extraoral cross-sectional imaging such as CT and MRI are required for the topography and the fine structure of the lesion.

The available treatment of the odontogenic lesions remains controversial. Treatments of most odontogenic lesions are generally classified as conservative or aggressive. Conservative treatment includes simple enucleation, with or without curettage, decompression, or marsupialisation. Aggressive treatment generally includes hemimandibulectomy, peripheral ostectomy, chemical curettage with Carnoy's solution, liquid nitrogen cryotherapy, electrocautery and resection, segmental resection or marginal resection (Güler *et al.*, 2012). However, the choice of treatment modality is based on numerous factors, including patient age, history of previous treatment, soft tissue involvement, size, localization and histological variant of the lesion.

2.2 Ameloblastoma

Ameloblastoma or frequently known as solid/multicystic ameloblastoma, is an expansible, locally aggressive but a histologically benign intraosseous progressively growing epithelial odontogenic neoplasm, virtually with no metastatic potential. It

represents the most common of all central and peripheral odontogenic tumours (such as peripheral odontogenic fibroma, peripheral calcifying odontogenic cyst, peripheral ameloblastoma, and peripheral calcifying epithelial odontogenic tumour), although it has an estimated annual incidence of only 0.5 cases per million population (Larsson & Almeren, 1978). The vast majority of ameloblastomas, approximately 80%, are developed in the mandible, frequently in the posterior region, followed by anterior mandible, posterior maxilla, and anterior maxilla, may involve the associated root resorption and unerupted teeth. Ameloblastoma has a strong tendency for local recurrence, especially after conservative treatment if it is not adequately removed. It occurs over a wide age range with a peak incidence in the fourth to fifth decades of life and generally with equal incidence in men and women (Reichart *et al.*, 1995). Clinically, ameloblastoma often presents as an otherwise asymptomatic painless swelling of the jaw. Radiographically, ameloblastoma commonly present as unilocular or multilocular "soap bubble-like" corticated radiolucency with or without hyperostotic borders that may result in a honeycomb appearance.

2.2.1 Epidemiology

The aetiology of ameloblastoma is unknown. However, mutations in genes that belong to the MAPK pathway, including of K-Ras, FGFR2 and tumour suppressor genes (e.g. p53 and MDM2) have been reported in almost 90% of all ameloblastomas (Garg *et al.*, 2015). In addition, oncoviruses such as HPV and EBV also showed their participation in 42% and 48% of ameloblastoma lesions respectively (Sand *et al.*, 2000; Ayoub *et al.*, 2011). Based on a retrospective study of ameloblastoma, it is noted that ameloblastoma forms 1% of all tumours and cyst of the jaws, and the relative frequency of ameloblastoma in relation to odontogenic tumours is ranged between 11 – 92%, ranked as the most frequent odontogenic tumour in some parts of the world, including Africa, Hong Kong, China and Turkey (Wu & Chan, 1985; Günhan *et al.*, 1990; Reichart *et al.*, 1995; Arotiba

et al., 1997; Lu *et al.*, 1998). In Malaysia, ameloblastoma formed 1.1% of all oral lesions and 12.4% of all odontogenic tumours and cysts cases as reported (Ramanathan *et al.*, 1982; Siar & Ng, 1993). The racial differences in the distribution of ameloblastomas are observed among various ethnic groups in Malaysia, with Malays accounting for 47.6%, Chinese 34.8%, Indians 7.0% and other races 10.6% (Siar *et al.*, 2012).

2.2.2 Histopathology

Ameloblastomas are histopathologically grouped into follicular, plexiform, acanthomatous, granular, basaloid and desmoplastic type (Angadi, 2011). The most common type is follicular type, which resembles the epithelial component of the enamel organ, populated by peripheral basal cells and stellate reticulum within a fibrous stroma; the peripheral cells are columnar to cuboidal shapes, with hyperchromatic nuclei and palisaded with reverse polarity, and central core is occupied by loosely arranged angular stellate reticulum-like cells. The plexiform type ameloblastoma is the second most common type, composed of anastomosing strands of ameloblastomatous epithelium with an inconspicuous stellate reticulum and cyst-like stromal degeneration. Other histological types like acanthomatous is composed of squamous epithelium in the centre and variable keratinization of stellate reticulum-like cells, granular type is composed of granular eosinophilic cytoplasm that often located within the stellate reticulum-like cells and basaloid type is the least common type, composed of peripheral rim of cuboidal hyperchromatic epithelial cells without the presence of centre stellate reticulum-like cells in the centre of the nest. The desmoplastic ameloblastoma consists of flattened or cuboidal rather than tall columnar peripheral cells with central spindle-shaped cells and densely collagenous stroma. Often, admixed histopathological types are found in ameloblastoma, and the lesion is commonly classified based on the predominant pattern.

2.2.3 Clinicopathologic classification

2.2.3.1 Unicystic type

Unicystic ameloblastoma (UAM) is a variant of intraosseous ameloblastoma, accounting for 5% – 22% of all ameloblastomas (Reichart *et al.*, 1995). UAM is present as a single cystic cavity that may be accompanied by luminal proliferation and mutation in BRAF is the most common site of mutation in UAM to date. The unicystic variant occurs at a younger age, peaked at the second decade of life. UAM may associate with an impacted tooth and generally shows a slight male preponderance; however, UAM not associated with an impacted tooth shows a minor female predilection. UAMs are often located in the mandibular third molar area and ascending ramus. UAMs can also be found in the posterior maxilla, inter-radicular and edentulous areas. Radiographically, it presents as an expansive unilocular radiolucency with a well-demarcated border may involve an unerupted tooth, root resorption, or cortical perforation. In Malaysia, UAMs represent about 28% of ameloblastomas and mostly affected Malay ethnic group with no gender predilection, peaked at the first and second decades of life and often located in the posterior mandible (Siar *et al.*, 2012).

UAMs are histopathologically grouped into luminal, intraluminal and mural type. The luminal type UAM is a simple cyst lined by ameloblastomatous epithelium, composed of cuboidal or columnar basal cells with hyperchromatic nuclei and nuclear palisading with polarization, overlying with loosely arranged stellate reticulum-like cells. The intraluminal type is characterized by the intraluminal proliferation of ameloblastic epithelium, often in a plexiform pattern. Hence, intraluminal UAM is sometimes referred to as the plexiform unicystic ameloblastoma. The mural type is the most aggressive subtype, involved mural extension of the ameloblastomatous epithelium into the cystic wall.

UAM is a relatively benign cyst-like odontogenic tumour exhibited a better response to conservative treatment with a lower recurrence rate. Accordingly, initial treatment of UAM often consists of conservative treatments such as enucleation, especially in younger populations due to its lower devastating impacts on patients. UAMs require long-term follow-up due to its extended recurrence period with recurrence rate of 30.5% after enucleation, much higher than resection with a recurrence rate of 3.6% after treatment (Lau & Samman, 2006). Therefore, the further treatment of UAM is determined by the pattern and extent of ameloblastomatous proliferation. Among the subtypes of UAM, mural type has the highest recurrence rate of 35.7% and therefore resection just as the conventional AM or other more radical modalities should be given; whilst luminal and intraluminal type have a relatively lower recurrence rate of 6.7% and may be justified by conservative management (Li *et al.*, 2002).

2.2.3.2 Extraosseous/peripheral type

Extraosseous ameloblastoma is an extremely rare variant accounting for 0.6% ameloblastomas in Malaysia (Siar *et al.*, 2012). Histologically, this lesion is defined as an ameloblastoma develops in the gingiva, or occasionally from other extraosseous sites including the alveolar areas. The extraosseous type peaked at fifth to seventh decades of life with a slight male preponderance. The most common location of extraosseous type is the soft tissues in the mandibular retromolar area and maxillary tuberosity. Generally, extraosseous type lacks the locally aggressive nature of central tumours and does not infiltrate the underlying bone, but it may infiltrate into the surrounding tissues, mostly the gingival connective tissue (Gardner & Corio, 1984). The actual histogenesis of extraosseous AM still remains controversial. Basically, it is suggested to derived from remnants of the dental lamina, odontogenic remnants of the vestibular lamina or the pluripotent cells from the minor salivary glands and in the basal cell layer of the mucosal epithelium (Isomura *et al.*, 2009). In the majority of the cases, extraosseous type usually

shows no radiological evidence of bone involvement, but a superficial bone erosion or bony depression (cupping or saucerization) of the underlying periosteum may be detected at surgery.

Microscopically, extraosseous AM involved the ameloblastic growth of nests of loosely connected stellate reticulum-like cells, surrounded by a layer of columnar cells with well-polarized nuclei within a squamous epithelial layer, resemblances the intraosseous ameloblastoma. The growth is usually presented as a sessile or pedunculated and exophytic lesion with a smooth, granular or warty surfaced solid mass of cells, with the presence of minute cystic spaces within the masses (Vanoven *et al.*, 2008).

The non-aggressive nature of extraosseous ameloblastoma and low recurrence rate of 9% as reported by Lin *et al.* (1987). The recurrence of this type is rare, but since it often produces a shallow depression in the underlying bone, rather than infiltration, conservative removal such as local surgical excision with proper disease-free margins is usually the common curative treatment management and accompanied with a long-term follow-up (Pogrel & Montes, 2009).

2.3 Bone remodelling

Bone is a mineralized connective tissue that composed of multiple cell types and a calcified extracellular organic matrix. It is a highly dynamic tissue with a capacity for continuous remodelling, coordinated by a group of specialized cell types in a cycle known as bone remodelling. The two principal cell types, osteoblast, and osteoclast are the major effectors in the turnover of bone matrix. Bone remodelling is a finely balanced cycle operates continually, involved the bone breakdown and bone synthesis simultaneously, widely known as the coupling of bone resorption and bone formation. The bone remodelling process comprises of three sequential phases: the initiation of bone

resorption by activated osteoclasts, the transition period from bone resorption to new bone formation, and bone formation by osteoblasts (Meghj *et al.*, 1998).

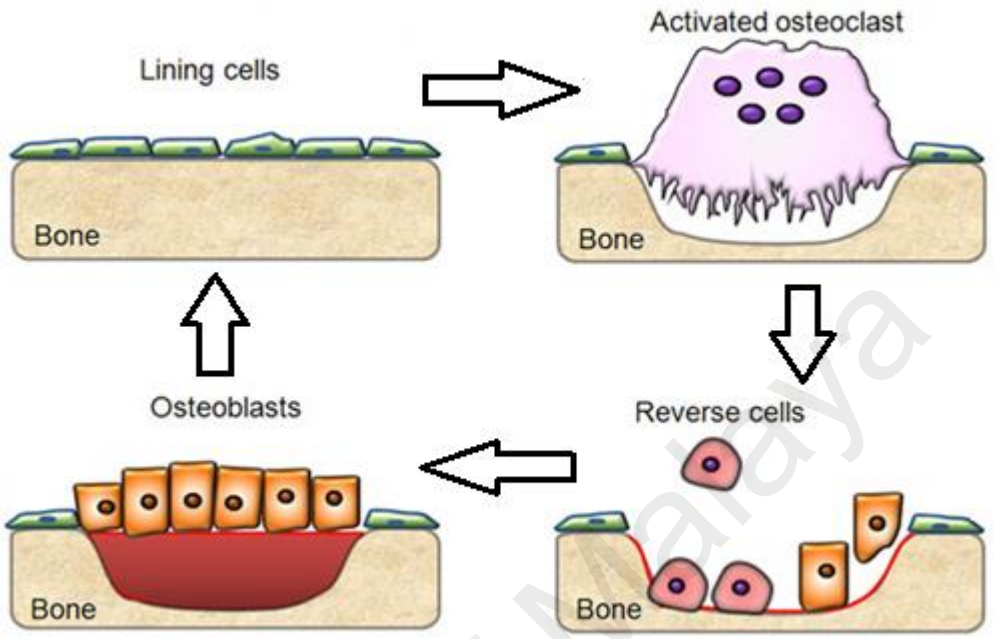

Figure 2.1:Bone remodelling cycle.

Schematic representation of the continual bone remodelling process: starting from the initiation and orchestration of activated osteoclasts and regulated by coupled crosstalk between osteoblasts and osteoclasts.

Figure adapted from Del Fattore *et al*., 2012.

2.3.1 Bone resorption

Bone resorption is a process involves the removal of mineral and organic components of the bone extracellular matrix by the activity of osteolytic cells, of which the osteoclast plays the most important role. The process is regulated by local and/or systemic regulatory systems, involves the recruitment of mononuclear osteoclast precursors to the bone surface, osteoclast differentiation and activation by cell-to-cell interaction between osteoclast and osteoblast at the surface of the mineralized bone, and ultimately the activity of the functional osteoclasts that work in concert to remove both mineral and organic components of the bone matrix through the action of protease enzymes. The activated osteoclasts also dissolve the bone mineral by lowering the pH of their microenvironment,

achieved by actively transport protons into the extracellular space through ion channels on their cell membrane (Meghj *et al.*, 1998). Bone resorption process is governed by the locally controlled autoregulatory mechanism. The paracrine and autocrine chemical signalling factors that released during resorption further inhibit the resorption via negative feedback control system, suppresses the osteoclast formation and stimulates osteoblastogenesis, and therefore the lifespan of osteoclast is presumably 8 – 10 days.

2.3.2 Bone formation

The formation of new bone by mononuclear osteoblasts, mediated by both local and systemic factors, essential for the maintenance of bone mass and bone strength. Generally, the process involves three basic steps: attraction and deposition of osteoprogenitor cells to the resorbed surface, differentiation of osteoprogenitor cells into mature osteoblasts, and the synthesis of new collagenous organic matrix and regulation of matrix mineralization by mature osteoblasts, leading to new bone deposition. The bone extracellular matrix that synthesized and secreted by osteoblasts consisting of collagenous proteins, primarily type I collagen (90%), the non-collagenous proteins, including osteonectin, proteoglycans, osteopontin, osteocalcin, bone sialoprotein II, bone morphogenetic proteins (BMPs) and matrix GLA protein, alkaline phosphatase, and growth-regulatory factors. After the completion of bone formation, approximately 50% to 70% of osteoblasts undergo apoptosis. In the secreted bone matrix, the remaining osteoblasts are known as bone lining cells, retained the ability to dedifferentiate into osteoblasts upon stimulation, or become osteocytes, which represent the terminally differentiated osteoblast that maintain connection with bone surface lining cells, osteoblasts and other osteocytes via their gap junctions between cytoplasmic processes extending from the cell body, to support bone homeostasis.

2.3.3 Mediators of bone remodelling

Bone remodelling is controlled by both local and systemic factors. The highly dynamic mechanism is mediated by the interplay of local factors, like growth factors, cytokines and prostaglandins expressed by bone cells that act in a paracrine or autocrine manner; systemic factors include PTH, calcitonin, androgens, and oestrogens. These factors are the central player in this mechanism and so it is important for the maintenance of bone homeostasis. The local factors expressed by osteoblastic cells, for instance, M-CSF alone is inadequate for the differentiation of osteoclast precursors into mature osteoclasts. RANKL/RANK/OPG signalling system, perhaps the most completely described molecular mechanism that plays a crucial role in osteoclastogenesis (Boyce & Xing, 2007b; Kohli & Kohli, 2011). RANKL, receptor activator of NF-κB ligand, also known as osteoprotegerin ligand (OPGL), function in homotrimer form and may express as a membrane adhered molecule on the cell surface (mRANKL) or soluble molecule (sRANKL). The expression of RANKL by bone marrow stromal cells, activated T lymphocytes, osteoblasts, chondrocytes, osteocytes, and thymocytes is triggered upon the stimulation of systemic factors, including PTH, PTHrP, vitamin D3, IL-1, TNFα, and PGE2. RANKL is recognized as the osteoclast master regulator cytokine, plays a pivotal role in the regulation of osteoclastogenesis, essential in the development of osteoclasts under the complex interplay with M-CSF (Boyce & Xing, 2007a). Osteoclastogenesis is a multistep process triggered by prolonged stimulation with RANKL. This strictly regulated RANKL-induced osteoclastogenesis is comprised of several stages including progenitor survival, differentiation to mononuclear pre-osteoclasts, cell fusion to multinucleated mature osteoclasts, and activation to bone resorbing osteoclasts. In fact, RANKL exhibits a dual antagonistic effect on osteoclastogenesis, depends on the receptor interacted, RANK or OPG. RANK, receptor activator of NF-κB is expressed on the surface of chondrocytes, dendritic cells, osteoclast progenitor cells and mature

osteoclasts. In the context of bone remodelling, RANK-RANKL interaction stimulates the initiation of both osteoclastogenesis and activation of osteoclasts. On the other hand, OPG that produced by a wide range of cells, such as bone marrow stromal cells, follicular dendritic cells and osteoblasts, acts as a soluble decoy to prevent the binding of RANK to RANKL and, consequently inhibits the recruitment, proliferation, and activation of osteoclasts. Conclusively, the RANKL/RANK/OPG system is essential for the osteoclast differentiation directed by osteoblasts, and the balance of RANK-RANKL and OPG-RANKL play the most important role in the bone homeostasis.

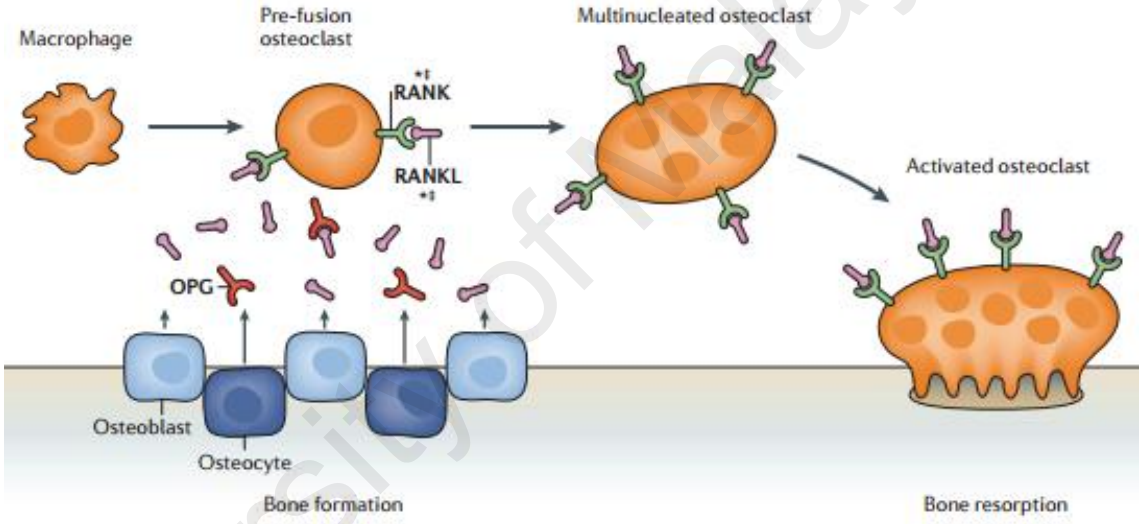

Figure 2.2: RANKL/RANK/OPG signalling mechanism for bone remodelling.

The interaction between sRANKL or mRANKL with membrane-bound RANK on the surface of osteoclast progenitor cells or mature osteoclasts triggers activation of osteoclast and the subsequent bone resorption. In contrast, OPG acts as a decoy receptor for RANKL, having an inhibitory effect on osteoclastogenesis.

Figure adapted from Richards *et al*., 2012.

2.3.4 Dysregulation of bone remodelling in ameloblastoma

Bone remodelling is an adaptive mechanism supported by the coordinated action of bone-forming osteoblasts and bone-resorbing osteoclasts, responsible for the maintenance of bone integrity and homeostasis. The importance of RANK/RANKL/OPG system as the determinant of equilibrium between bone resorption and bone formation is

well established. Recent molecular investigations and reviews supported that, the disruption of RANK/RANKL/OPG signal transduction pathway enhanced the osteoclast formation and activation, thereby accelerates bone resorption as seen in a wide range of bone lesion, including bone metastases (Chuang *et al.*, 2009). This trimolecular pathway formed the basis of the bone remodelling of ameloblastoma via the disruption of RANKL/OPG ratio (Qian & Huang, 2010). Also, the interactions between stromal and tumour cells have a subsequent role in tumour progression, local invasiveness and bone resorption in ameloblastoma. A study conducted by Kayamori *et al.* (2010) revealed that, IL-6 was expressed by both stromal and tumour cells at the tumour-bone interface and its role in inducing osteoclastogenesis through the activation of RANKL. Besides, the expression of bone-resorbing factors, such as cytokines and growth factors, acting in both autocrine and/or paracrine manner also responsible for cancer-associated bone resorption. Collaboratively, the upregulation of RANKL expression by osteoblasts leads to the subsequent uncoupled bone remodelling and ultimately causes bone destruction in ameloblastoma disease.

2.4 *In vitro* 3D cell culture model

The ability of the three-dimensional (3D) cell culture model to support the growth of a single type of cells or co-culture of multiple cell types and maintaining its normal shape and structure into a 3D spheroids or aggregates as their *in vivo* counterparts have received much attention from scientists. 3D cultured cells are generally grown on scaffold/matrix, within a scaffold/matrix or even in a scaffold-free manner (Edmondson *et al.*, 2014). Due to the nature of the 3D models, cell attachment could occurs around the entire cell membrane surface, allowed the cultured cells embedded in the extracellular matrix (ECM) to have an opportunity for cellular contact in a complex 3D fashion (Baker & Chen, 2012). This setting of 3D culture system may be critical in the establishment of cell-to-cell and cell-to-ECM interactions, organizing communication among adjacent

cells and their microenvironment as achieved in the *in vivo* state, important for an *in vivo*-like structural organization and a more precise depiction of cell polarization (Edmondson *et al.*, 2014; Antoni *et al.*, 2015). The artificial responses and reduced stress in cell adaptation to the flat, two-dimensional (2D) growth surface enabling a more suitable and natural environment for optimal cell growth, cell differentiation and cell function can significantly alter their ECM proteins expression and morphological changes that leads to subsequent impairment on cellular functions and metabolism (Zhang *et al.*, 2005; Knight & Przyborski, 2014).

An emerging evidence suggests that the 3D-cultured cells have improved physiological relevant morphology, and cell-to-cell contact, which is not present in 2D cultures (Vinci *et al.*, 2012). Cells cultured 3D also show characteristics in terms of cellular heterogeneity, mass transport and complex cell-matrix interaction more closely related to their *in vivo* counterparts (Khaitan *et al.*, 2006; Lin & Chang, 2008). In addition, gene expression analysis, microRNA and metabolic profiles of cells grown in 3D model indicated that, genotypes of 3D-cultured cells are significantly more relevant to the *in vivo* state, as compared to the genotypes of cell grown in conventional 2D cultures (Edmondson *et al.*, 2014). It is worth mentioning that 3D models serve as an ideal *in vitro* model that allowed the co-culture of multiple types of cells to more closely recapitulate the natural *in vivo* environment. Such 3D multicellular system is useful for the study of the roles of cell-cell interactions, particularly the interactions between stromal cells and tumour cells in the tumour microenvironment (Wang *et al.*, 2010). In addition, 3D models exhibited a greater stability than 2D monolayer culture and thus, cells cultured in 3D models have a relatively stable and longer lifespan of at least up to 4 weeks (Antoni *et al.*, 2015). Taken together, these findings embark on the physiological relevance of 3D model, providing greater support for cell complexity and functionality of varying degrees as in the native environment. Hence, the model is capable of bridging the gap between *in*

vitro and *in vivo* conditions, potentially acts as a promising alternative towards the traditional 2D cell culture system with more reflective cellular responses against drug treatments as of *in vivo* conditions.

2.4.1 Application of 3D cell culture model

3D cell culture system has been used extensively in studying of hallmarks of cancer, basically referred to the biological capabilities that acquired during the multistep development of tumours (Fischbach *et al.*, 2009; Truong *et al.*, 2016; Klimkiewicz *et al.*, 2017). However, *in vitro* culture of tumour cells in the scientifically-rigorous 3D culture system with customized microenvironments are genuinely better mimic the cells growing within the living tumours.

Chantravekin and Koontongkaew (2014) have established *in vitro* 3D co-culture model for head and neck squamous cell carcinoma (HNSCC), harbouring HNSCC cell lines (HN4 and HN12) and ameloblastoma-associated fibroblasts (AAFs) or gingival fibroblasts (GFs). The model provided a valuable tool to investigate the role of tumour stroma in the ameloblastoma biology. By using the established 3D co-culture model, both AAFs and GFs have shown a tendency to stimulate tumour cell growth. However, the difference in TGF-β expression suggested AAFs have a higher tendency to stimulate the proliferation and induce invasion of tumour cells. Moreover, lung cancer cells cultured in the *in vitro* 3D laminin-rich ECM models developed by Cichon *et al.* (2012) have displayed an observable development of multicellular structures that reflective of the phenotypic alterations controlling of the cancer cell malignancy. These outcomes have further embarked on the importance of cell-ECM interactions in cellular function. 3D cell culture system is a promising model being employed in many areas of biological research, especially a representative *in vitro* model for the study of cancer-relevant patterns of cellular processes due to the physiological relevance of the model. It was found that HepG2 liver cells culture in 3D models by Bokhari *et al.* (2007) exhibits a greater viability

and structural integrity. Thus, 3D-cultured HepG2 liver cells are less susceptible to cytotoxin-induced cell death even at a high concentration in comparison to their *in vitro* 2D counterparts. HepG2 cells occupied a 3D environment exhibit a normal metabolic activity and capable of interact with adjacent cells to maximize their surface area as in the natural cellular environment. In addition, the nature of 3D models allowed Härmä *et al.* (2010) to monitor and modulation of invasive processes of prostate cancer cells in such organotypic environment, including the growth modes, migration, and invasion of cancer cells.

At present, 3D models of the normal oral mucosa are well established. The use of 3D *in vitro* oral mucosa models constructed with a dysplastic and/or malignant cell line have extensively adapted by researchers to recapitulate of the *in vivo* oral dysplasia and oral cancer. Eriksson *et al.* (2016) cultured the AM-1 construct and the bone-like construct composed of human osteosarcoma (HOS) cells in a joined collagen construct using an acellular support gel to assess the cell-cell interactions. The constructed 3D *in vitro* co-culture model shown the migration of AM-1 cells through the bone-like part of the construct in the presence of HOS cells. These results suggested the role of stromal cells as key contributors to the tumour microenvironment and promotes the invasive properties of AM-1 cells. In AM co-cultures, the reciprocal interaction between HOS and AM-1 cells strongly impact on the local invasiveness of AM-1 cells through bone. The presence HOS cells in the microenvironment upregulates the expression of RANKL in AM-1 cells, in turn, AM-1 cells downregulated the OPG and NF-κB expression of bone-like construct. Collectively, interactions between these cells lead to the increased rate of bone resorption. Besides, Duong *et al.* (2005) cultured oral squamous carcinoma cells (OSCC) in 3D fashion to model the invasiveness of OSCC cells. In the established 3D model, OSCC cells were seeded atop of a layer of connective tissue containing oral mucosa fibroblasts, separated by a reconstituted basement membrane. Such setting of 3D models allowed the

demonstration of the invasion of OSCC cells into the connective tissue stroma through the underlying basement membrane. The *in vitro* model allows the investigation of the mechanisms associated with the invasive OSCC cells migration in varying culture conditions and treatments at different time intervals. In essence, these studies embrace the potentials of 3D model in narrowing the gap between cellular physiology and *in vitro* cell culture systems, and the physiological relevance of the model potentially arise as an excellent *in vitro* model system to accurately recapitulate of the *in vivo* microenvironment.

2.4.2 Challenges of 3D model

The biological nature of the scaffold/matrix used in the scaffold/matrix-based 3D culture systems is the major technical challenge of the system. Of the scaffold/matrix, 3D models that use matrices of animal origin components encountered difficulties during the implementation of the model for clinical work. Matrices originated from tissues such as basement membrane extracts potentially contain unknown intracellular contaminants or undesired components, including growth factors and viruses. Hence, the utilization of these matrices into 3D fibrous networks for cell culture is having a major effect on the matrix architecture and the corresponding growth and development of the cultured cells. In addition, the application of cell-adhesive matrix further complicated the handling of the 3D model. The *in vitro* cell-matrix attachment has limits the utility of such model, in particular, difficulty in effectively removing adhering cultured cells in the matrix and thus this model still presents challenges in developing assays and obtain fast, automated assay readouts from these more complex assays (Fawcett, 2013). Generally, collagen hydrogels and Matrigel are the bio-scaffold often used in 3D cultures. However, the viscosity and density of these scaffolds have direct implications on their functionality during biomedical applications. Hence, extra care must be taken when handling these hydrogels to enable effective cell manipulation and cell attachment, assuring the cell viability in the

3D culture system. In particular, the concentration of the hydrogel has a remarkable influence on the porosity and pore distribution of the scaffold. In essence, the choice of hydrogel as scaffold for 3D model, taking into the consideration of the concentration and exposed surface area of the scaffold, significantly affect the architecture of the generated ECM, determine the distribution and penetration of cells within the scaffold volume.

The culture conditions, such as temperature and pH are vital for the functional and effectiveness of cell cultures in the *in vitro* 3D hydrogel and must be very carefully controlled to create an ideal environment for the cultured cells. Therefore, the reproducibility and consistency between sets of experiments are the major issues in culturing cells in 3D model. Besides, the increased size and tortuosity of the *in vitro* 3D scaffold undoubtedly lead to the difficulty in cell extraction from the bio-scaffold for analysis. Moreover, the construction of 3D cell construct can be very complicated and laborious due to the requisition of many different components. In addition, the imaging of 3D model can be difficult in accordance with the size of the 3D scaffold and transparency of material used. The assays currently available for the investigation of cellular responses to drug interactions, including cell-to-cell and cell-to-matrix interactions, cell migration and dose-dependent cell viability are not optimized for the increasingly sophisticated 3D models. Conclusively, these technical difficulties and also the post-culturing processing embarking on the user-unfriendly nature of the 3D model (Antoni *et al.*, 2015). Therefore, a universal standardized model with systematic optimization and characterization is highly necessary to specifically prepared 3D culture model in order to fully utilize the benefits of the model in most of the experimental approaches, which ultimately facilitates the development of various biological research.

2.5 Immortalized cell lines

It has been well-documented that primary cells reach replicative senescence after a limited number of cell divisions (Stewart & Weinberg, 2002). Therefore, immortalized

cells are often used in research in place of primary cells. In addition, immortal cell lines also easy to use and bypass the ethical concerns on the use of animal and human tissues, providing a pure population of cells possess functional features and phenotype as close to the primary cells. In the mid-twentieth century, a vast collection of immortalized cells was blossomed, especially after the establishment of the HeLa, a first mammalian cell line in 1951.

Primary cells are not capable of extended proliferation due to telomeres shortening after rounds of proliferation. Primary cells can be manipulated in several methods to circumvent senescence of cells and thus immortalizing cells. Viral genes, such as simian virus 40 (SV40) T antigen was used to induce immortalization of mouse Sertoli cell line (MSC-1) (Peschon *et al.*, 1992). The over-expression of telomerase reverse transcriptase protein, stimulated by SV40 is able to maintain a sufficient telomere length to avoid replicative senescence of cells (Lundberg *et al.*, 2000; Fridman & Tainsky, 2008). Likewise, the over-expression of oncogenes, such as Ras or Myc T58A and inactivation of tumour suppressor genes, such as p53 and Rb have also found to be able to achieve immortalization of some primary cell types (Lundberg *et al.*, 2000; Sears *et al.*, 2000).

2.5.1 AM-1 cell line

Ameloblastoma-1, AM-1 cell line was established from a mural, plexiform-type ameloblastoma tissue of a 20-year-old woman. Briefly, Harada *et al.* (1998) produced an immortalized AM-1 cell line by transfection with human papillomavirus type-16 using plasmid pMHPV16d as a vector. Cultures of AM-1 cell grew slowly and composed of closed packed small and polygonal cells, showing morphological and histochemical resemblances to *in situ* ameloblastoma and those in primary cultures. This cell line maintains epithelial cell morphology and expresses cytokeratins K8, K14, K18, and K19 but a weak expression of vimentin and negative expression of enamel proteins. Furthermore, the product of bcl-2 gene, a protein product which prevents apoptosis of the

cell, is consistently expressed. The established AM-1 cells grew in a monolayer over foci of collagen degradation as evidenced by the formation of a pronounced depression on the surface of the collagen gel and could invade the collagen gel at such sites, gave rise to long processes or duct-like structures at their perimeters that penetrated the gel.

2.5.2 KUSA/A1 cell line

Umezawa *et al.* (1992) immortalized bone marrow stromal cells of female C3H/He mice by transfection with a plasmid containing middle T antigen (MTAg) gene from tumour-inducing polyomavirus. The monoclonal cell populations were isolated from clones of transfected stromal cell lines by limiting dilution and continuous passage. Following that, among the mesenchymal progenitor cell lines (KUMs) identified, only KUSA cells exhibited osteoblastic properties and fibroblastic appearance with flat, elongated spindle-shaped. From *in vivo* cell mass of KUSA cells, independent sublines KUSA/A1, KUSA/M1, KUSA/D, KUSA/H1 and KUSA/O were isolated and established. However, KUSA/A1 is the only sub-clone possessed the most remarkable osteogenic ability both *in vivo* and *in vitro*, with rapid mineralization and marked calcium deposition in inducing condition. Interestingly, high ALP activity was detected in KUSA/A1 cell in both inducing and non-inducing conditions even before mineralization. These findings augmented that KUSA/A1 cell has a unidirectional potential for osteogenesis. Differential expression of osteogenic markers served as the indicator of the stage of osteogenesis. In the context of KUSA/A1 cell, it showed osteocalcin expression in both inducing and non-inducing conditions after confluency. Whilst, osteopontin expression is upregulated only in the inducing condition indicates the stage of KUSA/A1 differentiation *in vitro* (Kawashima *et al.*, 2005).

2.5.3 ST2 cell line

The stromal cell line, ST2 is derived from bone marrow culture of BC8 mice in accordance with the method as described by Whitlock *et al.* (1987). Generally, ST2 cells

have characteristics of preadipocytes and none of the osteoblastic phenotype in standard cultures. ST2 was found to developed characteristics of typical osteoblast, including ALPase activity, expression of osteoblastic differentiation marker proteins such as osteocalcin, and the formation of mineralized nodules under the induction of ascorbic acid, suggested the significance of ascorbic acid for the osteoblastic differentiation of ST2 (Otsuka *et al.*, 1999). Ascorbic acid-induced ALPase activity and also enhanced the calcium deposition of ST2 cells in a dose-dependent manner. On the other hand, β-glycerophosphate was found not involved in the activation of ALPase activity in ST2 cells although it has been reported to increase the expression of ALPase in osteoblastic cells. However, BMPs were able to induce the differentiation of ST2 cells into osteoblast-like cells in the absence of ascorbic acid, as evidenced by the enhanced dose-dependent ALPase activity of ST2 cells with the induction of exogenous BMP-2. In addition, BMP-2 and ascorbic acid synergistically enhanced the ALPase activity in ST2 cells, emphasizes the presence ascorbic acid in promotes the efficiency of the BMP system, further embark on the importance of ascorbic acid in osteoblastic differentiation of ST2 cells.

2.5.4 MC3T3-E1 cell line

The osteoblastic cell line, MC3T3-E1 developed by Kodama *et al.* (1981). was established via independent sub-culturing of the calvaria cultures of newborn C57BL/6 mice on a rigid 3T3 sub-culturing schedule and selected based on high alkaline phosphate (ALP) activity in the resting state. Several clones with ALP activity were initially isolated but MC3T3-E1 was amongst the clones that found to possess the highest ALP activity. These cells exhibited fibroblast-like morphology and have the capacity to deposit collagenous extracellular matrix and differentiation into osteoblast- and osteocyte-like cells, expressing osteoblastic phenotypes such as ALPase activity and osteocalcin expression, demonstrated to form calcified tissue *in vitro* similarly to their *in vivo* counterparts under the induction of ascorbic acid.

2.6 Cellular biomarkers

Hulka (1990) first defined biomarkers as cellular, biochemical or molecular alterations that are measurable in biological media such as human tissues, cells or fluids. In 2001, the definition has been broadened to include biological characteristics that can be objectively measured and evaluated as an indicator of normal biological processes, pathogenic processes, or pharmacological responses to a therapeutic intervention, agreed by the Biomarkers Definitions Working Group (Naylor, 2003). The application of biomarkers is especially well-known in the diagnosis and management of cancer (Easton *et al.,* 1995; Locker *et al.,* 2006; Allegra *et al.,* 2009). It is based on the quantitative or qualitative alteration of biomarkers that expressed by tumour cells or normal host cells may be due to the cause or effect of the malignant process. The spectrum of biochemical tumour markers as reported is very wide, classified based on their origin, structure, biological function or relationship to the event in tumour growth or formation.

2.6.1 Epithelial marker, cytokeratin

Cytokeratin (CK), a highly cell type-specific intermediate filament (IF), which represent the most abundant proteins in epithelial cells. They are multigene family of proteins, make up the largest subgroup of IF proteins that differ in their distribution in different types of epithelia. Two types of cytokeratins are distinguished that form heterodimers, namely acidic type I (CK 9-23) and basic type II (CK 1-8) cytokeratins. Depending on their expression pattern, cytokeratin serves to distinguish different epithelial cells and hence it also a valuable adjunct in the diagnosis and classification of tumour cells. The pattern of cytokeratin expression in OTs helps in the elucidation of histogenesis and biologic behaviour of the tumour. Virtually, the differential expression of cytokeratins in ameloblastomas enable it to differentiate them from other odontogenic neoplasms (Yoon *et al.,* 2011; Pal *et al.,* 2013). In general, the expression of cytokeratins

in ameloblastomas, although their expression may vary in some subtypes has reiterates their odontogenic epithelial origin.

2.6.2 Mesenchymal marker, vimentin

Vimentin is a widely expressed and highly conserved type III intermediate filament protein. Vimentin is often expressed in undifferentiated and proliferative cells of mesenchymal origin and thus, it is frequently used as a mesenchymal marker and also as an epithelial-mesenchymal transition (EMT) marker. Interestingly, vimentin is expressed in a cell type- and developmental stage-specific manner (Tapscott *et al.*, 1981). Lian *et al.* (2009) reported the high expression of vimentin in immature osteoblasts and a low level in fully differentiated osteoblasts, which represents the decreased of vimentin expression over time during the course of osteoblastic differentiation.

2.6.3 Osteoblastic markers

2.6.3.1 Osteocalcin

Osteocalcin, a major non-collagenous protein component of bone ECM that synthesized and secreted exclusively by fully functional and differentiated osteoblastic cells. Therefore, osteocalcin is often a late stage marker of osteoblasts differentiation and identified as a specific marker of osteoblast function that concomitantly with mineralization. In addition, osteocalcin as the osteoblast-related proteins also used as a non-invasive biochemical marker of bone formation and at least in part, reflects the bone turnover that exhibited clinical significance within-subject variability.

2.6.3.2 Osteopontin

Osteopontin, a secreted phosphorylated glycoprotein first identified in osteoblasts in year 1986. Osteopontin is a multifunctional protein that exists both as a soluble cytokine and non-collagenous component of the bone matrix. Osteopontin mediates diverse biological functions, also involves in osteoclast differentiation and the osteoblast

recruitment and function (Rittling *et al.*, 1998). In addition, osteopontin is highly expressed in bone by both osteoblasts and osteoclasts, functions in the osteoclast migration to the sites of bone resorption, and thus, it has been implicated as a crucial factor in bone turnover for balance bone homeostasis (Chellaiah *et al.*, 2003). Interestingly, osteopontin expression peaks twice during osteoblast growth, once in the proliferation phase and then again in the later stage of osteoblast differentiation (Aubin, 2001). Therefore, osteopontin can be used as osteoblast differentiation marker and the selective expression of osteopontin allows the evaluation of the differentiation state of osteoblastic cells.

2.6.3.3 Bone sialoprotein

Bone sialoprotein (BSP), an early marker of osteoblast differentiation, is an acidic, non-collagenous glycoprotein abundantly expressed in the bone extracellular matrix. BSP is expressed in several cell types that associated with mineralized tissues, but it is mainly expressed in abundance by osteoblasts. The actual role of BSP still remains unknown; however, several studies suggested the role of BSP in the development of mineralized tissue (Chen *et al.*, 1992; Chen *et al.*, 1994). Gordon *et al.* (2007) demonstrated the role of BSP in aiding osteoblast differentiation by directly modulating the activity and expression of osteoblast-associated factors and maintaining the osteoblast phenotype of fully functional and differentiated osteoblasts.

2.7 Histologic examination

The histologic examination involves the microscopic study of cell and tissue specimens under a microscope, either electron or light microscope. Various methods are used to study the characteristics and microscopic structures of the cells of a tissue and the examination is made possible with the aid of histological staining. Histological staining is a series of technique processes in the preparation of specimen, generally involves five key stages: fixation, processing, embedding, sectioning and staining using histological

stains. Histological staining is an aid in the microscopic study because it is significant in highlighting the important features of the tissue or cells and to flag nucleic acids, proteins and other biological components of a cell, enhancing the tissue contrast (Alturkistani *et al.*, 2016). In more recent, various multiple staining methods, such as differential staining, double staining or the multiple staining are used in some other cases to enhance the effectiveness of the staining process.

2.7.1 Hematoxylin and Eosin staining

Hematoxylin and eosin, or the H&E stain is the most frequently used combination of stains as far back as the 1870s. H&E staining is the standard histology stain for a typical tissue section. Hematoxylin is a basic dye that binds to acidic structures such as nuclei acids, give rise to nuclei of cells a blue-purple stain. On the other hand, eosin binds to basic structures of the cell, such as cytoplasm and the surrounding matrix giving it a varying degree of pinkish staining. H&E staining has the capability to reveal the structural information of a cell or tissue with specific functional implications. However, H&E staining is insufficient to provide all the diagnostic answers required because not all features of a cell or tissue can be provided, and special stains or advanced staining techniques are necessary (Martina *et al.*, 2011).

2.7.2 Alizarin Red S staining

Alizarin Red S (ARS), an anthraquinone dye, has been widely used to identify calcium deposits in tissue sections or cell cultures. It reacts with calcium and forms a birefringent Alizarin Red S-calcium complex in a chelation process. The versatility of ARS staining making it to be possible to extracted from the stained cells and readily assayed. The ARS staining is not strictly specific for calcium and interference of other minerals such as magnesium, barium, strontium, and iron may be occurred. However, elements other than calcium usually occur in finite concentration and thus hardly to interfere with the staining for calcium deposition (Puchtler *et al.*, 1969).

2.8 Immunohistochemistry

Immunohistochemistry (IHC) introduced in the 1930s is a multistep technique, aimed to detect the presence of a target antigen in tissue specimen with a specific antibody tagged with a visible label for visualization. IHC is frequently used for disease diagnosis, drug development and biological research. The detection of the presence of specific biomarkers with IHC able to identify the cell origin and cell type and the efficacy of test drug. Antibody-mediated antigen detection approaches are separated into direct and indirect methods, both using antibodies for the detection of the target antigen. However, the selection of the suitable method largely depends on the level of target antigen expression, availability and desired readout.

2.8.1 Direct method

In direct detection method, the primary antibody is directly conjugated to a fluorophore-labelled and so it is reacting directly with the antigens of interest in the tissue sections. Direct detection is straightforward and less time-consuming, allows immediate visualization of highly expressed targeted antigens since only one antibody is utilized. On the downside, the direct method is usually insensitive and lack the ability amplify weak signals (Chen *et al.*, 2010).

2.8.2 Indirect method

The indirect method utilizes an unlabelled primary antibody to detect the presence of the antigen of interest in the tissue, and a secondary labelled antibody is then bound to the primary antibody to give rise to signal visualization. This method is comparatively more sensitive as it amplifies weak antigen signals in the tissue through two or more labelled secondary antibody reactions with different antigenic sites on the primary antibody. In addition, it is also a greater choice because it is economy since the labelled secondary antibodies can obviously be used with many different primary antibodies to identify different antigens of interest (Chen *et al.*, 2010).

2.8.2.1 Peroxidase anti-peroxidase (PAP) method

The PAP method was introduced by Sternberger in 1979. This method is a further development of the indirect method, involving a third layer of anti-peroxidase antibody generated in the same species as the primary antibody, coupled with peroxidase to make a very stable PAP complex. This three-step approach amplified the antigenic signals with high sensitivity of about 100 to 1000 times higher since the peroxidase molecule is immunologically bound to the anti IgG, and thus retains its enzyme activity (Bratthauer, 1995). The high sensitivity of PAP method allows much higher dilution of the primary antibody, thus eliminating many of the unwanted antibodies and reducing non-specific background staining. However, the primary antibody and the PAP complexes must be from the same species, but a particular PAP complex may not be available for all cases of primary antibody and the ready-made PAP complexes from multiple species to accommodate the primary antibodies available is costly and not easy.

2.8.2.2 Avidin-biotin complex (ABC) method

ABC method consists of an unlabelled primary antibody, a biotinylated secondary antibody and a complex of avidin-biotin peroxidase. Biotin, a low molecular weight vitamin that capable to conjugated to a vast variety of biological molecules, such as antibodies and peroxidase enzyme reporter for the detection of the target antigen. Avidin, a large glycoprotein that contains four identical subunits has a high affinity for biotin; thus, a total of four biotin molecules can bind to a single avidin molecule. In the context of IHC, the avidin-biotin complexes allow more peroxidase enzyme to be located at the antigenic site and enhancing the sensitivity of the method (Bratthauer, 2010). Fortunately, the biotinylated secondary antibodies are inexpensive, readily available commercially and reactive against immunoglobulin from a wide variety of species. The strong non-covalent avidin-biotin binding and high affinity of avidin for biotin make ABC method less prone to errors related to assay condition and more sensitive than PAP method.

2.8.2.3 EnVision system

EnVision system is a two-step polymeric method in which application of the primary antibody is followed by a polymeric conjugate consisting of a large number of secondary antibodies bound directly to an activated HRP labelled dextran backbone. This unique polymeric conjugate permit binding of a large number of HRP molecules, hold up to 100 HRP molecules and 20 antibodies per backbone. The polymeric conjugate enhanced the sensitivity of EnVision system and allows the amplification of poorly expressed targeted antigen of interest. In addition, EnVision system usually allows the high dilutions of primary antibody to minimized non-specific background staining, enable it to maintain the specificity of the reaction. Furthermore, EnVision system provides some other additional advantages that in relation to its intrinsic structural characteristics, such as the lack of endogenous biotin activity and the reduction in the total number of assay steps as compared to conventional techniques (Ulrike *et al.*, 2001).

2.8.2.4 Histofine method

Histofine method is a simplified staining step uses a labelled polymer, consisting of Fab' fragment of secondary antibody conjugated to an amino acid polymer and multiple enzyme molecules such as peroxidase. This method allows no cross-reactivity of the labelled polymer with endogenous biotin and thus; minimizing the background staining and enhances the sensitivity of the staining (Kasamatsu *et al.*, 2010).

2.9 Quantitative analysis

Traditionally, IHC data are semi-quantified by pathologist visual scoring of staining such as calculation of H-Score. However, the semi-quantification method of analysis is subjective in interpretation, costly and impractical. Therefore, computer-aided analysis of digitized whole slide images, such as ImageJ, an open source Java scientific image analysis program for biomedical image analysis, is often chosen because it is time-saving, improves IHC data quality and promise to overcome these limitations of traditional IHC

analysis (Schneider *et al.*, 2012). The whole-slide imaging systems are widely available and precise in ranges of staining that appear weak to the naked eye (Rizzardi *et al.*, 2012).

T-test tests the null hypothesis if the population means estimated by two independent samples differ significantly. The three main types of t-test: an independent sample t-test that compares the means of two groups, a paired sample t-test that compares means from the same group at different times and a one sample t-test that tests the mean of a group against a known mean. Student t-test is a parametric statistical test that is used to compare the means of two independent groups with prerequisites, the assumption of normality that specifies the normal distribution of the mean of the sample group and the assumption of equal variance of the sample group (Altman & Bland, 2009).

CHAPTER 3: MATERIALS AND METHODS

3.1 Materials

3.1.1 General reagents and consumables

General laboratory chemicals and reagents were obtained from Life Technologies Inc. (Canada) and Sigma-Aldrich Co. LLC (Tokyo, Japan), unless otherwise stated. All reagents for molecular studies were from Abcam Inc. (Cambridge, MA, USA), Dako (Glostrup, Denmark), Takara Bio Inc. (Shiga, Japan), IBL Co., Ltd. (GunmaJapan) and Cosmo Bio Co., Ltd. (Tokyo, Japan). Tissue culture plastics and flasks were all purchased from Sigma-Aldrich Company Ltd or Falcon (Becton Dickinson Labware, NJ), whereas other tissue culture reagents and materials were purchased from Life Technologies Inc. (Canada) or Sigma-Aldrich Company Ltd, unless otherwise stated.

3.2 Methods

3.2.1 Monolayer cell culture

3.2.1.1 AM-1 cell line

The ameloblastoma cell line, AM-1 was kindly provided by Dr. Hidemitsu Harada from Iwate Medical University, Japan. These cells are stored in liquid nitrogen for preservation. On resuscitation of these frozen cells stored in liquid nitrogen, cell vial collected from liquid nitrogen storage was subjected to quick-thawed by rubbing gently and wiped with a tissue soaked in 70% alcohol prior to opening to decrease the risk of contamination. As soon as the cells were thawed, the whole content of the cell vial was quickly transferred to the 50 ml conical centrifuge tube (Falcon, Becton Dickinson Labware, NJ) containing 10 ml of 1X PBS (Phosphate Buffered Saline) solution (Takara Bio Inc., Shiga, Japan) to remove cryoprotectant by centrifugation for 5 minutes (mins) at 1,000 rotations per minute (rpm) at room temperature. Thereafter, the supernatant was discarded, and the pellet was resuspended in appropriate volume of fresh supplemented Keratinocyte-Serum Free Medium (K-SFM: recombinant epithelial growth factor, EGF,

bovine pituitary extract) (all from GIBCO, El Paso, TX, USA) to achieve the correct cell seeding density. An appropriate volume of cell suspension was plated on 100 mm × 20 mm cell culture dishes (Sigma-Aldrich, St. Louis, MO, USA) and incubated in the humidified incubator at 37ºC with 5% CO_2. The cells were passage by when nearly confluent and the culture medium was changed every three days. The culture medium was changed every three days until the cells were nearly confluent and passage using accutase (Innovative Cell Technologies, San Diego, CA, USA).

3.2.1.2 KUSA/A1 cell line

KUSA/A1, the mouse pre-osteoblastic cell line was the courtesy of Dr. Akihiro Umezawa from Keio University, Tokyo, Japan. Similarly, these frozen cells stored in liquid nitrogen also resuscitated as above mentioned. However, the thawed cells were transferred to the 50 ml conical centrifuge tube containing 10 ml of Minimal Essential Alpha Medium (α-MEM) (GIBCO, Burlington, ON, Canada) supplemented with 10% fetal bovine serum and 1% antibiotic-antimycotic (GIBCO, USA) and centrifuged for 5 mins at 1,000 rpm at room temperature to pellet cells. Thereafter, the cell pellet was resuspended in appropriate volume of fresh α-MEM containing 10% fetal bovine serum and 1% antibiotic-antimycotic to achieve the correct cell seeding density. Following that, an appropriate volume of cell suspension was plated on 100 mm × 20 mm cell culture dishes (Sigma-Aldrich, St. Louis, MO, USA) and incubated in the humidified incubator at 37ºC with 5% CO_2. The culture medium was changed every 3 days until the cells were nearly confluent and passage using 0.05% trypsin-ethylenediaminetetraacetic acid (EDTA) (GIBCO, Canada).

3.2.1.3 ST2 cell line

ST2 cells, a clone of stromal cells derived from mouse bone marrow was obtained from RIKEN BRC (Tsukuba, Japan) and stored in liquid nitrogen for preservation. These frozen ST2 cells were resuscitated by quick-thaw and then transferred to 50 ml conical

centrifuge tube containing 10 ml of α-MEM supplemented with 10% fetal bovine serum and 1% antibiotic-antimycotic for centrifugation at 1,000 rpm for 5 mins at room temperature. Following that, the cell pellet was resuspended in appropriate volume of fresh α-MEM containing 10% fetal bovine serum and 1% antibiotic-antimycotic to achieve the correct cell seeding density. An appropriate volume of the cell suspension was plated on 100 mm × 20 mm cell culture dishes and incubated in humidified incubator at 37ºC with 5% CO_2. The cell culture medium was changed every 3 days until the cells were nearly confluent and passage using 0.05% trypsin-EDTA.

3.2.1.4 MC3T3-E1 cell line

MC3T3-E1, the mouse osteoblastic cell line was purchased from RIKEN BRC (Tsukuba, Japan) and was stored in liquid nitrogen. Similarly, these cryopreserved cells were resuscitated by quick-thaw and then transferred to 50 ml conical centrifuge tube containing 10 ml of α-MEM supplemented with 10% fetal bovine serum and 1% antibiotic-antimycotic for centrifugation for 5 mins at 1,000 rpm at room temperature. The cell pellet obtained was resuspended in appropriate volume of fresh α-MEM with 10% fetal bovine serum and 1% antibiotic-antimycotic to achieve the correct cell seeding density. Thereafter, an appropriate volume of the cell suspension was plated on 100 mm × 20 mm cell culture dishes and incubated in humidified incubator at 37ºC with 5% CO_2. The cell culture medium was changed every 3 days until the cells were nearly confluent and passage using 0.05% trypsin-EDTA

3.2.1.5 Cell culture maintenance

Culture medium was removed from cell culture dish with cultured cells of nearly 80% confluency. Adherent cells attached on culture dish were washed in 10 ml of 1X PBS solution and l ml of 0.05% trypsin/EDTA or accutase (AM-1 only) was added for 5 mins (or 3 mins for AM-1) at room temperature. Cell detachment is promoted by gently tapping on the sides of the culture dish and was monitored under a light microscopy. Following

that, the activity of the trypsin/EDTA was neutralized by addition of 10% FBS-containing medium at a volume of 4× the volume of trypsin/EDTA added to terminate their action on cells. On the other hand, the detached AM-1 cells are resuspended in 10 ml of 1X PBS solution and then the cell suspension in the conical centrifuge tube was centrifuged for 5 mins at 1,000 rpm at room temperature. The supernatant was discarded and the cell pellet was resuspended in supplemented K-SFM. Cells were then either reseeded such that the split ratio is 1:5 in a number of new culture dish for monolayer culture or in 24- or 96-well culture plate to establish the 3D *in vitro* cell culture model.

3.2.1.6 Cell counting

A known volume of growth medium or PBS (AM-1 only) was added to the cell suspensions and 10µl of the diluted cell suspension was transferred to each counting chamber of the haemocytometer. The cell counting was performed under ×100 magnification, aided by a hand tally counter. Four individual corner squares within the haemocytometer were counted. The total cell number in the suspension was calculated using the formula as shown in the table below:

Cell number per cell suspension volume = Mean cell count × total cell suspension volume (ml) × 10^4

3.2.2 Cell culture in 3D

3.2.2.1 AM-1s in Matrigel matrix

Matrigel (BD Biosciences, Bedford, MA) was defrosted on ice and diluted (1:1) in α-MEM supplemented with 10% FBS, 0.1% of 50 µg/ml ascorbic acid and 0.5% of 1M β-glycerophosphate (all from Sigma-Aldrich, Dorset, England, UK) prior to the addition of AM-1 cells. The tube was placed on ice, and the cell pellet of AM-1 cells were re-suspended in the prepared polymerizing Matrigel at density of 4.0×10^6 cells/ml. The cells are then gently mixed with the Matrigel solution to evenly dispersed the cells

throughout the cold homogenised Matrigel mixture and for a total of 1.4 ml out of which 100 µl was added into the wells of a 96-well culture plate with the layout as shown in Figure 3.1. The plate was incubated for 90 mins at 37ºC after which 100 µl of mineralization medium (α-MEM containing 0.1% of 50 µg/ml ascorbic acid and 0.5% of 1M β-glycerophosphate) was gently added to the top of each polymerized gel and placed back in the incubator. The mineralization medium was changed routinely every three days.

3.2.2.2 KUSA/A1s in Matrigel matrix

The Matrigel method for KUSA/A1 cells was as described (Section 3.2.1.1) for AM-1 cells.

3.2.2.3 AM-1s in 3D collagen type I gels

Atelocollagen, Eagle's MEM (Koken, Tokyo, Japan) was defrosted overnight in a 4°C refrigerator a day before use. To set up cells in 1.0 mg/ml collagen gels, equal volumes of α-MEM supplemented with 10% FBS, 0.1% of 50 µg/ml ascorbic acid and 0.5% of 1M β-glycerophosphate were mixed on ice prior to the addition of AM-1 (4.0×10^6 and 8.0×10^5 cells/ml gel in 96-well and 24-well plate respectively with layout as shown in Figure 3.1) cells. The cells are then gently mixed with the collagen solution to evenly dispersed the cells throughout the cold homogenised collagen mixture prior to the addition of a 100 µl aliquot of the cold collagen mixture into the wells of a 96-well culture plate (or 0.5 ml/well in a 24-well plate). Both 96- and 24-well culture plates were placed in the humidified incubator at 37ºC with 5% CO_2. 100 µl of mineralization medium (Section 3.2.2.1) was gently added to the top of each gel (or 1 ml in the 24-well plate) after the polymerization of the gel (nearly 90 mins). The culture plates were placed back in the 37ºC incubator and the medium was changed routinely every three days.

3.2.2.4 KUSA/A1s in 3D collagen type I gels

The collagen gel method for KUSA/A1 cells was as described (Section 3.2.2.3) for AM-1 cells.

3.2.2.5 ST2s in 3D collagen type I gels

The collagen gel method for ST2 cells was as described (Section 3.2.2.3) for AM-1 cells, but with the following modifications:

1. ST2s were set up at a concentration of 3.3 x 10^5 cells/ml gel for plating in a 24-well culture plate.
2. 0.75 ml of the collagen mixture was added to each well in the plate prior to the addition of 1.5 ml of mineralization medium.

3.2.2.6 MC3T3-E1 in 3D collagen type I gels

The collagen gel method for MC3T3-E1 cells was as described (Section 3.2.2.3) for AM-1 cells, but MC3T3-E1s were only set up at a concentration of 8.0 × 10^5 cells/ml gel for plating in a 24-well culture plate.

3.2.3 *In vitro* 3D tumour-fibroblast co-culture

3.2.3.1 Co-culture of AM-1 and KUSA/A1 in Matrigel matrix

The Matrigel method for co-culture of AM-1 and KUSA/A1 cells was as described (Section 3.2.1.1) for AM-1 cells, by addition of total cell concentration of 8.0 × 10^6 and 4.0 × 10^6 cells/ml gel in each well of a 96-well culture plate at 1:1 ratio of AM-1 to KUSA/A1 cells (Figure 3.2).

3.2.3.2 Co-culture of AM-1 and KUSA/A1 in collagen matrix

The collagen gel method for co-culture of AM-1 and KUSA/A1 cells was as described (Section 3.2.2.3) for AM-1 cells, by addition of total cell concentration of 8.0 × 10^6 and 4.0 × 10^6 cells/ml gel in each well of a 96-well culture plate (or 1.6 × 10^6 and 8.0 × 10^5

cells/ml gel in each well of a 24-well culture plate) at 1:1 ratio of AM-1 to KUSA/A1 cells.

3.2.3.3 Co-culture of AM-1 and ST2 in collagen matrix

The collagen gel method for co-culture of AM-1 and ST2 cells was as described (Section 3.2.2.3) for AM-1 cells, by addition of total cell concentration of 8.0×10^6 and 4.0×10^6 cells/ml gel in each well of a 96-well culture plate (or 6.6×10^5 and 3.3×10^5 cells/ml gel in each well of a 24-well culture plate) at 1:1 ratio of AM-1 to ST2 cells.

3.2.3.4 Co-culture of AM-1 and MC3T3-E1 in collagen matrix

The collagen gel method for co-culture of AM-1 and MC3T3-E1 cells was as described (Section 3.2.2.3) for AM-1 cells, by the addition of total cell concentration of 1.6×10^6 and 8.0×10^5 cells/ml gel in each well of a 24-well culture plate at 1:1 ratio of AM-1 to MC3T3-E1 cells.

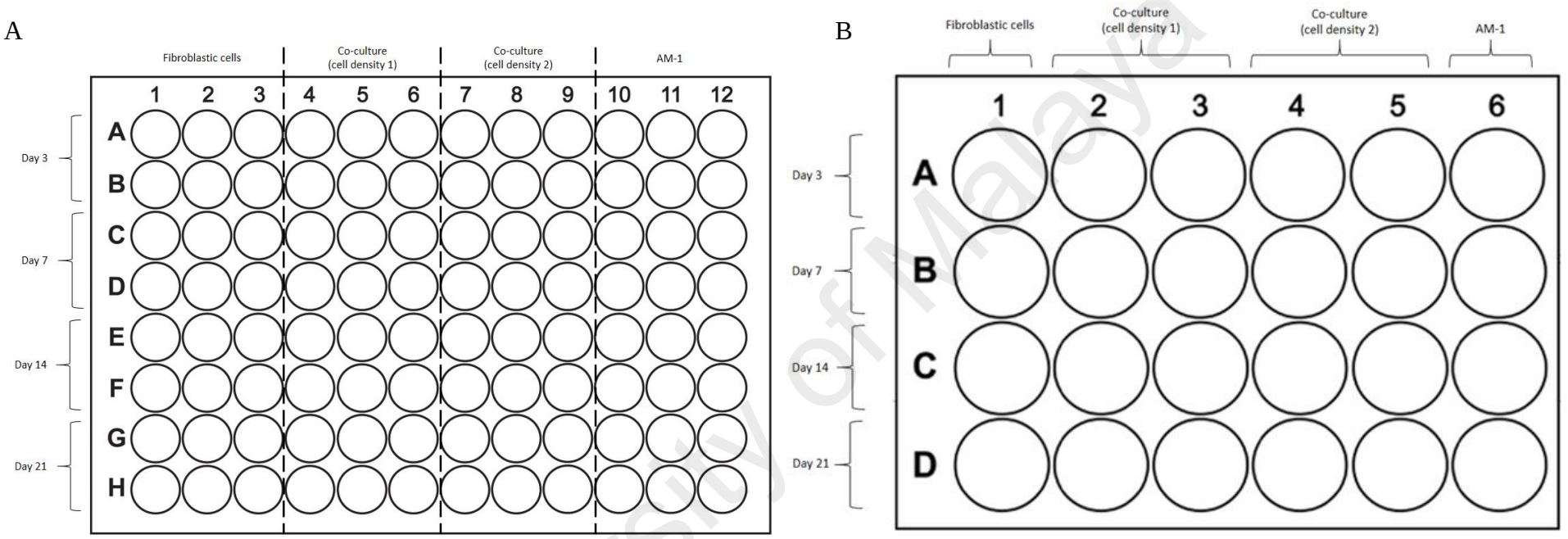

Figure 3.1: Layout of 3D cell cultures.

The monocultures and AM co-cultures was seeded into a (A) 96-well culture plate and (B) 24-well culture plate bathed in mineralization medium for the development of scaffold-based 3D *in vitro* cell monoculture constructs and AM co-culture constructs.

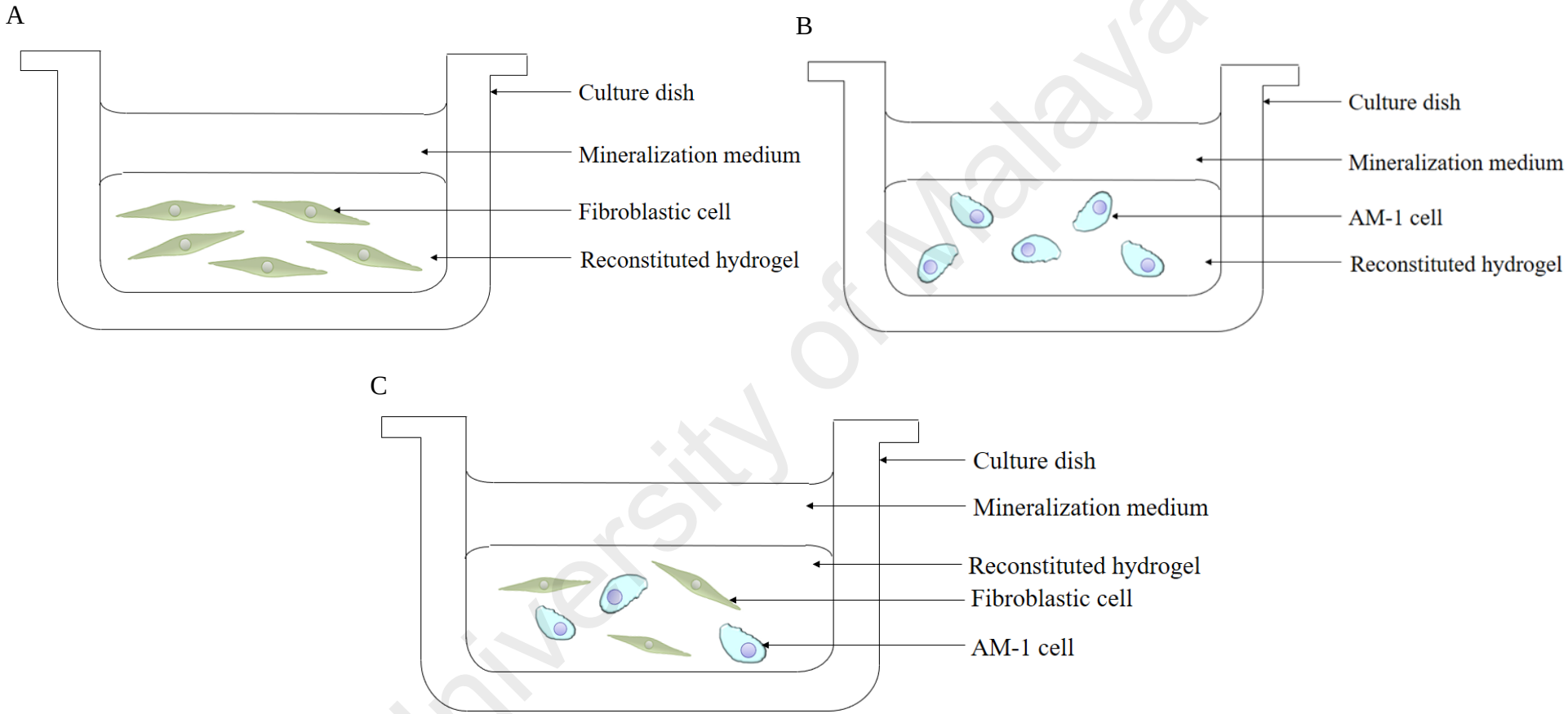

Figure 3.2: *In vitro* 3D cell cultures.

The establishment of (A) fibroblastic cell monoculture construct, (B) ameloblastoma cell monoculture and (C) ameloblastoma cell/fibroblast co-culture construct, seeded in reconstituted hydrogel matrices that overlaid with mineralization medium.

3.2.4 Histological analysis of type I collagen gels and/or Matrigel

3.2.4.1 Fixation of gels

Cell culture in 3D was maintained in mineralization medium (Section 3.2.2.1) and outputs analysed after 3, 7, 14 and 21 days. Initially, medium was discarded prior to the fixation of gels. Then, the whole gel was removed from the culture plate by gently detached from the walls and bottom of the wells by passing a syringe needle around the perimeter of the wells. Gels harvested from monocultures of single cell types (AM-1, n=3; KUSA-A1, n=3; ST2, n=3; MTCT3-E1, n=3) and co-culture constructs (AM-1/KUSA-A1, n=12; AM-1/ST2, n=12; AM-1/MTCT3-E1, n=12) were placed in individual 1.5 ml (or 5 ml) tubes and fixed in 1 ml (or 2.5 ml) of 10% formalin depending on the size of the gel overnight at room temperature. The 10% formalin was removed, and the gel was placed in a separate embedding cassette using forceps and marker with mercurochrome (Kozakai Pharmaceutical, Tokyo, Japan) before washed in 70% ethanol in shaker overnight.

3.2.4.2 Tissue processing of gels

The whole washed gels in the embedding cassette were processed overnight in the tissue processor CT-Pro20 (Genostaff Co., Ltd, Tokyo, Japan) which involved them being rinsed sequentially in formalin, ethanol (70%; 90%; 100%), xylene and paraffin.

3.2.4.3 Embedding of gels in paraffin wax

The individual processed gels were embedded in paraffin wax using the Tissue-Tek TEC 5 paraffin embedder (Sakura Finetek Japan Co., Ltd, Tokyo, Japan). For this process, a little of the melted wax was placed in a stainless-steel base mould and the whole harvested gel was carefully removed from the cassette using forceps, placed flat and cross-sectionally in the mould, topped with more melted paraffin wax and finally with cassette left on the top of the mould. It was then placed on the cold plate and leave until

the wax is solidified. The embedded sample was then popped out of the mould prior to sectioning.

3.2.4.4 Sectioning of gels

For all specimens from monocultures (AM-1, n=3; KUSA-A1, n=3; ST2, n=3; MTCT3-E1, n=3) and two specimens per time point from co-culture constructs (AM-1/KUSA-A1, n=6; AM-1/ST2, n=6; AM-1/MTCT3-E1, n=6), 10 µm thick paraffin sections were cut using the large sliding microtome type TU-213 (Yamato Kohki Industrial Co., Ltd, Saitama, Japan) with the aid of slide warmer PS-51 (Sakura Finetek Japan Co., Ltd, Tokyo, Japan) and mounted on individual Matsunami adhesive slide (MAS)-coated slides (Matsunami, Tokyo, Japan). All slides were placed in a 60ºC incubator for 4 – 5 hours on slide racks tilted at a 45º angle prior to staining or storage for later use.

3.2.4.5 H&E staining of gels

Refer to Appendix A.

3.2.4.6 Alizarin Red S staining for the detection of calcified nodules

Refer to Appendix B.

3.2.4.7 IHC staining of gels

IHC staining was undertaken on individual sections using antibodies specific for cytokeratin, vimentin, osteocalcin (OC), osteopontin (OPN), bone sialoprotein (BSP), RANK, RANKL and OPG (Appendix C). All IHC analysis was undertaken at the same time for each protein being tested for all experimental representatives. Immunostaining was scored as negative (-) when none of the cells were positively stained in the cytoplasm, membrane or nucleus; mild (+), <25% cells positive; moderate (++), 25-50% cells positive; and strong (+++), >50% cells positive.

3.2.4.8 IHC staining protocol

Refer to Appendix D.

3.2.5 Confocal microscopy of 3D type I collagen gels

3.2.5.1 Fixation of collagen gels

One representative specimen was selected from d 3 co-culture constructs (AM-1/KUSA-A1, n=1) seeded collagen gel in 24-well culture plate for confocal microscopy and fixed as described (Section 3.2.3.1). The whole gel was prepared for specific immunofluorescent staining for pan-cytokeratin, vimentin and 4', 6-diamidino-2-phenylindole (DAPI) labelling of nuclei.

3.2.5.2 Double-label immunofluorescent staining of cytokeratin and vimentin

Refer to Appendix E.

3.2.6 Statistical analysis of data

At each time point, the number of cytokeratin- and vimentin-positively stained cells was counted at 200x magnification from the selection regions in the mono- and co-culture constructs. In each section, quantification was performed using ImageJ, a Java-based image processing program developed at the National Institutes of Health for Windows. Relative cell number in both configurations was calculated from 5 randomly selected defined regions of interest in each case. Results were expressed as means $\pm$ standard deviation (SD).

All experiments were conducted in duplicates with same passages of the cell lines. Statistical analysis was performed using IBM SPSS software version 18.1 (IBM, Armonk, NY, USA) for Windows. Data on cell count were presented as means $\pm$ SD. Comparisons between mean variables of two groups were performed using the Student *t* test. Level of significance was set as $p<0.05$.

CHAPTER 4: RESULTS

4.1 Optimum culture conditions selection

4.1.1 Effect of hydrogel used on morphology of cultured cells

In hydrogel preparation, the feasibility of the reconstituted hydrogel prepared by serial dilution of atelocollagen or Matrigel was evaluated. Previous studies have shown that the concentration of reconstituted hydrogels was inversely proportional to their rigidity. Meanwhile, the concentration of hydrogels reported to determines the density of the matrix and pore size, hence influences the navigation of culture cells through the gel. The use of collagen gels instead of Matrigel was best for our model due to the physiologically relevant cellular structure of cells cultured on collagen gel (Figure 4.1). Taken together, collagen diluted with equal volume of α-MEM is the key characteristics in synthesis of hydrogel matrices for three-dimensional culture of cells as developed in the present study.

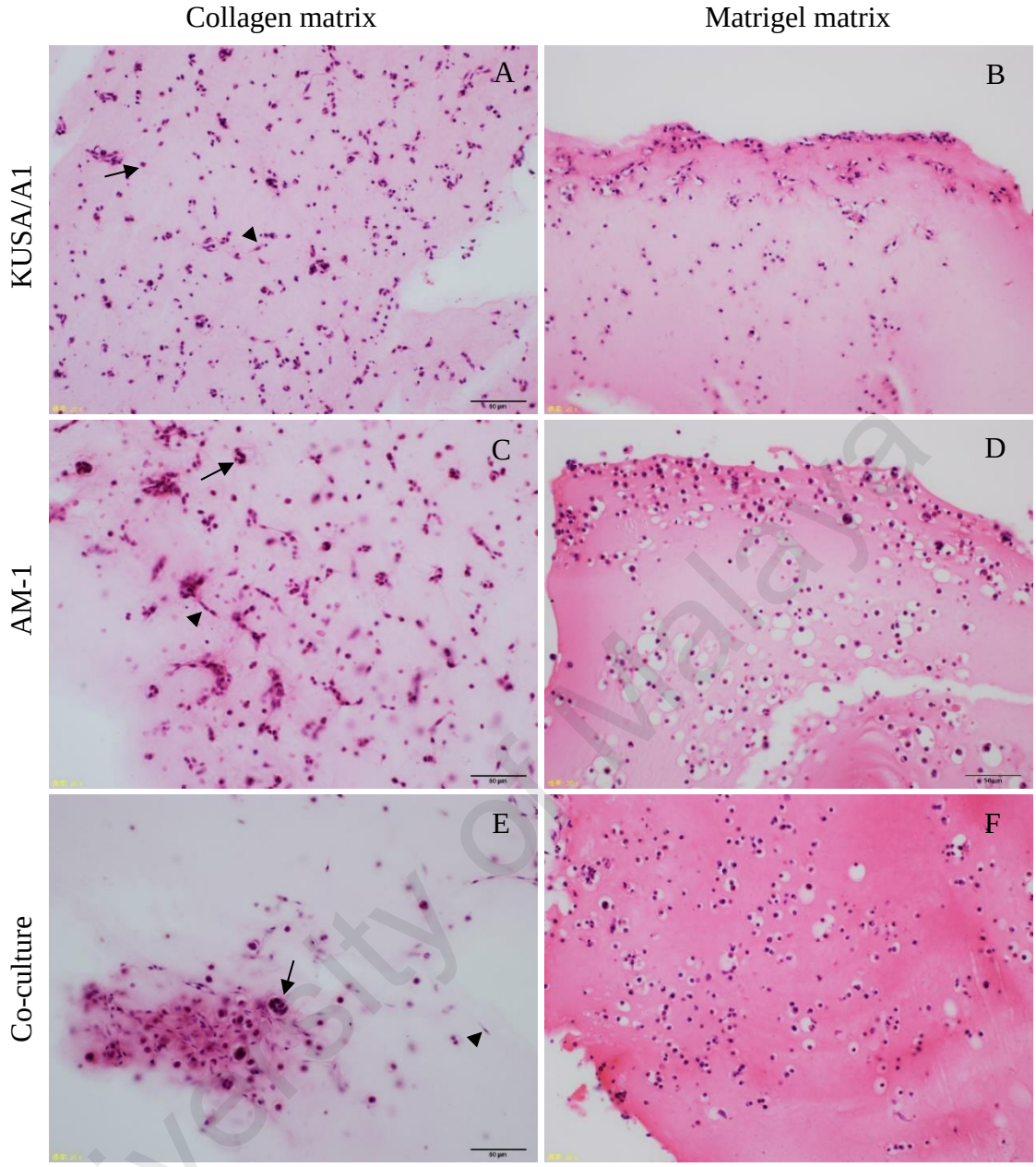

Figure 4.1: Characterization of *in vitro* 3D cell culture constructs in hydrogels.

H&E stained histologic sections of KUSA/A1 and AM-1 cell monocultures and co-cultures in collagen and Matrigel matrices at day 7. (A) KUSA/A1 and (C) AM-1 cell monocultures in collagen matrices exhibit spindle-shape (arrow-heads) and round-shape (arrows) morphology respectively that not visible in (B) KUSA/A1 and (D) AM-1 cell monocultures in Matrigel matrices. Both morphologies as observed in monocultures can be seen in (E) co-cultures cultured in collagen matrices but not distinguishable in (F) co-cultures cultured in Matrigel-based matrices.

4.1.2 Effect of exposed surface area of culture substrate on cell behaviour and morphology

To evaluate the effect of exposed surface area of culture substrate to culture medium on cell behaviour and morphology in 3D, cells were entrapped within collagen matrices at the same concentration in 96-well culture plate (32.0 mm^2) and 24-well culture plate (2.0 cm^2). Significant differences in the appearance of KUSA/A1 cells cultured either on 24-well or 96-well culture plate were revealed through H&E staining (Figure 4.2). KUSA/A1 cell monocultures grown on 24-well culture plate for 3 days formed elongated spindle-shaped structures and started to cluster. After 7 days, KUSA/A1 cells cultured on 24-well plate clustered into colonies of closely packed cells and from aggregates. The opaque regions within the matrices of KUSA/A1 monocultures grown for 14 days on 24-well plate represent the onset of mineralization. KUSA/A1 cells grown on 96-well culture plate were generally disorganized in appearance and scattered throughout the collagen matrices and formed spindle-shaped structures after 14 days. Furthermore, co-cultures grown either on 24-well or 96-well culture plate were also examined (Figure 4.3). In general, co-cultures grown on 24-well culture plate showed the close association between the adjacent cells and indicative of the establishment of an intercellular network between two cell populations with distinctive morphology. In contrast, such interaction between adjacent cells was not seen in co-cultures grown on 96-well culture plate.

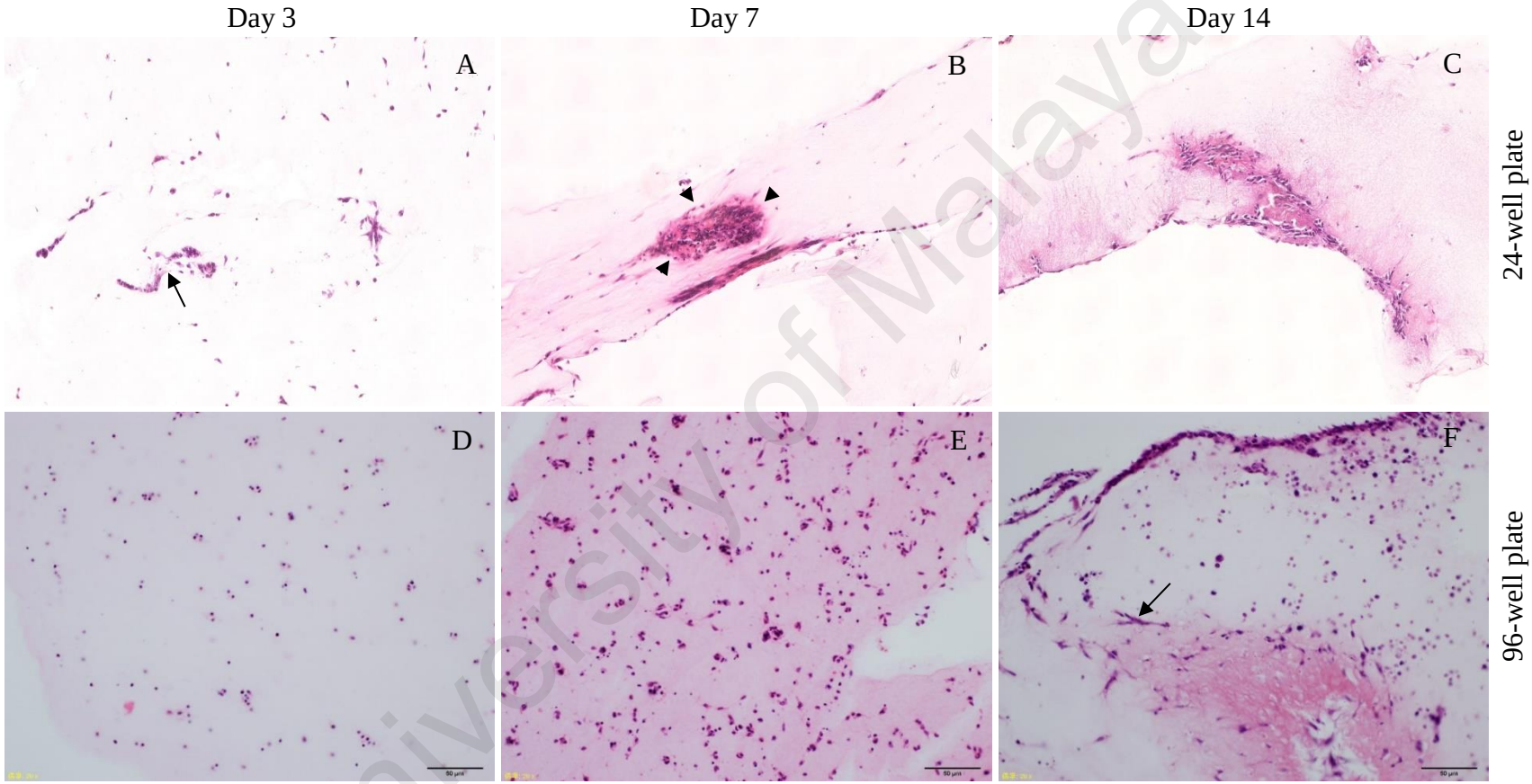

Figure 4.2: Exposed surface area of culture substrate on morphology and structure of KUSA/A1 cells in 3D monoculture construct.

H&E stained histologic sections of KUSA/A1 cell monocultures in collagen matrices cultured in 24-well plate (A-C) and 96-well plate (D-F) at day 3, 7 and 14. KUSA/A1 cells grown for 3 days in 24-well plate (larger surface area) were generally spindle-shaped (arrow) in appearance (A), started to cluster and form aggregates (arrow-heads) after 7 days (B) and shown characteristics of matrix mineralization (M) after 14 days (C). KUSA/A1 cells grown in 96-well plate (smaller surface area) scattered throughout the matrices for 7 days (D, E) and started to appear spindle-shaped (arrow) in morphology at day 14 (F).

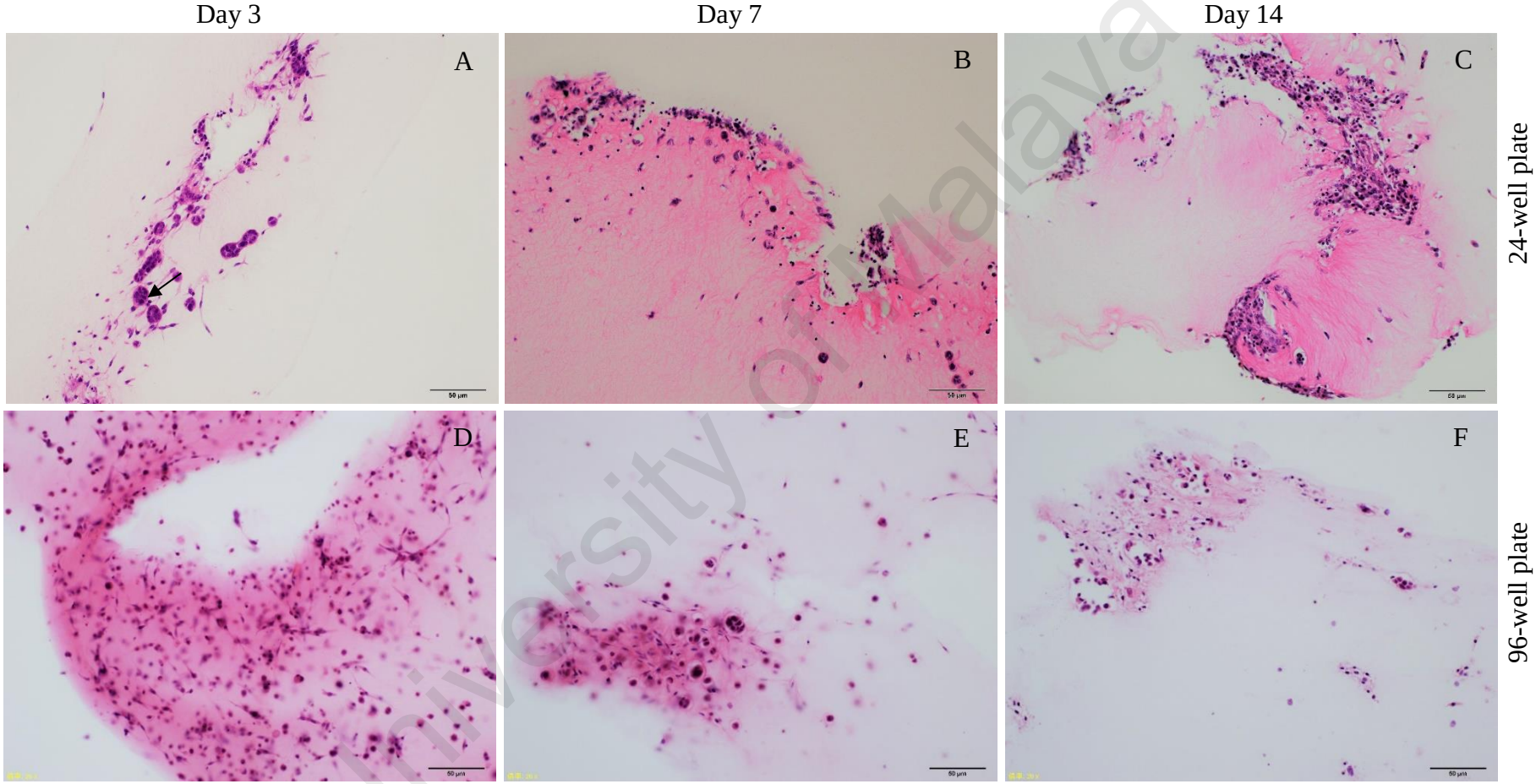

Figure 4.3: Exposed surface area of culture substrate on cell morphology and structure of 3D AM-1/KUSA-A1 co-culture construct.

H&E stained histologic sections of co-cultures of KUSA/A1 and AM-1 cells in collagen matrices cultured in 24-well plate (A-C) and 96-well plate (D-F) at day 3, 7 and 14. Co-cultures grown for 3 days in 24-well plate were generally indicated a greater interaction between adjacent cells (arrow) growing on the scaffold (A), proliferated and gradually maximise their surface area (B, C). Co-cultures grown in 96-well plate scattered throughout the matrices at day 3 (D) and day 7 (E) but reduced in cell number after 14 days (F).

4.1.3 Optimal seeding density for co-cultures in 3D collagen matrices

Co-cultures of KUSA/A1 and AM-1 cells were entrapped within collagen matrices on 24-well culture plate in a 1:1 ratio at the total seeding density of 4.0×10^6 cells/mL and 8.0×10^6 cell/mL. Cell behaviour and morphology were evaluated at days 3, 7 and 14 by H&E staining (Figure 4.4). Two distinctive morphology of cells was observed for the lower cell density. Cell population with round-shaped and nest-like in appearance is surrounded by another population of cells with elongated and spindle-shaped in appearance after 3 days of incubation. For the higher cell density, no distinguishable cell morphology was observed after 3 days of culture, as well as the intercellular network between two cell populations. Along the time of culture, massive cell proliferation was observed for both seeding densities tested. As shown in Figure 4.4, the better cellular interaction between two distinct cell populations observed in lower density co-cultures may have resulted from a more favourable culture condition, and the eventual efficient intercellular signalling, more prone to occur under this seeding density.

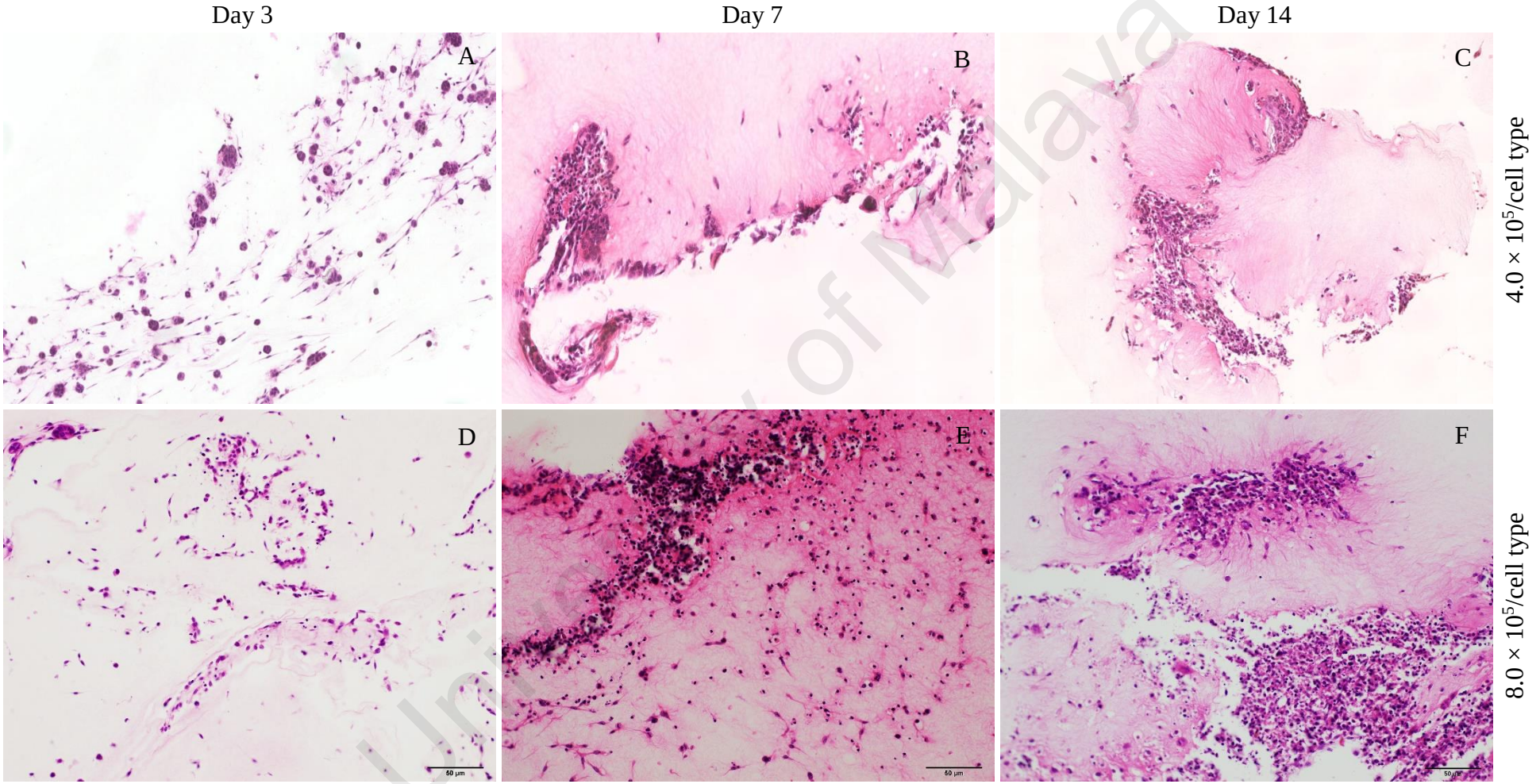

Figure 4.4: Seeding density on cell morphology and structure in 3D co-culture construct.

H&E stained histologic sections of co-cultures comprise of KUSA/A1 and AM-1 cells grown in collagen matrices on 24-well culture plate at low cell density (A-C) or high cell density (D-F) at day 3, 7 and 14.

4.2 Characterization of cell cultures in 3D collagen-fiber network model

4.2.1 Morphology and structure of monocultures in 3D

After specific time point in culture, monocultures of the fibroblastic cell, as well as ameloblastoma tumour cells were harvested, fixed, dehydrated and embedded in paraffin prior to H&E staining. Figure 4.5 represents the H&E stained histologic sections of 3D *in vitro* monocultures of the fibroblastic cell: KUSA/A1 (A-C), MC3T3-E1 (D-F), ST2 (G-I) and ameloblastoma cell, AM-1 (J-L) at day 3, 7 and 14. As presented, flat and elongated appearance is common for all fibroblastic cell lines. However, a distinguishable difference in behavioural characteristics was observed amongst 3D *in vitro* monocultures of fibroblastic cell lines entrapped in collagen matrices. KUSA/A1 and MC3T3-E1 fibroblastic cells monoculture grown in 3D collagen matrices for 3 days generally formed round or flat, elongated shapes structure and arranged in a dissociated manner. Importantly, it is observed that cells started to cluster into colonies of closed packed cells within the collagen matrices, resembling small multicellular aggregates. On the other hand, ST2 cells exhibited flat and elongated appearance as the two other fibroblastic cells and cells were scattered throughout the collagen matrices. In contrast, cell aggregates were not seen in monocultures of ST2 cell grown in collagen matrices throughout the culture period. Furthermore, with increased culture duration (7 to 14 days), cell aggregates as observed in the KUSA/A1 cell monocultures were developed into a larger size, but cell aggregated in MC3T3-E1 cell monocultures were relatively dispersed and scattered throughout the collagen matrices. KUSA/A1 cells in 3D culture showed excessive proliferation in comparison to ST2 and MC3T3-E1 cells. Cells of line AM-1 in collagen matrices were scattered in a dissociated manner with round shapes and without observed cell aggregates formation throughout the culture period. In addition, no visible evidence of extensive cellular proliferation was seen in AM-1 cell monoculture. Overall,

regions of fibroblastic and AM-1 cell monocultures grown for 21 days appeared unhealthy (data not shown).

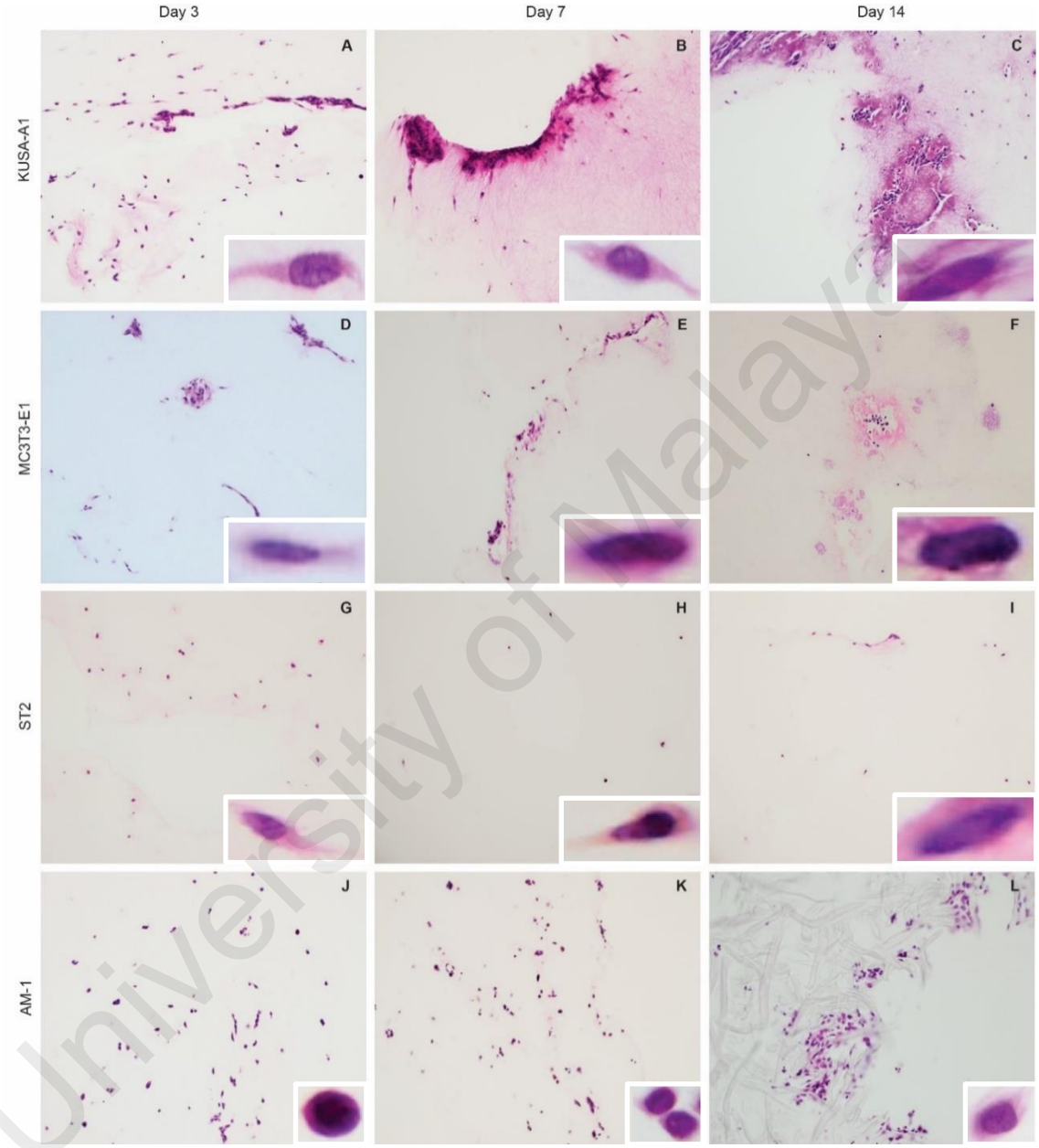

Figure 4.5: Characterization of monocultures in 3D model.

H&E stained histologic sections of monoculture of fibroblastic cells: KUSA/A1 (A-C), MC3T3-E1 (D-F) and ST2 (G-I), as well as the monoculture of AM-1 cells (J-L) in collagen matrices cultured on 24-well plate at day 3, 7 and 14.

4.2.2 Morphology and structure of *in vitro* 3D co-culture construct

We compared the morphological differences in co-cultured cells grown in different 3D *in vitro* tumour-fibroblast co-culture model comprises of AM-1 and different fibroblastic cells: KUSA/A1, MC3T3-E1 and ST2. As presented in Figure 4.6, AM-1 and KUSA/A1 cell co-culture grown 3 days in collagen matrices were generally heterogeneous in appearance and consisted of two populations of cell with distinct morphologies: one population interconnected to another population that found organized into colonies of closely packed cells resembling multicellular aggregates through cytoplasmic processes extending from the cell body, forming an extensive interconnected intercellular network. However, such distinguishable morphologies as observed in AM-1 and KUSA/A1 cell co-cultures were not seen in both AM-1 and MC3T3-E1 cell co-cultures and AM-1 and ST2 cell co-cultures throughout the culture period.

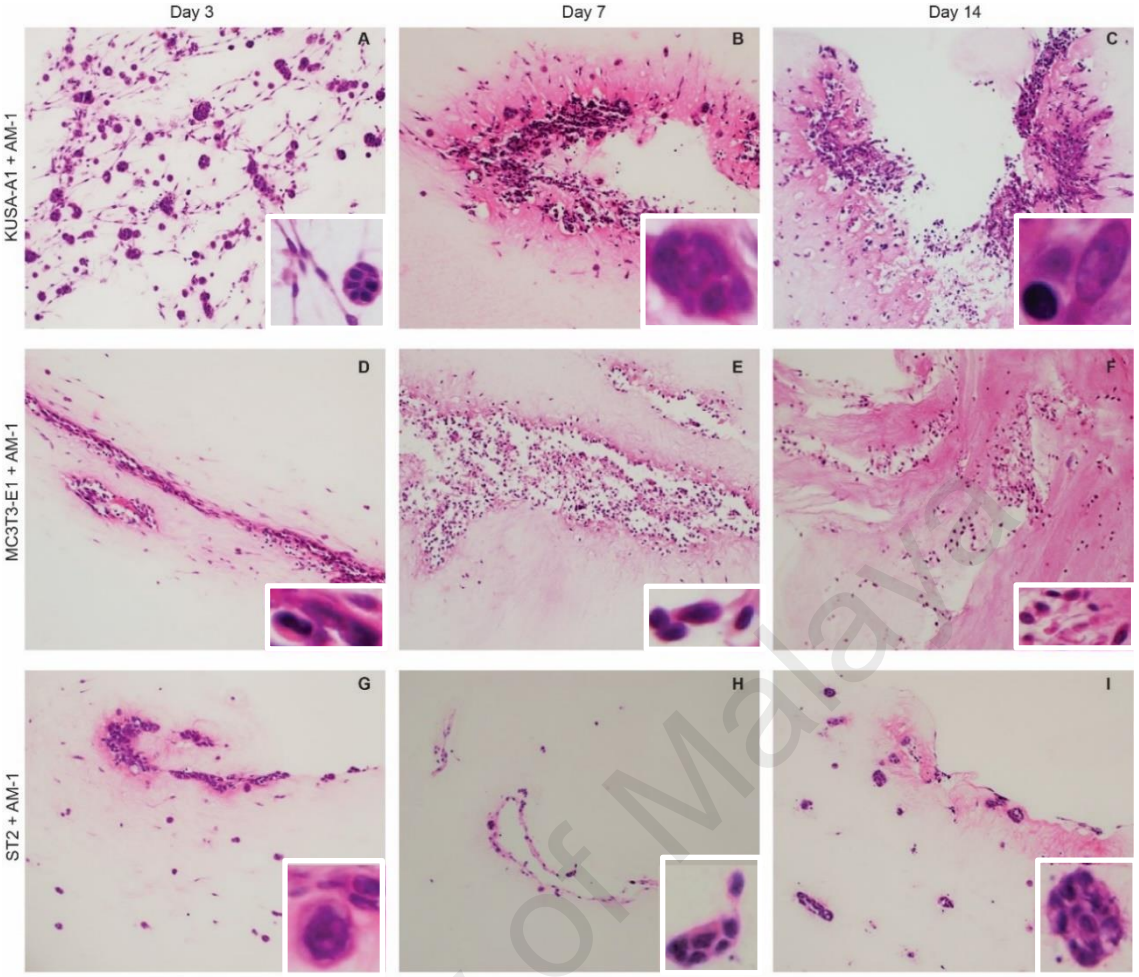

Figure 4.6: Characterization of AM co-cultures in 3D model.

H&E stained histologic sections of 3D *in vitro* tumour-fibroblast co-culture of AM-1 and different fibroblastic cells, KUSA-A1 (A-C), MC3T3-E1 (D-F) and ST2 (G-I) in collagen matrices at different time points – day 3, 7 and 14.

4.3 Validation of cell-cell interaction in 3D *in vitro* AM co-cultures

We compared the morphological differences in cells grown in the 3D *in vitro* tumour-osteoblast co-culture construct and monoculture construct through H&E staining (Figure 4.7). Nest-like structures are seen in AM co-culture comprises of AM-1 and KUSA/A1 cells, but not visible in AM-1 cell monocultures. Further, KUSA/A1 cell monoculture construct shown a visible extracellular matrix but not in the co-culture construct under the same culture condition.

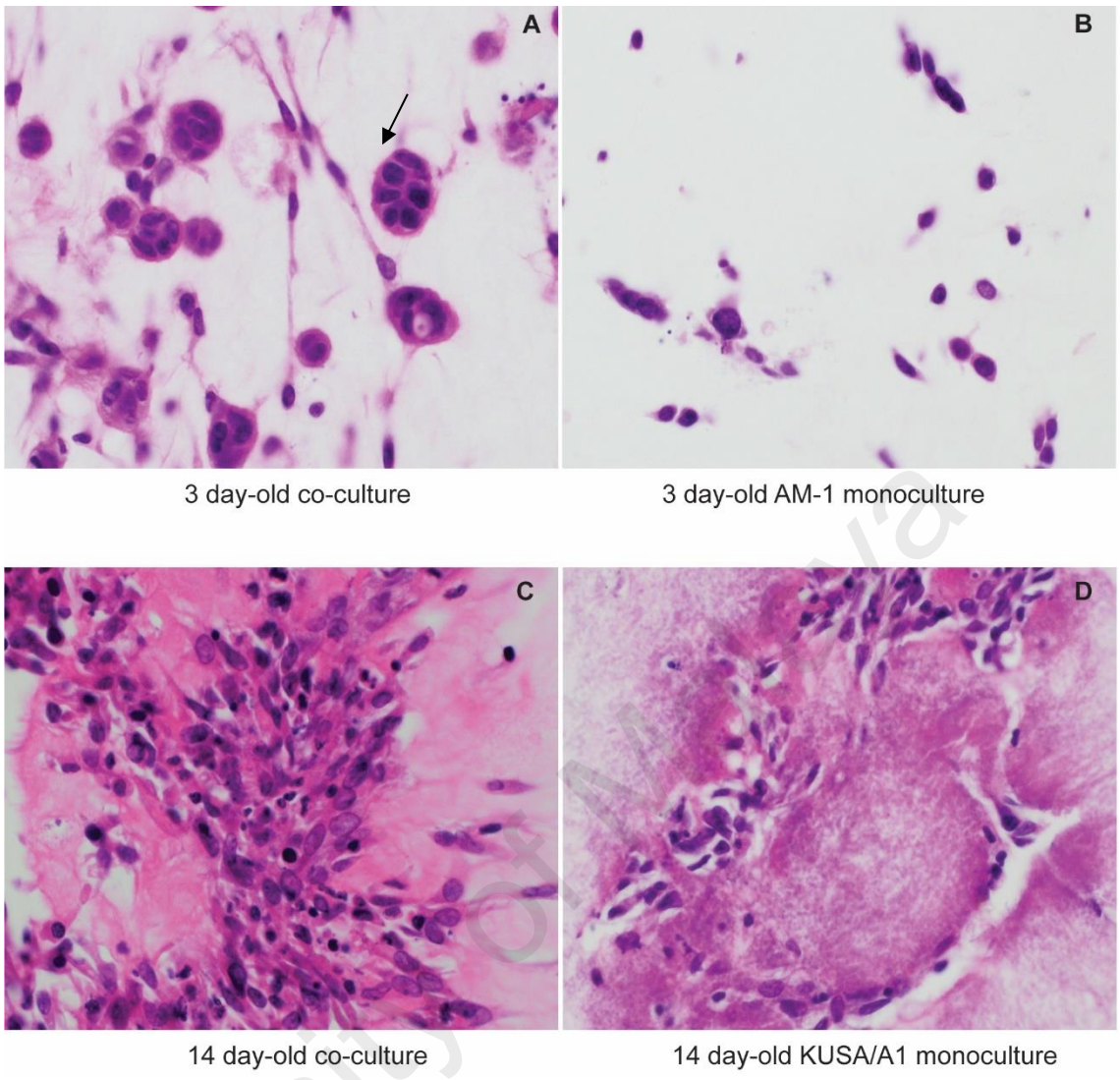

Figure 4.7: Validation of cell-cell interaction on cell count and mineralization characteristic of monocultures against AM co-cultures.

Comparison of the microscopic image of the 3D *in vitro* AM co-culture and AM-1 monoculture at day 3 (A&B) and the 3D *in vitro* AM co-culture and KUSA/A1 monoculture at day 14 (C&D). At day 3, AM-1 cells in the 3D *in vitro* AM co-culture form cohesive clusters (arrow). Extracellular matrix is not visible in AM co-culture grew for 14 days, in contrast to KUSA/A1 monoculture that shows extracellular matrix (M) after 14 days.

4.3.1 Extracellular matrix mineralization

The extracellular matrix mineralization of 3D *in vitro* osteoblastic cell and AM-1 cell monocultures incubated with mineralization medium was examined. After 14 days in culture, collagen matrix of KUSA/A1 cell monoculture shown evidence of mineralization as depicted by the intense Alizarin Red S staining (Figure 4.8H). However, the collagen matrix of AM-1 cell monocultures and osteoblastic cell monocultures of other cell lines,

MC3T3-E1 and ST2 has no evidence of mineralization as no visible Alizarin Red S staining was observed (data no shown) over the culture period.

On the other hand, the collagen gel cultures of KUSA/A1 and AM-1 cell co-culture incubated with mineralization medium for 14 days shown evidence of reduced Alizarin Red S staining (Figure 4.8G) as compared to the KUSA/A1 cell monoculture. Further, the collagen matrix of co-culture of AM-1 cells with other osteoblastic cell lines (MC3T3-E1 and ST2) also has no evidence of mineralization as no observable Alizarin Red S staining (data no shown).

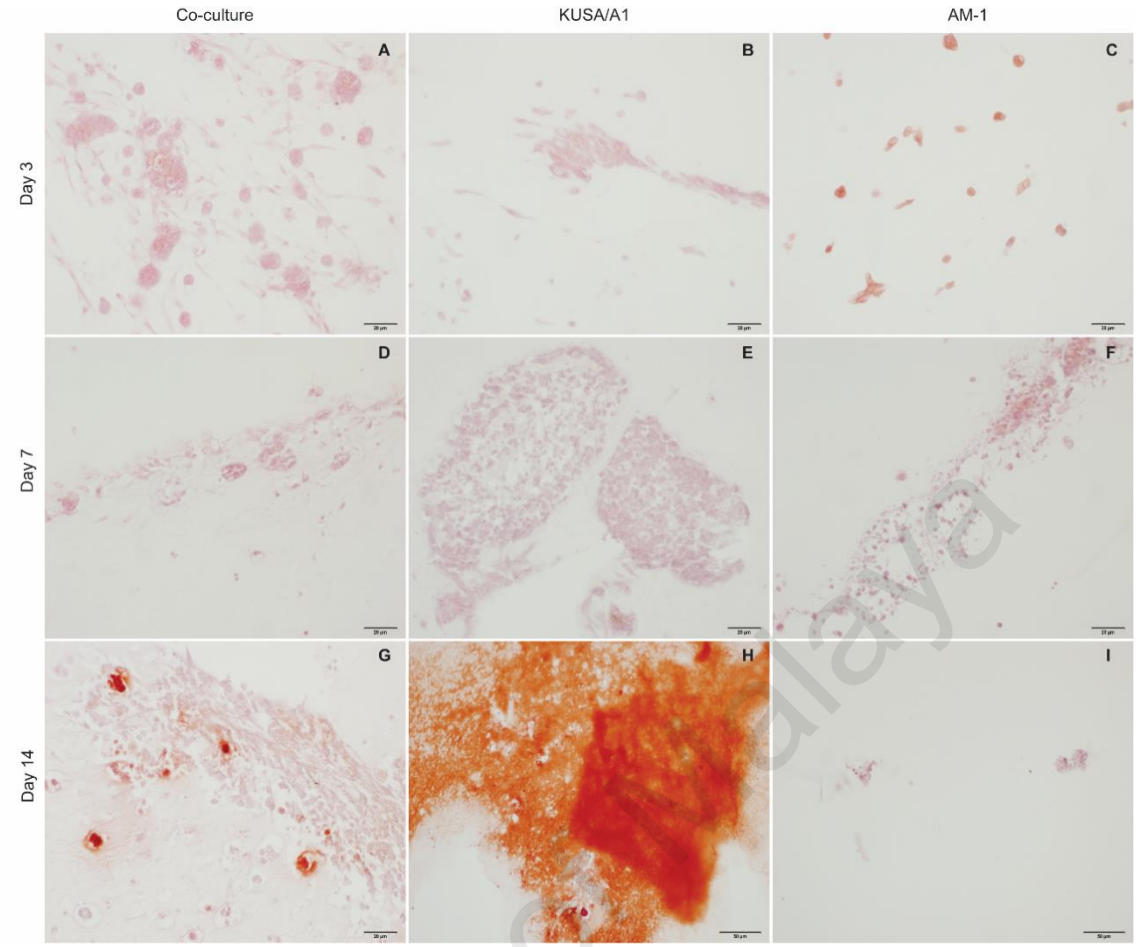

Figure 4.8: Mineralization characteristics of mono- and co-culture cells.

Extracellular matrix mineralization: 3D *in vitro* co-culture and 3D *in vitro* KUSA/A1 and AM-1 cell monoculture entrapped in the collagen matrices incubated with mineralization medium. Extracellular matrix mineralization in 3D *in vitro* cultures was visualized by Alizarin Red S staining. No visible staining was seen in the cultures incubated for one week (A-F). Collagen matrix of KUSA/A1 and AM-1 cells co-culture showed reduced staining (G) as compared to intense Alizarin Red S staining as seen in collagen matrix of KUSA/cell monoculture (H).

4.3.2 AM-1 cell density

With increased culture duration (7 to 14 days), a noticeable increase in AM-1 cell density was observed in the AM-KUSA/A1 co-culture construct in comparison to AM-1 cell monocultures (Figure 4.9). Whilst, cell density in both AM-1 and MC3T3-E1 cell co-cultures and AM-1 and ST2 cells co-cultures was relatively less enhanced. Similarly, all three different types of co-culture grown for 21 days appeared unhealthy (data not shown).

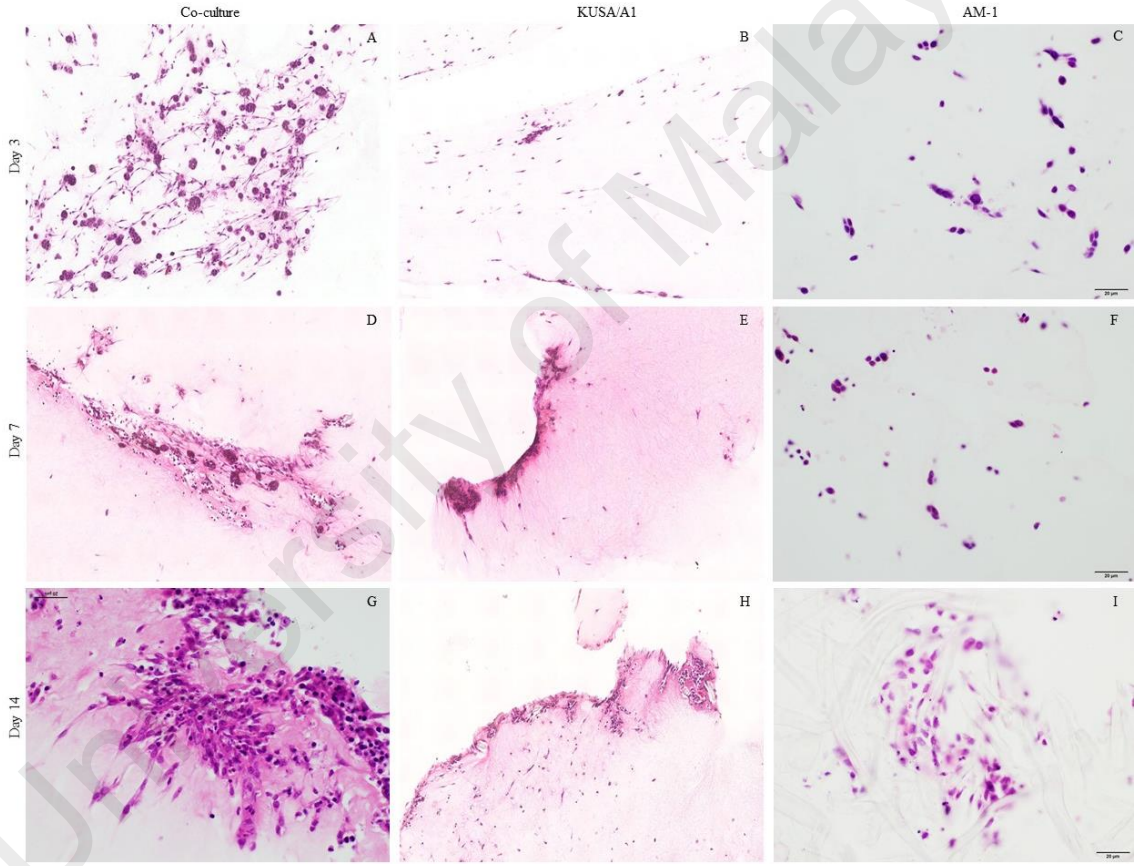

Figure 4.9: Morphological characteristics of mono- and co-culture cells.

H&E stained histologic sections of 3D *in vitro* AM co-culture and KUSA/A1 and AM-1 cell monocultures in collagen matrix at different time points – day 3, 7 and 14.

4.4 Effect of cell-matrix interaction on collagen gels contraction

Collagen gel contraction mediated by cells cultured in a 3D collagen gel was examined by the change in diameter of the gel (Figure 4.10). Monocultures of the fibroblastic cell, KUSA/A1 and AM-1 cell at the same seeding concentration induced small but not significant contraction as examined (Figure 4.10A-B). However, alterations in cell volume were shown to be involved in the decrease in the collagen gel diameter. KUSA/A1 and AM-1 co-cultures seeded at a high concentration (8.0×10^6 cells/mL) induced a significant contraction of the collagen gel and the subsequent reduction in the size of the collagen gel (Figure 4.10C). Co-cultures at a low concentration (4.0×10^6 cells/mL) as in the mono-cell cultures had no significant effect on the contraction of the collagen gel (Figure 4.10D). The time-dependent and concentration-dependent manner of collagen gel concentration reflected the clear indication of the influence of cell-matrix interaction.

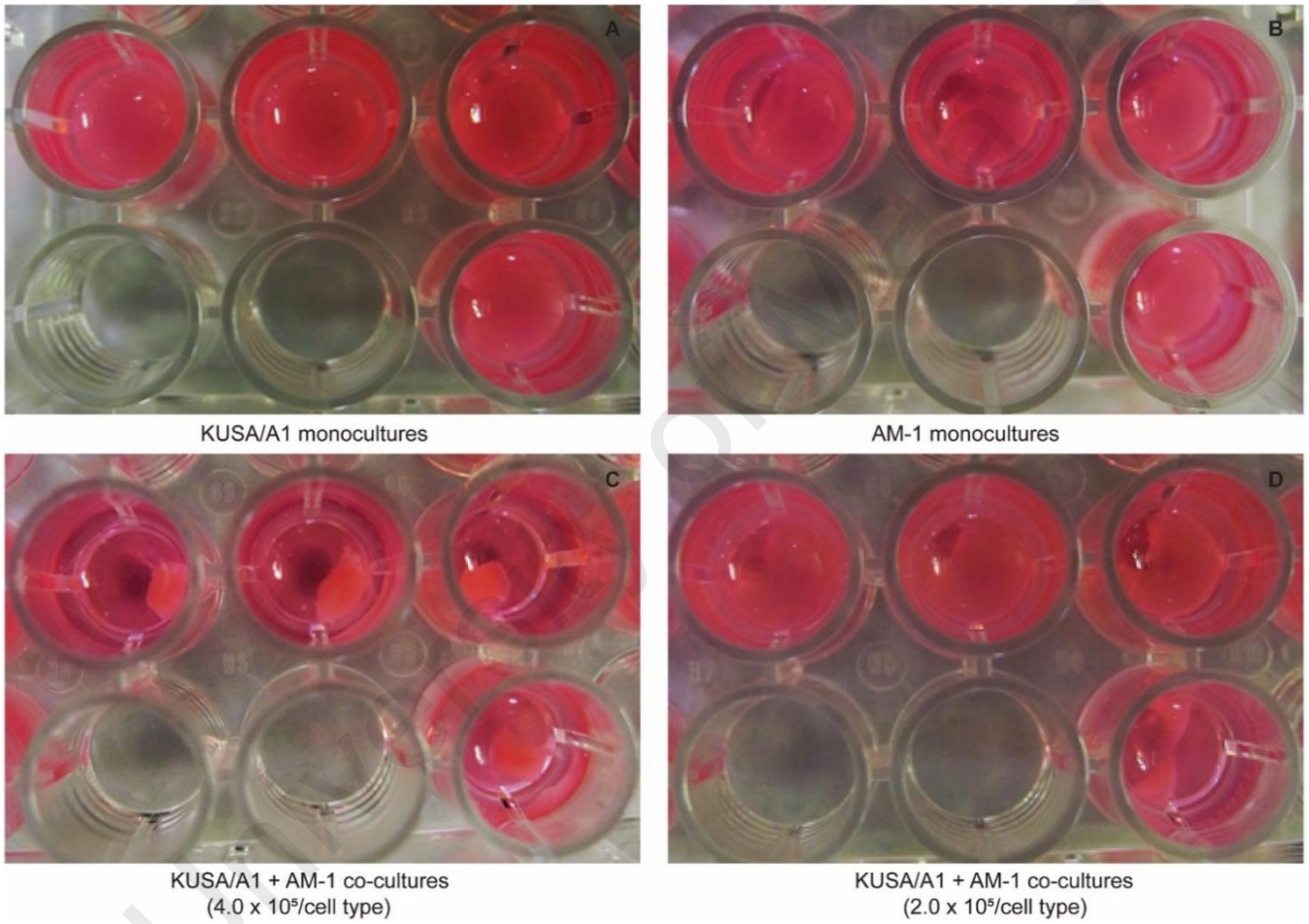

Figure 4.10: Hydrogel contraction of mono- and co-culture constructs.

Effect of cell-matrix interaction on collagen hydrogels contraction mediated by KUSA/A1 or AM-1 or both cells. Photographs of collagen gel cultures of (A) KUSA/A1 cells, (B) AM-1 cells, (C) KUSA/A1 and AM-1 at concentrations of 8.0×10^6 cells/mL and (D) KUSA/A1 and AM-1 at concentrations of 4.0×10^6 cells/mL incubated for 21 days.

4.5 Protein expression of 3D monoculture cells

4.5.1 Cytokeratin expression

Analysis of cytokeratin expression in KUSA/A1 cells in collagen matrices in a 3D monoculture configuration revealed that KUSA/A1 cell stained negative for cytokeratin throughout the culture period (Figure 4.11A-C). Whilst, AM-1 cells in 3D monoculture configuration stained positive for cellular cytokeratin with similar intensities at each time point (Figure 4.11D-F).

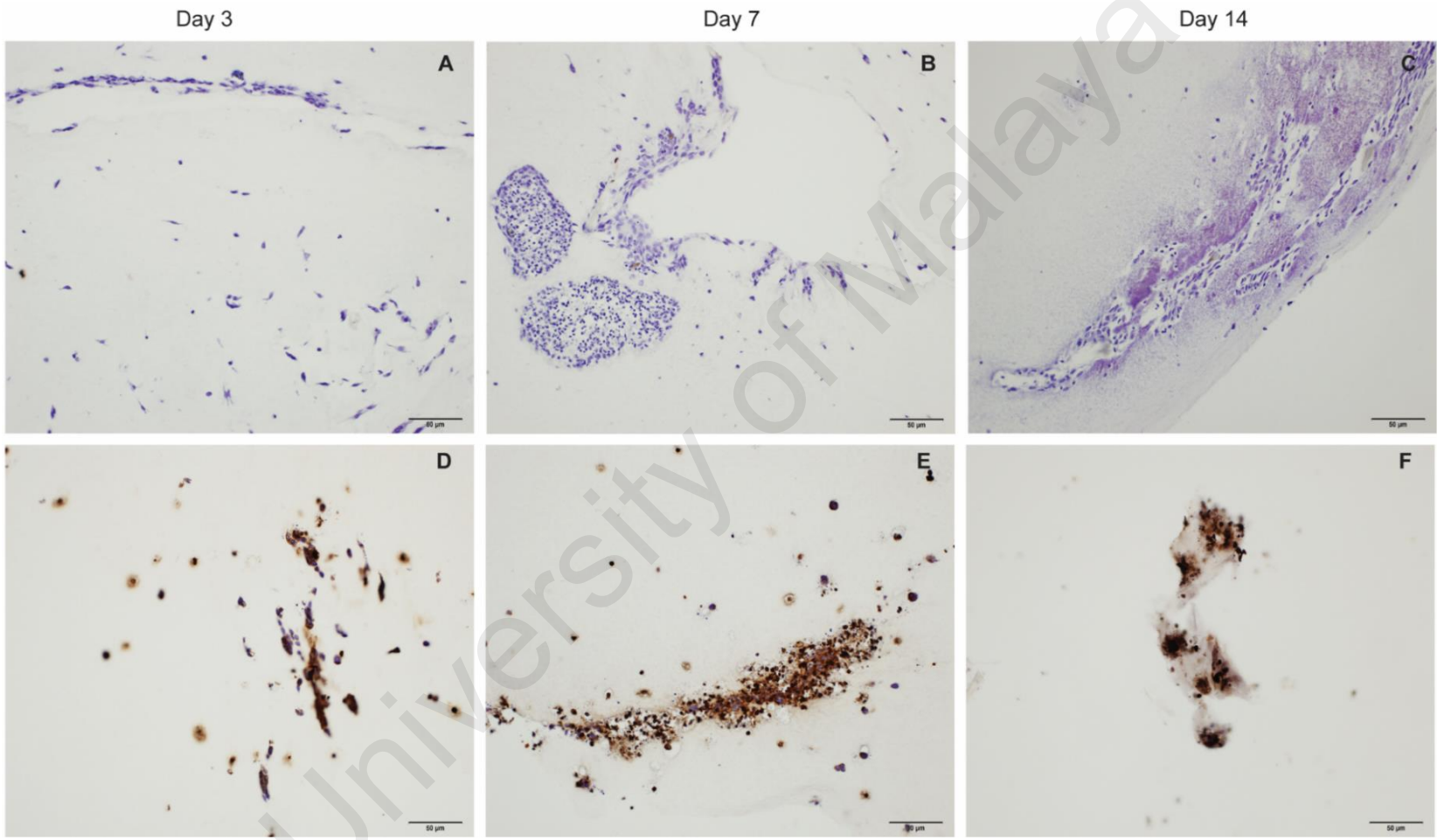

Figure 4.11: Cytokeratin expression of monoculture cells.

Cytokeratin protein expression in KUSA/A1 cells and AM-1 cells in collagen matrices in a 3D monoculture configuration. KUSA/A1 cells (A-C) and AM-1 cells (D-F) were maintained in mineralization medium for 3, 7 or 14 days, prior to fixation, processing and sectioning of the individual gels and counterstained with haematoxylin.

4.5.2 Vimentin expression

Analysis of vimentin in KUSA/A1 cells in collagen matrices in a 3D monoculture configuration revealed that KUSA/A1 cell stained positive for vimentin, but varies at each time point. The cellular staining intensity of KUSA/A1 cells in 3D monoculture configuration appeared to be lightest on day 3, and this had increased and reached its maximum on days 7 before returning to a lower level of expression on day 14 (Figure 4.12A-C). In contrast, AM-1 cells in a monoculture configuration did not show any cellular staining throughout the culture period (Figure 4.12D-F).

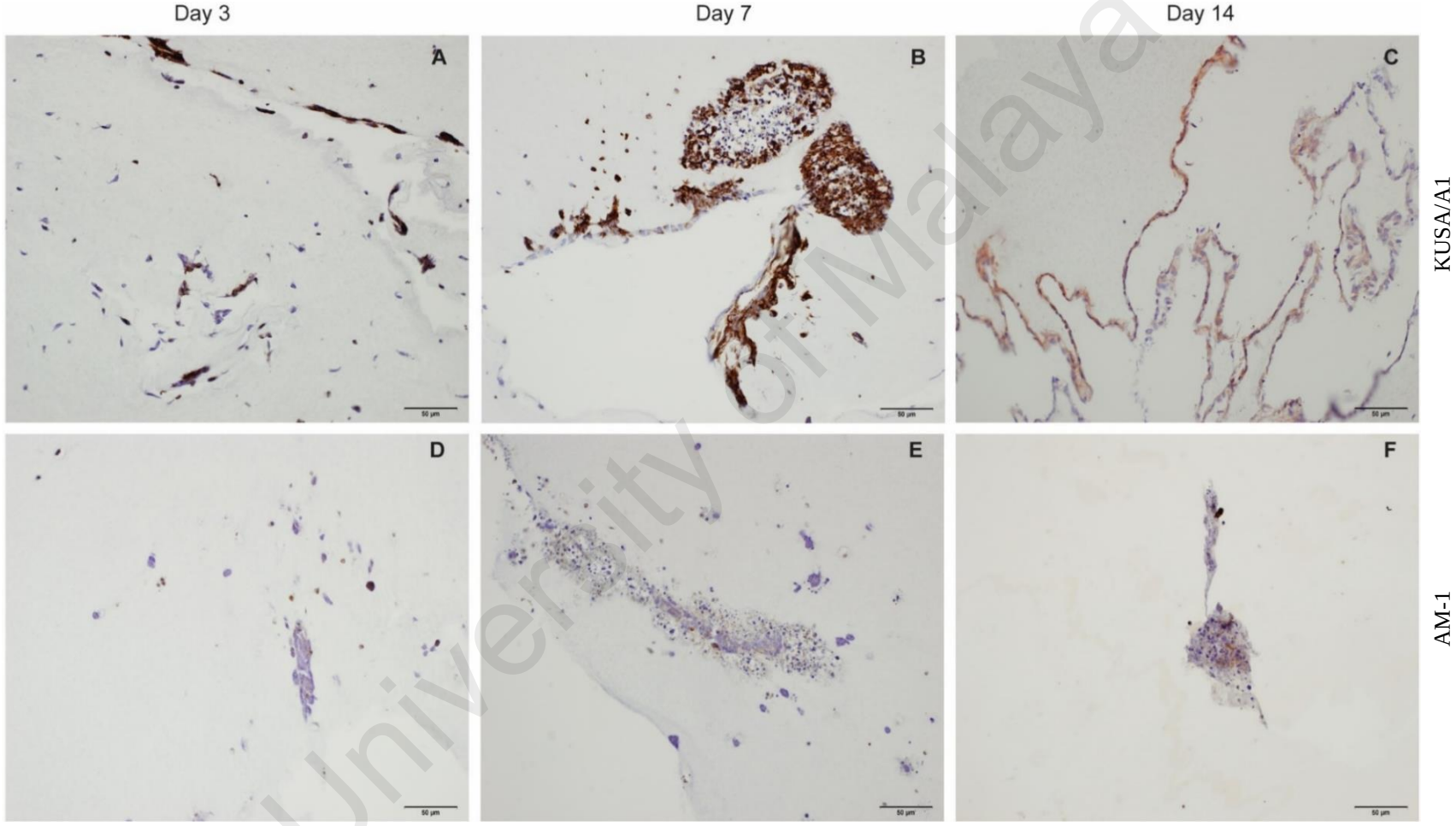

Figure 4.12: Vimentin expression of monoculture cells.

Vimentin protein expression in KUSA/A1 cells and AM-1 cells in collagen matrices in a 3D monoculture configuration. KUSA/A1 cells (A-C) and AM-1 cells (D-F) were maintained in mineralization medium for 3, 7 or 14 days, prior to fixation, processing and sectioning of the individual gels and counterstained with haematoxylin.

4.5.3 Osteocalcin expression

Osteocalcin expression in both KUSA/A1 cells and AM-1 cells entrapped in collagen matrices in a 3D monoculture configuration showed weak cellular staining at day 3, and then increased at day 7 (Figure 4.13). On days 14, KUSA/A1 cells did not show any osteocalcin cellular staining, but the three-dimensional KUSA/A1 cell monoculture matrices stained positive for osteocalcin. However, the intensity of osteocalcin expression in AM-1 returned to a lower level of expression on day 14.

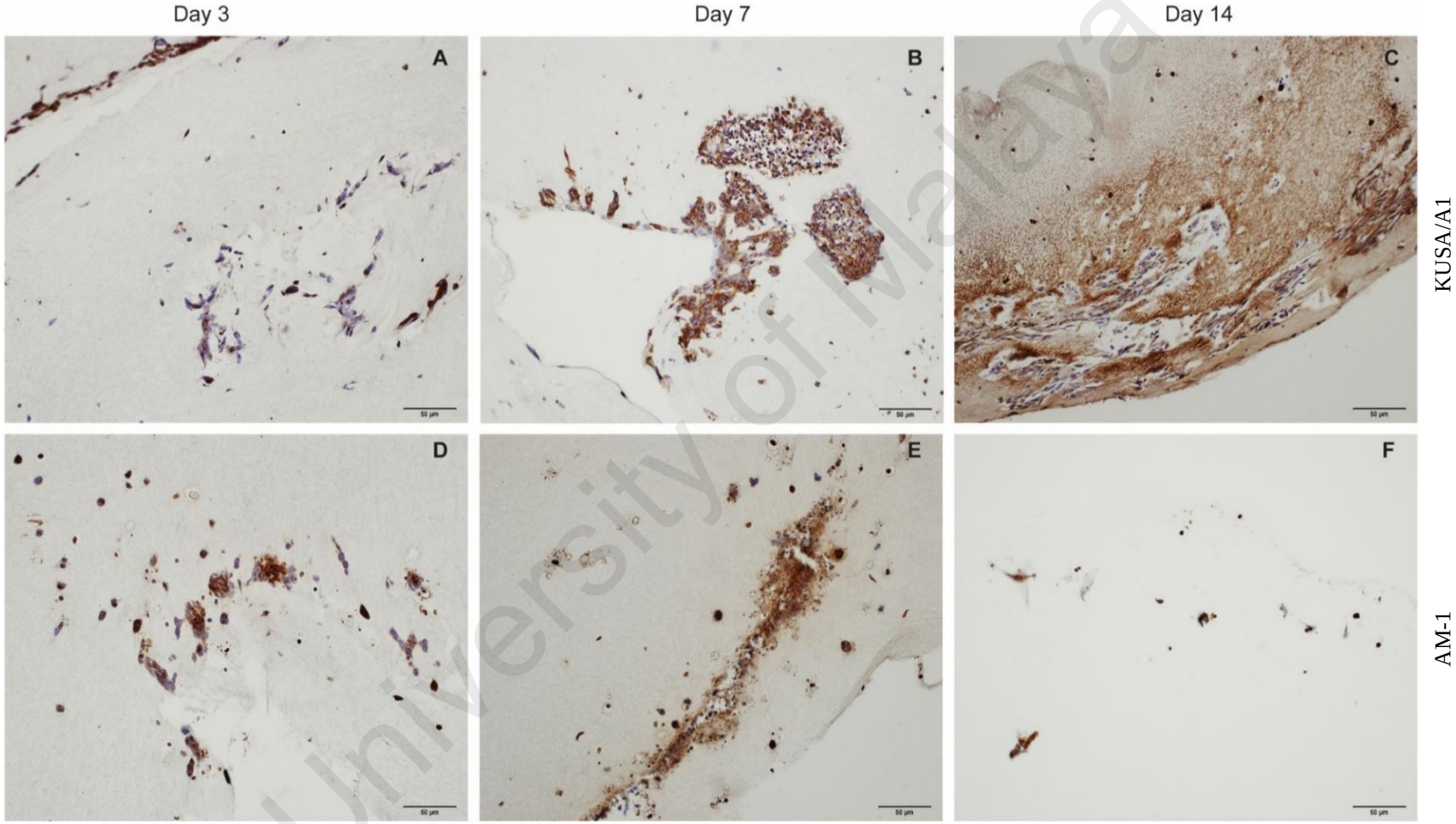

Figure 4.13: Osteocalcin expression of monoculture cells.

Osteocalcin protein expression in KUSA/A1 cells and AM-1 cells in collagen matrices in a 3D monoculture configuration. KUSA/A1 cells (A-C) and AM-1 cells (D-F) were maintained in mineralization medium for 3, 7 or 14 days, prior to fixation, processing and sectioning of the individual gels and counterstained with haematoxylin.

4.5.4 Osteopontin expression

Osteopontin expression in KUSA/A1 cells in 3D monoculture did not show any staining at day 3 and day 7, but there was faint positive staining at day 14 in KUSA/A1 cells (Figure 4.14A-C). However, AM-1 cells in 3D monoculture did not show any staining for osteopontin expression throughout the culture period (Figure 4.14D-F).

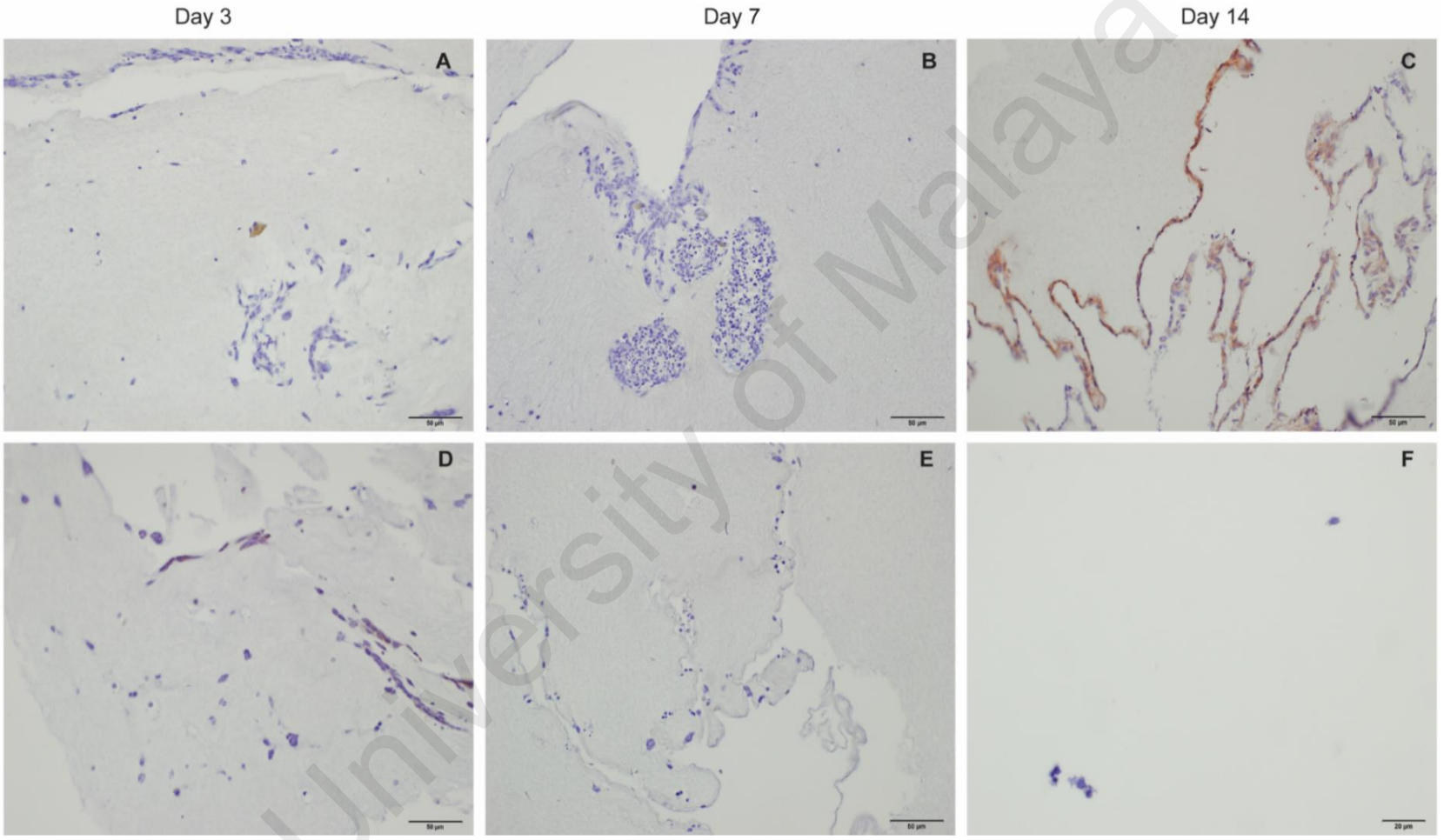

Figure 4.14: Osteopontin expression of monoculture cells.

Osteopontin protein expression in KUSA/A1 cells and AM-1 cells in collagen matrices in a 3D monoculture configuration. KUSA/A1 cells (A-C) and AM-1 cells (D-F) were maintained in mineralization medium for 3, 7 or 14 days, prior to fixation, processing and sectioning of the individual gels and counterstained with haematoxylin.

4.5.5 Bone sialoprotein expression

Analysis of bone sialoprotein (BSP) expression in KUSA/A1 cells in a 3D monoculture configuration revealed that KUSA/A1 cell and the 3D KUSA/A1 cell monoculture collagen matrices stained positive for BSP at day 3 (Figure 4.15A). On days 7, KUSA/A1 cells nor its matrices show any BSP staining, but the intensity of BSP staining in collagen matrices of KUSA/A1 monocultures returned to a lower level of expression on day 14. However, AM-1 cells and its matrices in a monoculture configuration did not show any BSP staining throughout the culture period (Figure 4.15D-F).

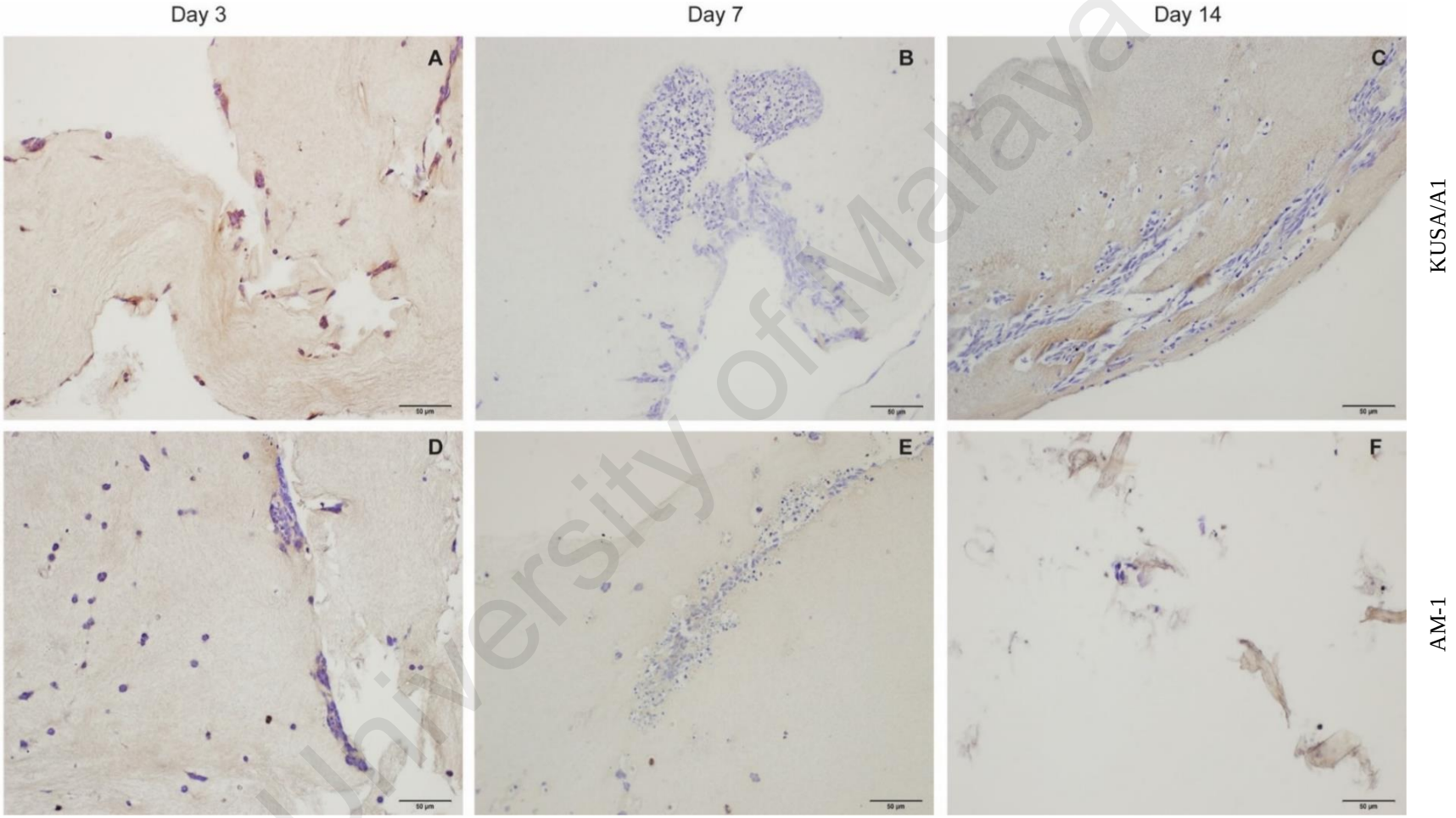

Figure 4.15: Bone sialoprotein expression of monoculture cells.

Bone sialoprotein (BSP) expression in KUSA/A1 cells and AM-1 cells in collagen matrices in a 3D monoculture configuration. KUSA/A1 cells (A-C) and AM-1 cells (D-F) were maintained in mineralization medium for 3, 7 or 14 days, prior to fixation, processing and sectioning of the individual gels and counterstained with haematoxylin.

4.6 Protein expression of 3D co-culture cells

4.6.1 Expression of extracellular matrix proteins affects mineralized nodule formation in co-cultures of KUSA/A1 and AM-1 cells

Formation of a mineralized matrix is a definite hallmark of osteoblastic differentiation. To determine whether extracellular matrix protein expression influences on the mineral formation, IHC of osteocalcin, osteopontin and bone sialoprotein expression in co-cultures of KUSA/A1 and AM-1 cells entrapped in collagen matrices in inducing condition were performed as presented in Figure 4.16.

4.6.1.1 Osteocalcin expression

Analysis of osteocalcin expression in co-cultures of KUSA/A1 and AM-1 cells in collagen matrices in inducing condition by IHC, in which darkly cellular staining but no evidence of matrix staining was observed throughout the culture period (Figure 4.16A-C).

4.6.1.2 Osteopontin expression

Osteopontin in KUSA/A1 and AM-1 co-cultures in collagen matrices in inducing condition incubated for 3 days and 7 days have no visible evidence of cellular staining nor matrix staining (Figure 4.16D-E). On days 14, there was faint positive cellular staining but no evidence of matrix staining for osteopontin expression in the cultures (Figure 4.16F).

4.6.1.3 Bone sialoprotein expression

Analysis of bone sialoprotein expression in co-cultures of KUSA/A1 and AM-1 cells in collagen matrices in inducing condition by IHC revealed that, cultures have no evidence of cellular and matrix for bone sialoprotein expression on days 3 and days 7 (Figure 4.16G-H). When the same cultures were maintained in the same condition, there

was faint positive cellular staining for bone sialoprotein expression on day 14 with no evidence of matrix staining as presented in Figure 4.16I.

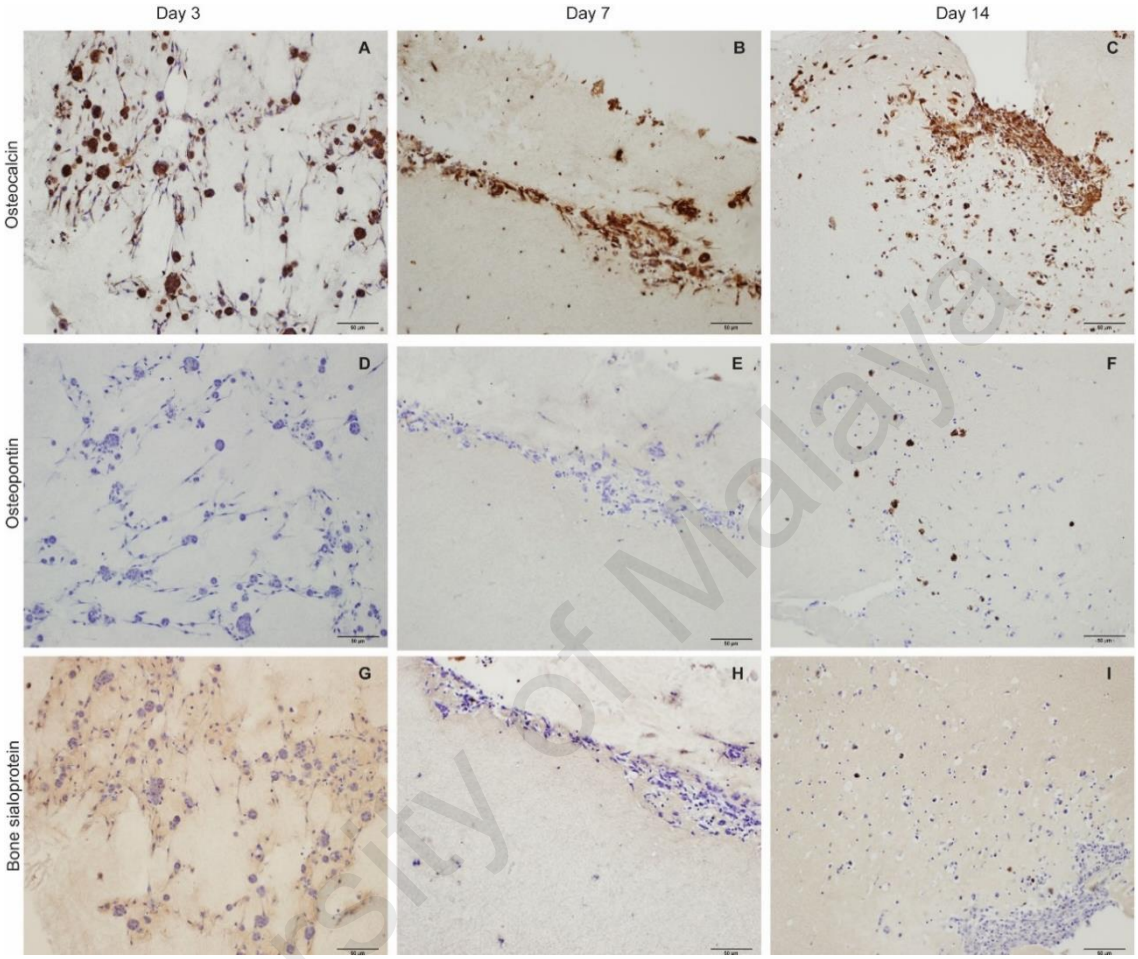

Figure 4.16: Osteopontin expression of co-culture cells

Osteocalcin, osteopontin and bone sialoprotein expression in 3D *in vitro* KUSA/A1 and AM-1 cell co-cultures entrapped in collagen matrices in mineralization medium. Co-cultures were maintained in mineralization medium for 3, 7 or 14 days. Individual gels were fixed, processed and sectioned prior to IHC for osteocalcin (A-C), osteopontin (D-F) and bone sialoprotein (G-I) expression and were counterstained with haematoxylin.

4.6.1.4 RANK, RANKL and OPG expression

Analysis of RANK, RANKL and OPG expression in three-day-old AM-1/KUSA-A1 co-culture revealed that, both round cell nest-like structures and elongated spindle-shaped cells in co-culture strongly expressed RANK, mildly for RANKL and OPG (Figure 4.17A-C).

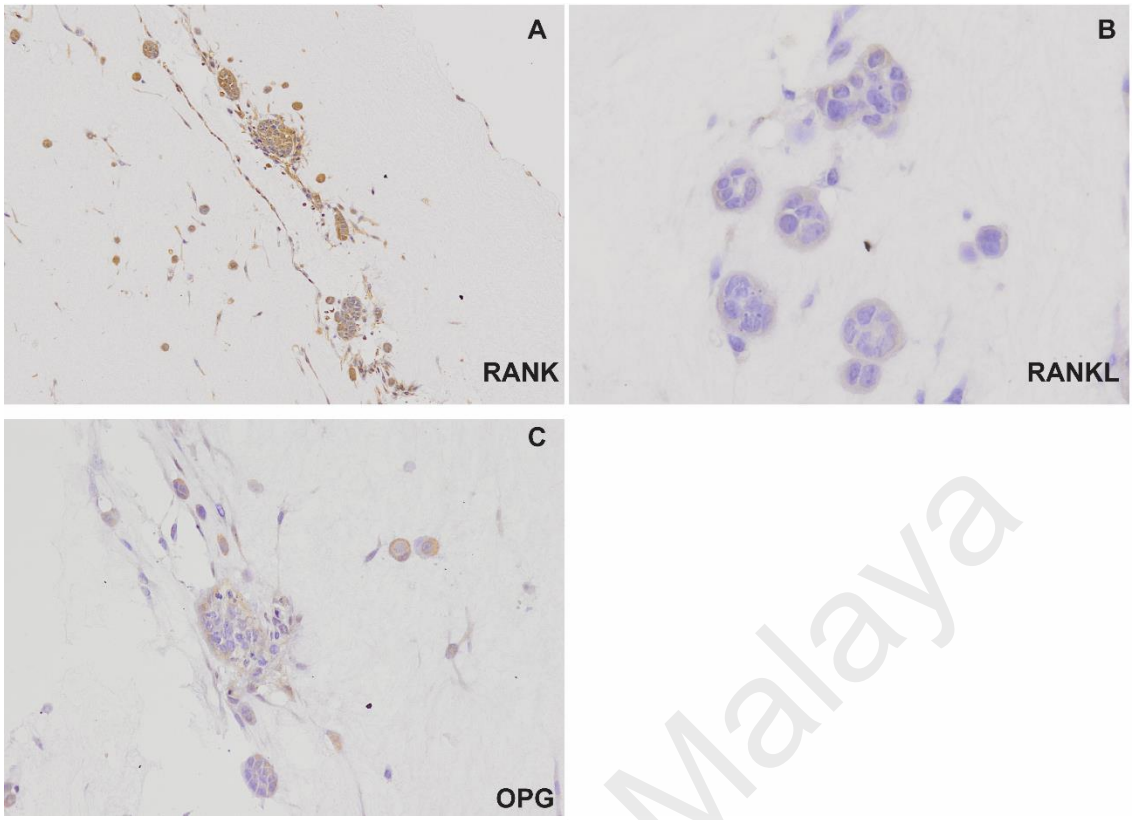

Figure 4.17: A RANK-high, RANKL-low and OPG-low immunoprofile.

Representative sections of KUSA/A1 and AM-1 co-culture constructs showing immunohistochemical staining for RANK, RANKL and osteoprotegerin (OPG) (A-C). RANK reaction was strong in the membrane and cytoplasm of round nest-like structures and elongated spindle-shaped cells (A). RANKL expression was weak to absent in the cytoplasm of both cell types (B). OPG was weakly expressed in both cell types (C). (Original magnification: A-C, x200).

4.6.2 Morphological characteristics of co-culture cells in related to the expression of cytokeratin and vimentin protein

The results of the immunohistochemical labelling of 3D *in vitro* tumour-fibroblast co-cultures entrapped in collagen matrices in mineralization medium with cytokeratin and vimentin at day 3, 7 and 14 are presented in Figure 4.18. Analysis of cytokeratin and vimentin expression of three-day-old 3D *in vitro* co-cultures of AM-1 and KUSA-A1 cells revealed that, cytokeratin-expressing cells are found formed into nest-like aggregates of closely packed cells; whilst vimentin-expressing cells grew as flat, elongated shape in appearance and scattered around the cytokeratin-expressing cell population. Note, with increased culture period, cultured cells in the co-culture condition

undergo substantial growth despite the density at which these co-cultures were initiated until the cells were confluent.

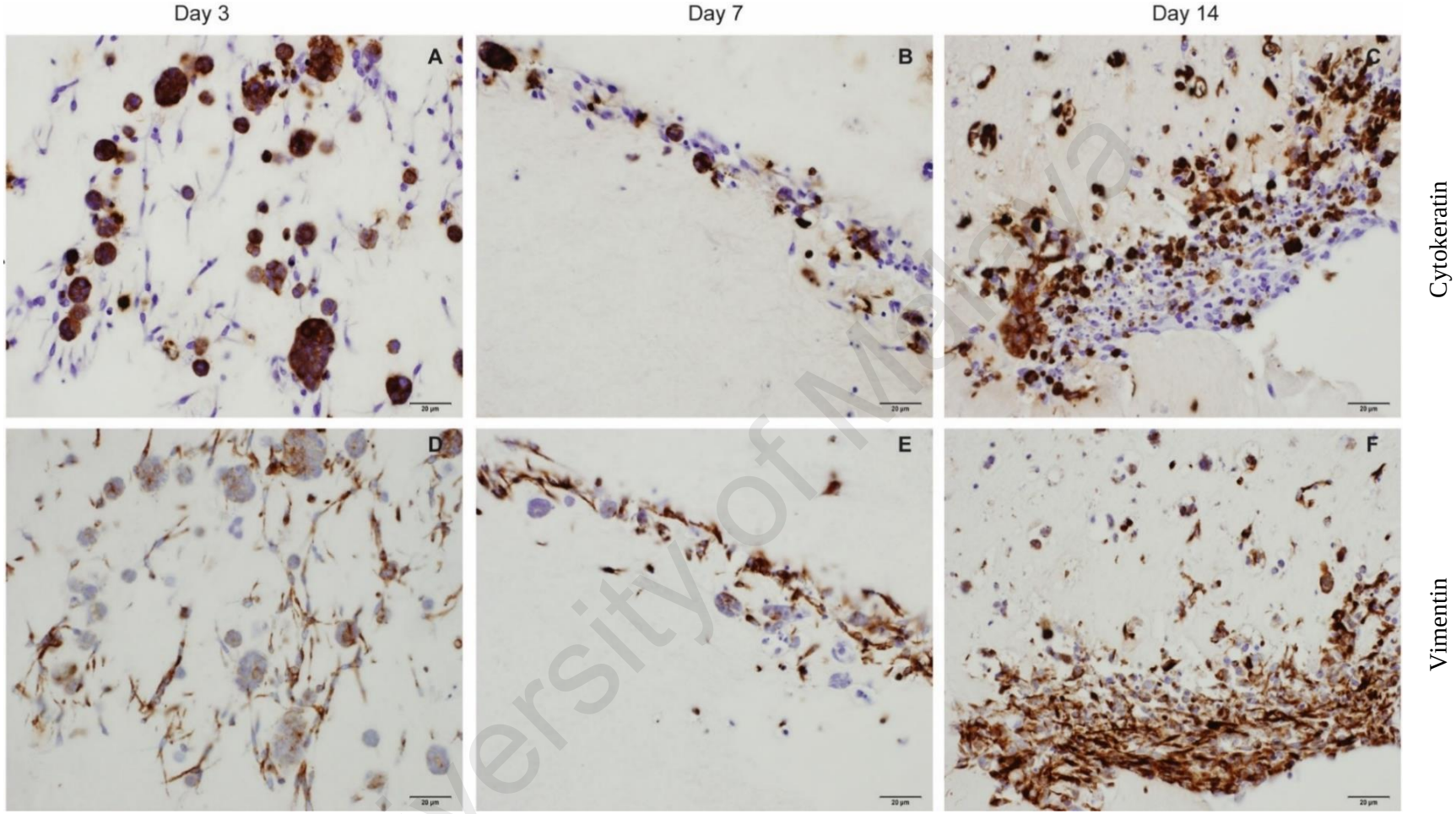

Figure 4.18: Cytokeratin and vimentin protein expression in co-culture cells.

Cytokeratin and vimentin protein expression in KUSA/A1 and AM-1 cells entrapped in collagen matrices in 3D in vitro tumour-fibroblast co-culture model. Co-cultures were maintained in mineralization medium for 3, 7 or 14 days, prior to fixation, processing and sectioning of the individual gels and counterstained with haematoxylin.

4.7 Tumour-fibroblast interactions affect the organization of cells

Immunofluorescent staining demonstrated the distribution of cytokeratin-expressing cells and vimentin-expressing cells cultured in 3D *in vitro* co-culture configuration entrapped in collagen matrices in mineralization medium (Figure 4.19). In KUSA/A1 and AM-1 co-cultures incubated for 3 days, vimentin-expressing cells are found flat, elongated in their appearance with long cytoplasmic processes scattered around the cytokeratin-expressing cells that found organized into nest-like aggregates in the 3D collagen scaffold. This was indicative of the interaction between adjacent cells growing across and into the structure of the matrices, forming an interconnected cellular network between two cell lines.

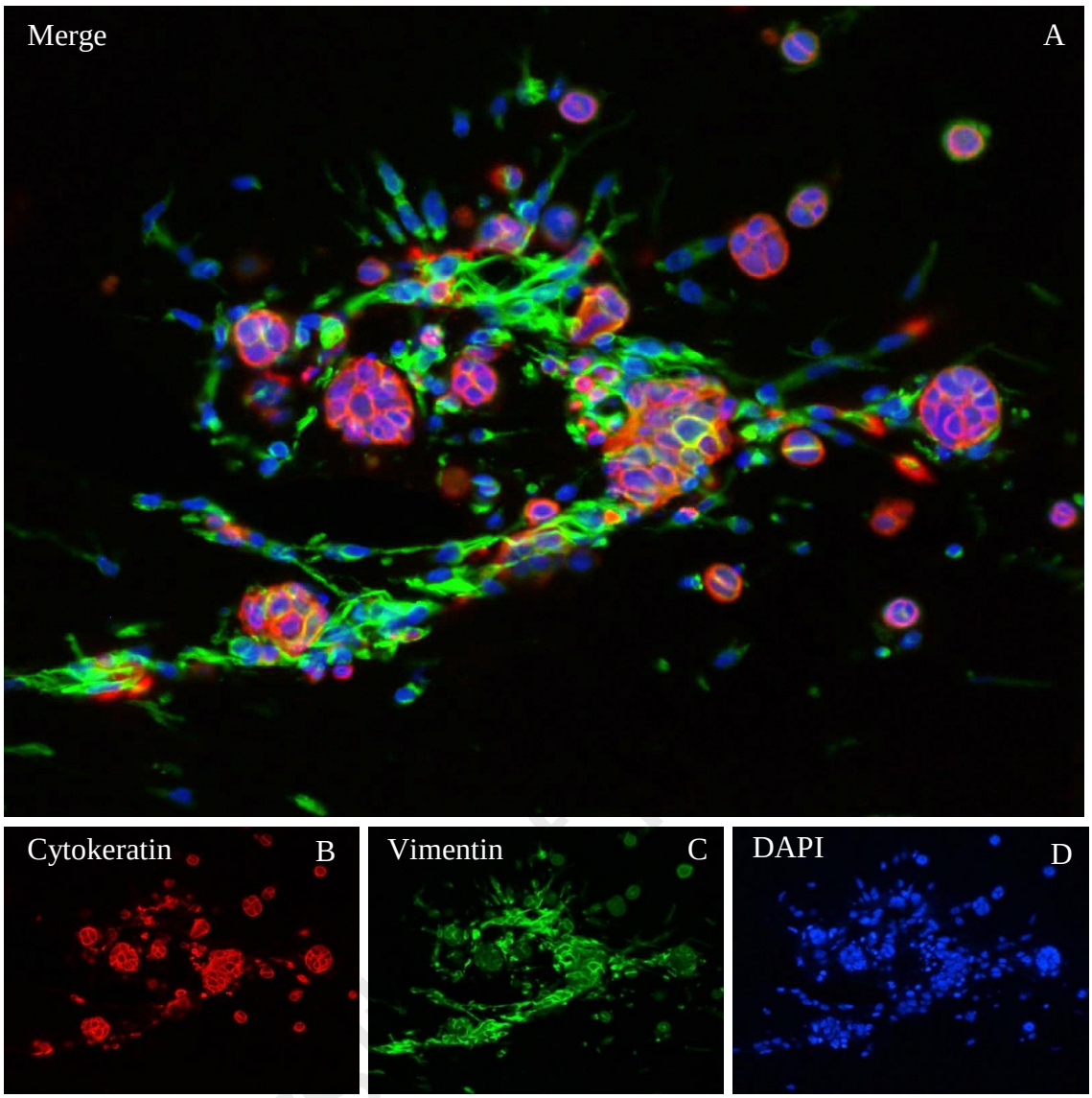

Figure 4.19: Cell organization in AM-1/KUSA-A1 co-culture construct.

Indirect multiple immunofluorescence images of three-day-old 3D *in vitro* KUSA/A1 and AM-1 cell co-cultures entrapped in the collagen matrices in mineralization medium. Red, cytokeratin; green, vimentin; blue, DAPI staining. Note that cytokeratin-expressing cells formed into nest-like aggregates of closely packed cells, surrounded by vimentin-expressing cells that appeared as flat, elongated in shape and scattered around the cytokeratin-expressing cell population.

4.8 Cell count of mono- and co-culture cells

Immunoreactivity scores for cytokeratin, vimentin, RANK, RANKL and OPG for KUSA/A1 and AM-1 cells in mono- and co-culture constructs at different time points are shown in Table 4.1. Statistical analysis of cell count in mono- and co-cultures is shown in Table 4.2 and illustrated in Figure 4.20. Both KUSA/A1 and AM-1 in co-cultures showed a drop in cell count at day 7 but regained back at day 14. At the end of culture period (day 14) both KUSA/A1 and AM-1 in co-cultures showed a significant increase in cell count compared to their monoculture counterparts ($p<0.05$).

Table 4.1: Immunoreactivity scores for cytokeratin, vimentin, RANK, RANKL and osteoprotegerin (OPG)

Factors	Monoculture cell lines		Co-culture cell lines	
	KUSA/A1	AM-1	KUSA/A1	AM-1
Cytokeratin	-	+++	-	++++
Vimentin	+++	-	+++	-
RANK	+	+	+++	+++
RANKL	±	±	+	+
OPG	-	-	+	+

Table 4.2: Statistical analysis of mean ± SD cell count at different time points for KUSA/A1 and AM-1 cell lines in 3D monocultures and co-cultures.

Period (d)	KUSA/A1, mean ± SD (range)				*p*-value	AM-1, mean ± SD (range)				*p*-value
	n	Monoculture	n	Co-culture		n	Monoculture	n	Co-culture	
3	1	137.2 ± 36.27	2	163.8 ± 56.62	0.0536	1	117.6 ± 44.91	2	206.2 ± 76.92	0.0629
7	1	186.2 ± 98.15	2	135.8 ± 35.85	**0.0148**	1	172.6 ± 49.13	2	135.8 ± 77.55	**0.0046**
14	1	243.8 ± 100.59	2	256 ± 237.41	**0.0319**	1	63.2 ± 52.3	2	229 ± 118.62	**0.0161**

n, number of samples; Bold values indicate statistical significance. $p<0.05$.

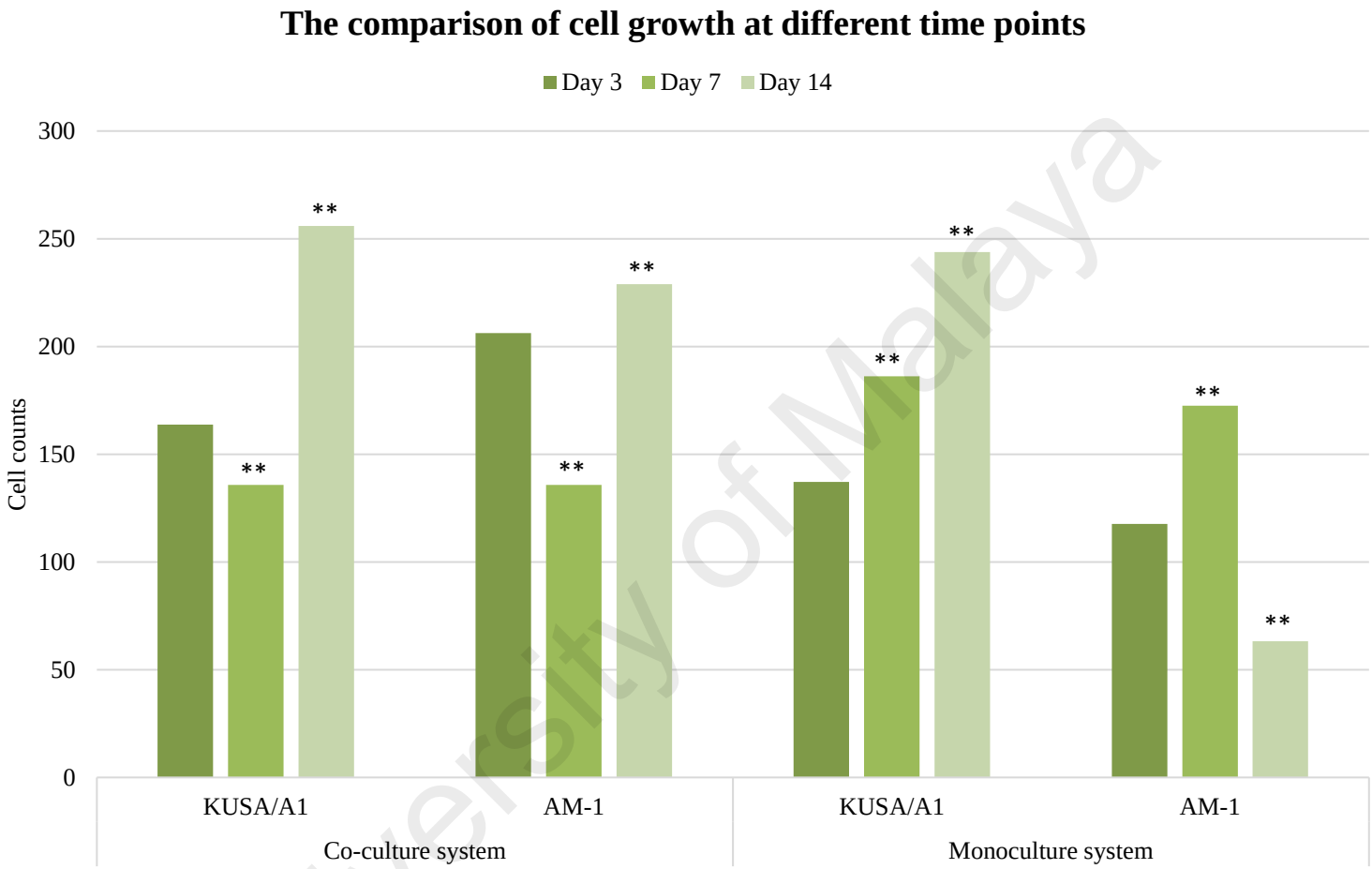

Figure 4.20: Ameloblastoma-osteoblastic interactions promoted tumour cell growth and growth inhibitory effect on osteoblasts.

Both KUSA/A1 and AM-1 in co-cultures showed a drop in cell count at day 7 but regained back at day 14. At day 14, AM-1 in co-culture showed a significant increase in cell count compared to their monoculture counterpart. ** denotes $p<0.05$.

CHAPTER 5: MAJOR FINDINGS

A key finding in the present study was significant increase in the number of AM-1 cells in 3D co-cultures compared to their monoculture counterparts. In contrast, cell count between co-culture and monoculture for KUSA/A1, MC3T3-E1 and ST2 cells was less distinctive at the end of the experiment. These observations imply that ameloblastoma-osteoblastic interactions may have a promotive effect on tumour cell growth and growth inhibitory effect on osteoblasts. The specific mechanism underlying this heterotypic interaction that stimulates tumour cell proliferation is unclear. It is known that AM-1 cells show downregulation of osteogenic genes including functional inactivation for WDR5, a factor which is essential for osteoblast differentiation (Sathi *et al.*, 2012). In osteoblastic metastases, cancer cell produces osteoblast-stimulating factors to induce osteoblastogenesis and the activated osteoblasts in turn secrete factors to promote cancer colonization and growth (Ottewell, 2016). Whether the latter signalling pathway occurs in ameloblastoma requires further investigation.

In the original work by Harada *et al.* (1998), primary culture AM-1 cells were described as predominantly closely-packed small and polygonal cells with an epithelial morphology. In the current study, AM-1 cells co-cultured with KUSA/A1 formed visible nest-like epithelial structures resembling ameloblastoma cells in their native state whilst KUSA/A1 remained as flat, elongated spindle-shaped cells. We interpreted this to mean that tumour-osteoblastic interactions induce morphodifferentiation of AM-1 cells but preservation of KUSA/A1 mesenchymal phenotype. The other notable observation was in the co-culture state, both cell types were in close proximity with each other. KUSA/A1 cells with their long cytoplasmic processes interspersed and encircled AM-1 nest-like aggregates suggesting heterotopic cell-cell interaction. Despite this closeness, AM-1 and KUSA/A1 maintained fidelity of their lineages by expressing cytokeratin and vimentin respectively.16 Lack of vimentin positivity in AM-1 cells further indicates absence of

epithelial-to mesenchymal transition and phenotypic switching (Siar & Ng, 2014). It is known that intercellular communication between cancer and surrounding stromal cells creates a local microenvironment that promotes tumour survival and growth (Wendler *et al.*, 2016). However, this feature of topographic closeness was not observed in AM-1 cells co-cultured with either MC3T3-E1 or ST2 cell lines. Emerging evidence suggests that differences in cell properties and genetic instability may be major reasons influencing interaction between these cells (Kim & Othmer, 2013; Fong *et al.*, 2016; Liu *et al.*, 2016).

In this study, a two-prong approach was used to assess local bone metabolism in the 3D co-culture system. Firstly, we examined KUSA/A1 and AM-1 in the co-culture construct for expression of bone remodelling molecules RANK, RANKL and OPG. A RANK-high, RANKL-low and OPG-low immunoprofile displayed by both cell types suggested a deregulated osteoclastogenesis. Osteoclasts are the cells responsible for bone resorption and the process of osteoclastogenesis is regulated by the complex RANK-RANKL-OPG pathway (Khosla, 2001; Proff & Romer, 2009). Binding of RANKL to RANK triggers differentiation and activation of pro-osteoclasts (osteoclastic precursor cells) to mature (active) osteoclasts (Proff & Romer, 2009). This RANKL-RANK interaction is inhibited by OPG, a soluble decoy receptor for RANKL, resulting in osteoclast inactivation. Our results differed from previous in vitro studies where a 700-fold increase in RANKL was detected in co-culture of AM-1 and human osteosarcoma cell lines, RANKL and OPG were well-expressed in AM-1 monoculture and in primary ameloblastoma co-cultured with neonatal rabbit bone marrow cells (Sandra *et al.*, 2006; Qian & Huang, 2010; Eriksson *et al.*, 2016). The reasons for this variability in *in vitro* findings are unclear. One possible explanation may be ascribed to differences in cell lines, and types of cell culture system used (Eriksson *et al.*, 2016). Other factors that might contribute to these disparities in findings include differences in the antibody sources used, methodologies related to tissue processing and histomorphometry. In clinicopathological

studies, reports on RANK-RANKL-OPG expression levels based on surgical materials of ameloblastoma show variations in bone remodelling activities between primary and recurrent tumours (Kumamoto & Ooya, 2004; Tay *et al.*, 2004; Sandra *et al.*, 2005; Andrade *et al.*, 2008; da Silva *et al.*, 2008; Tekkesin *et al.*, 2011; de Matos *et al.*, 2013; Siar *et al.*, 2015). A plausible explanation put forth is that RANKL up- or down-regulation in ameloblastoma might be reflective of the dynamic on-going process associated with tumour-induced bone remodelling (Siar *et al.*, 2015). In mineralization assays, KUSA/A1 monoculture demonstrated abundant Alizarin Red S positive mineralised areas whereas this was diminished in the co-culture. These observations lend further support to our immunohistochemical findings which suggests that tumour-osteoblast interaction induces an altered local bone metabolism.

CHAPTER 6: DISCUSSIONS

6.1 Optimum 3D cell culture condition

6.1.1 3D collagen construct to monitoring differentiation of cells

Collagen gel has good biocompatibility, degradability and low immunogenicity, can be used as a culture matrix in 3D cell culture for the growth of a variety of mammalian precursor cells. Huang *et al.* (2013) reported that 3D collagen gel promoted the differentiation of neurons stem cells into mature neurons, shown that collagen acts as a natural extracellular matrix providing a favourable condition for the growth of cultured cells. Furthermore, Matthews *et al.* (2014) also demonstrated the enhanced osteoblastogenesis of osteoblastic cells in the 3D collagen scaffold. The results from this study also indicated that the upregulation of the late-osteoblast markers in 3D collagen gels over the culture period is dependent on the 3D configuration of the scaffold since the expression level of these markers in cells growing on collagen-coated plates and uncoated plastic is similar.

In the present study, we demonstrated that KUSA/A1 pre-osteoblastic cells seeded within 3D collagen gels showed positive mineral staining at an earlier time point than cells growing in 2D model with similar culture condition. Mineralized nodules were first visible in 2D KUSA/A1 cultures on day 3 after confluency in the inducing condition, whereas 3D KUSA/A1 cultures spontaneously exhibited nodule-like structures and were stained strongly positive for Alizarin Red S after 14 days of culture, indicated the acceleration of KUSA/A1 cell differentiation seeded in the 3D collagen gel (Kawashima *et al.*, 2005). In contrast, matrix mineralization was not visible in both 3D MC3T3-E1 and ST2 cultures throughout the culture period (21 days), but studies first demonstrated mineralized nodules first visible in the 2D cultures after confluency in the inducing condition only on day 20 and day 24 respectively (Otsuka *et al.*, 1999; Kawashima *et al.*, 2005). Unlike the determination of the onset of matrix mineralization, the overall level of

matrix mineralization could not be directly compared between the two culture systems. However, this present work adequately indicated the acceleration of pre-osteoblastic KUSA/A1 cell differentiation in the 3D collagen gels even with the absence of comparison between the overall level of mineralization between 2D and 3D culture system.

In our experiment, the collagen solution of desired concentration was mixed thoroughly with cells before it has polymerized as a gel, and therefore the cells are allowed to settle directly into the 3D environment. The variation of parameters existed between the 2D and 3D culture system potentially contributed to the differential rate of osteoblast differentiation in these systems and cells cultured in the *in vivo*-like 3D model are superior to their 2D counterparts, with an accelerated cell differentiation. In addition, pre-osteoblastic cells cultured in the 3D collagen gels assumed a more *in vivo*-like morphology compared to the flat, adherent pre-osteoblastic cells on the 2D surface of the tissue culture dishes. The 3D configuration of gels in 3D cell culture system mimic the *in vivo* environment allows for more extensive cell-cell physical contact and the subsequent cell-cell interaction and cell-matrix interaction, which synergistically accelerated osteoblast differentiation. The present work characterized the growth of pre-osteoblastic cells and elucidated the acceleration of osteoblast differentiation in 3D collagen gel by comparing the osteoblastic matrix mineralization over a 14-day period.

6.1.2 Exposed surface area of culture substrate

For cell culture system, the exposed surface area of the culture substrate plays a major role, whose influence the penetration of nutrients within the scaffold volume in the vicinity of cells. In the present study, the exposed surface area shown significant influence on the cellular behaviour and morphology of cultured cells. Cells grown on the larger surface area were generally corresponding to the physiological relevance to their *in vivo* counterparts. Further, the close association between the adjacent cells in the co-culture

construct indicative of the establishment of an intercellular network between two cell populations of distinctive morphology.

6.1.3 Optimal cell seeding density

The seeding density in the cell culture system is important to ensure the optimal intercellular interactions between cells. For instance, AM co-cultures entrapped within collagen matrices in a 1:1 ratio at the total seeding density of 4.0×10^6 cells/mL is the optimal seeding density before the gel shrinkage and presented with the optimal intercellular interactions.

6.2 Validation of the 3D model

6.2.1 Differentiation of pre-osteoblastic cells

At present, the *in vitro* differentiation of osteoblastic cells cultured in 3D cultures have been reported by researchers to represent the physiological bone environment and offer a number of related biomedical applications (Ferrera *et al.*, 2002; Woo *et al.*, 2011; Prideaux *et al.*, 2014). However, there were only a few reports of the similar studies on pre-osteoblastic cells, especially the uncommercialized KUSA/A1 cells. In the present work, the established 3D *in vitro* collagen type I gel cell culture model characterizes the cultured pre-osteoblastic cells in inducing condition and allows *in vitro* studies of the differentiation of these cells in 3D cultures, which better represent the physiological bone environment compares with 2D cultures. Furthermore, the *in vitro* model as established in the present work demonstrated and characterized the developmental of osteoblastic cells. The model better exemplified the pre-osteoblastic cells at each stage of differentiation process, which would be represented by cells which have been in 2D cultures for at least 5 days after confluency in inducing conditions.

By using 3D *in vitro* cell culture model, this present work demonstrated for the first time the morphological and behavioural characteristics of the selected pre-

osteoblastic cell lines, which were previously not visible in conventional 2D cultures. In the present study, the designed 3D *in vitro* model in a mineralizing culture condition enhanced the differentiation of pre-osteoblastic cell line, KUSA/A1 cell into an osteocalcin, osteopontin and BSP expressing, mature osteoblast-like cell. In addition, cells in 3D inducing conditions expressed mature osteoblast markers and mineralized extracellular matrix within a shorter culture period compared to the cells in 2D cultures.

6.2.2 Modulation of 3D *in vitro* culture model

6.2.2.1 3D *in vitro* pre-osteoblastic cell monocultures

Modulation of the 3D *in vitro* pre-osteoblastic cell culture model possible to improves the model and maximise its role in the *in vitro* studies and biomedical application. Hence, it is possible that the model as developed in the present work could be targeted for the studies of a spectrum of bone disease. The establishment of an *in vitro* culture model better recapitulate of the *in vivo* osteoblastic differentiation and maturation is very important for a better understanding of the development and progression of related bone diseases and also fuel development of new treatment regimens. The work as described addressed this concept by investigating the growth of different pre-osteoblastic cell lines in the model developed. This study has selected three different pre-osteoblastic cell lines to assess the morphological and behavioural characteristics of cells in 3D collagen matrices, possible to establish and study stromal variation in the role of stromal-tumour cell interaction in impaired bone formation as well as the enhanced bone resorption in odontogenic tumours, especially ameloblastoma.

In the present work, the established 3D monoculture of pre-osteoblastic cell lines: KUSA/A1, MC3T3-E1 and ST2, revealed that these cell lines have an appearance of a typical fibroblastic cell in 3D collagen matrices. However, the most extensive growth in the 3D model as developed in the present work was best demonstrated by KUSA/A1 cell line. Both KUSA/A1 and MC3T3-E1 cells in 3D monocultures after incubated for 3 days

exhibited either a spindle or round shape in their appearance. These unique features of cellular morphology revealed the dynamic cell morphology and movement of cells across and into the structure of the collagen, probably due to the intercellular interactions or possibly the rearrangement of collagen fibres by the cellular contractile forces. Furthermore, the nature of 3D model allows enhanced cell-to-cell contacts and their subsequent cellular interaction as well-depicted by colonies of closely packed cells in KUSA/A1 and MC3T3-E1 monocultures after incubated for 7 days. Taken together, these factors give rise to collective cell movement of cultured cells in a self-organized manner.

There was an outgrowth of proliferating KUSA/A1 cells across and within the 3D collagen gels. Virtually, there were no obvious differences in the intensity and cellular distribution of MC3T3-E1 cells and ST2 cells in the developed 3D culture, probably due to the inhibitory effect of collagen gel on the proliferation and migration of MC3T3-E1 cells and ST2 cells. Besides, 3D *in vitro* monocultures of KUSA/A1 cell incubated for 14 days in mineralization-inducing media, showed calcification of the extracellular collagen matrix (ECCM). Collagen-containing scaffolds had reported to enhance the cellular attachment and proliferation (El-Jawhari *et al.*, 2016). However, 3D cultures of all pre-osteoblastic cell lines in collagen gel limited to 14 days, possibly due to hypoxia-caused cell death and/or the difficulty with medium penetration to cells deeper inside the construct. The present study highlighted the suitability of selected pre-osteoblastic cell lines for use in the developed 3D culture system. Collectively, the developed 3D model in the present study is a culture system best for KUSA/A1 cells. Such cell cultures allow better evaluation of cellular growth and morphology of KUSA/A1 cells, probably due to the existence of better cell-to-cell and cell-to-matrix interactions that potentially exert a synergistic effect on the proliferation and differentiation of KUSA/A1 cells.

6.2.2.2 3D *in vitro* ameloblastoma cell, AM-1 cell monocultures

The 3D growth of ameloblastoma, AM-1 cells in collagen matrix as in the developed model morphologically mimicking of the epithelial cell. AM-1 cells degraded the collagen matrix and expanded over the gel with a slower proliferation rate, which is consistent with the slow-growing but locally aggressive nature of AM tumour cells *in vivo*. demonstrated typical features of *in situ* ameloblastoma cells. The nature of infiltrativeness in AM-1 cells stimulates hypoxia-caused cell death and/or nutrient deficiencies with difficulty in medium penetration to cells deeper inside the construct, leads to unsteady growth of individual AM-1 cell and cell survival up to 14 days (Riffle *et al.*, 2017).

6.3 Co-culturing cells

The previous study by Eriksson *et al.* (2016) proposed the utility of the 3D *in vitro* model that incorporates AM tumour cells and human osteosarcoma (HOS) cells in the assessment of the impact of co-culture environment on AM tumour cells and their subsequent interactions on bone turnover. In the *in vitro* AM co-culture model developed by Eriksson *et al*., AM-1 cells seeded in collagen type I gel was placed next to 14-day-old bone-like scaffolds constructed from HOS cell line seeded in a separate collagen type I gel with acellular collagen gel as supporting layer formed the basis of the 3D cellularized model. However, a non-cancerous cell line is required to improve the 3D co-culture model in order to validate the AM growth and invasion. Therefore, an osteoblast model as developed in the present study by co-seeding both AM-1 cells and KUSA/A1 cells in a collagen type I gel aimed at investigating tumour-osteoblast interactions in order to gain some insights into the biological behaviour of this enigmatic neoplasm.

6.3.1 Evaluation of 3D *in vitro* osteoblast-AM co-culture model

Although it is evident that tumour-stroma crosstalk appears to play a significant role in tumour progression and resistance to therapeutic agents causes high attrition rate, few

in vitro models are available to examine these interactions in odontogenic tumours, especially ameloblastoma. 2D monocultures of AM tumour cells in which 3D co-culture set-up is lacking reduce its efficacy in minimizing the gap between *in vitro* cell culture models and their *in vivo* counterparts. Eriksson *et al.* (2016) have developed a novel *in vitro* AM organotypic co-cultures model for the characterization of AM tumour pathogenesis, growth and gene expression. Intriguingly, the model provided indications of AM towards bone absorption mechanism in the presence of human osteosarcoma cells. In the present work, AM co-culture model was developed from osteoblastic cell line to monitor intercellular interactions between the two cell types in the 3D *in vitro* co-culture setting and the role of these interactions on tumour progression. Data from the experiment comparing the AM co-culture model based on different pre-osteoblastic cell lines used putatively indicated that osteogenic differentiation rate exerts a differential impact on the interaction between tumour cells and osteoblasts. Using this model, it is revealed that osteogenic differentiation of osteoblastic cells potentially influences the tumour cell survival and therapeutic responses of the related therapeutic agents.

Upon co-cultivation of AM-1 tumour cells with different pre-osteoblastic cell lines in separate collagen gels, the morphology of the two cell types in the co-cultures was found to be from distinct sets of AM co-cultures. In fact, the co-culturing cells in some set of AM co-cultures arranged differently as monocultures indicating that there may be factors influencing the cell organization in co-cultures. In the present work, it is revealed that the organization of cells in AM-1 and KUSA/A1 co-culture can best address the tumour-osteoblast interaction in AM. As reported by Sellmyer *et al.* (2013), reporter cells in the *in vitro* co-culture assay, in closest proximity to the activator cells emitted the strongest signal. Accordingly, KUSA/A1 cells in close proximity neighbouring the AM-1 cells in the co-culture suggested that, cells within the matrix, in close proximity to each other can spatially catalyse the cellular interactions in co-culturing cells. Furthermore, cell-cell

direct physical contact was reported to play important roles in the mechanisms of cancer invasion through adhesion molecules such as N-cadherin (De Wever & Mareel, 2003). Hence, co-culture system was preferentially employed since it is possible for the study of cell-cell interactions by both paracrine and direct cell-cell contacts in cancer microenvironment, potentially contributes to the prognosis and testing of therapeutic responses of candidate drugs.

6.3.2 Effect of differentiation state of osteoblastic cells on AM co-cultures

KUSA/A1, MC3T3-E1 and ST2 apparently differed in calcium accumulation rates. KUSA/A1 form mineralized nodules 3 days after confluency in the inducing condition. However, MC3T3-E1 and ST2 cultured in the 2D culture system in the inducing condition formed these nodules on day 20 and day 24 after confluency. Although the absence of comparison between the calcium accumulation rate of pre-osteoblastic cells in 3D collagen gel, the difference in calcium accumulation rate of two-dimensionally-cultured cells indicated that the pre-osteoblast differentiation rate was remarkably different in distinct pre-osteoblastic cell lines. In the present study, we found that KUSA/A1 cells have the remarkable osteoblast differentiation rate amongst the pre-osteoblastic cells cultured in 3D collagen gel in inducing condition, which is consistent with the data obtained from 2D cultures. Further, our results demonstrated that AM co-cultures are best addressed by AM-1 and KUSA/A1 cells. These findings indicated that intercellular interaction between KUSA/A1 and AM-1 in the developed 3D co-culture model are enhanced during *in vitro* differentiation of KUSA/A1 that accompanied by expression of proteins that potentially promotes the survival and activation of AM-1 cells.

The secretion of soluble factors, such as cytokines and growth factors by tumour cells as well as the stromal cells into the microenvironment promotes tumour growth and invasiveness. Therefore, cell-to-cell communication through cytokines between stromal cells and tumour cells play important roles in providing a favourable microenvironment

favourable for tumour growth and progression. Interleukin-6 acts as a differentiation accelerator in pre-osteoblastic cells (Li *et al.*, 2008). A study conducted by Fuchigami *et al.* (2014) demonstrated that the *in vitro* cell-to-cell communications in ameloblastoma are activated reciprocally through IL-6. AM cells induce the surrounding osteoblasts to produced IL-6. Reciprocally, IL-6 from osteoblasts promoted the cellular motility and proliferation of AM cells. Taken together, these findings suggested that the increased expression of IL-6 receptor during *in vitro* differentiation of pre-osteoblastic cells could affect the extension of ameloblastomas. In conclusion, the differentiation of KUSA/A1 cells leads to the initiation of intercellular interactions between KUSA/A1 cells and AM-1 cells in the developed 3D *in vitro* culture model to provide a microenvironment that enhanced the invasion and growth of ameloblastoma.

6.4 Cell-mediated hydrogel contraction

Collagen I hydrogels have been the most common matrices used in 3D *in vitro* cell culture model and its mechanical properties is a popular measure of cell activation. In these models, the interplay of cell shape and cell-matrix interaction lead to cell-mediated gel contraction and the subsequent changes in cell volume. In the present work, control gels without cells did not shrink throughout the culture period. In contrast, collagen gels with higher cell seeding density shrank more rapidly and detached from the well walls. These results clearly indicated that the combined influence of cell proliferation and cell-matrix interaction on collagen gel contraction in a time-dependent manner. Hydrogels showed extensive shrinkage and reduction in gel volume after incubated for 21 days. As a result, cells seeded in these gels appeared unhealthy. Accordingly, these findings imply that massive shrinkage and reduction of gel volumes lead to considerable cell death causes the decrease in the number of viable cells. In explicit, hydrogels are capable of supporting survival of cultured cells even after gels started to condense and shrink. However, the increased stiffness of the gel as gel shrinks could have a significant effect on both

proliferation and differentiation of cultured cells (Mathieu & Loboa, 2012; Hwang *et al.*, 2015).

6.5 Validation of cell-cell interactions

6.5.1 Inhibition of osteogenic differentiation of pre-osteoblastic cells

We investigated the properties of pre-osteoblastic cell lines in 3D collagen gels. These cell lines have a unidirectional potential for osteogenesis in the inducing condition and their osteogenic potential were compared by mineralization activity. KUSA/A1 had a high ability for osteogenesis in the *in vitro* inducing condition. The osteogenic ability of KUSA/A1 was remarkable; it showed mineralization within 14 days in 3D collagen gel, whereas MC3T3-E1 and ST2 do not demonstrate any mineralized nodules over the culture time, indicated that these cell lines had a relatively low ability for osteogenesis. The rapid calcium deposition suggested that the KUSA/A1 completely differentiated into an osteoblastic cell with strong mineralization ability and high ALP activity of in the inducing condition.

KUSA/A1 showed reduced mineralization ability in co-culture construct with reduced mineralized matrix deposition, suggesting that the presence of AM-1 impairs osteoblast mineralization. In the present study, AM-1 cells within the collagen matrix in the 3D *in vitro* co-culture construct are morphologically and histochemically mimicking AM behaviour *in vivo*. The invasive nature of AM tumour cells was also demonstrated, in which AM tumour cells significantly reduced bone formation by interacting with the osteoblastic cells in the co-culture construct. These cell-to-cell contact-dependent mechanism mediated by cytokines directly act on osteoblastic cells in an autocrine/paracrine fashion and form a vicious cycle leading to extensive bone destruction and ameloblastoma cell expansion. A study conducted by Sathi *et al.* (2009) demonstrated that the secretion of sFRP-2 by ameloblastoma cells to the microenvironment is responsible for the decreased ALP activity and suppressed bone

formation in ameloblastoma disease. The sFRP-2 secreted by AM tumour cells probably blocks the canonical Wnt signalling, resulting in the continuation of cell proliferation without osteoblastic differentiation. In the developed 3D co-culture model, the co-culturing cells within the collagen matrix in close proximity to each other spatially catalyse the cellular interactions and stimulated cell-to-cell contact-dependent mechanism, which impairs the osteoblastic mineralization and plays a great effect on AM tumour growth and progression into the adjacent tissues and the cancellous bone.

6.5.2 Cellular nesting of AM tumour cell

The co-culture model for tumour-stromal interaction is advantageous and thus gained increasing attention because it allows physical contact between cells of interest and the subsequent homotypic communication and heterotypic interactions, increased physiological relevance of cellular microenvironment to their *in vivo* counterpart. Although conventional 2D monocultures have been for long the most popular *in vitro* models for cancer research, but only recently the *in vitro* 3D co-culture models have been used extensively to mimic the natural tumour microenvironment due to its physiological relevance. 3D co-culture model comprises of two different cell type of cancer tissues allows the evaluation of cell-cell interactions in these cancer microenvironments. The reciprocal interaction between breast cancer cell and cancer-associated fibroblasts (CAFs) in a 3D co-culture system promoted an increase in fibroblast membrane packing density and enhanced the fluidity of cancer cell membrane, determined a definite increment in tumour cell migration velocity and directionality (Angelucci *et al.*, 2011).

AM-1 cells within the collagen matrix in monoculture configuration are morphologically and histochemically mimicking epithelial cell, confirming the epithelial origin and epithelial nature of AM-1. AM-1 in co-culture construct has retained its epithelial nature and characteristics. Further, AM-1 showed tumour nest configuration in co-culture construct, suggested that the heterotypic cellular communication between AM-

1 and KUSA/A1 cells in the *in vitro* 3D co-culture construct. The physical contact between AM-1 and KUSA/A1 stimulates the subsequent heterotypic cellular communication, in which leads to the cellular nesting of AM-1 that tends to correlate with the aggressiveness of the tumour. Expectedly, the presence of tumour nest may predict a poor prognosis for the patient with AM. Further, these AM-1 tumour nest configurations may reflect the promotion of AM tumour cell proliferation and invasiveness as a result of strong interaction between tumour and host cells (Nakanishi *et al.*, 2001). Thus, cellular nesting of AM-1 is corresponded to the behaviour of tumour cells against stromal cells, indicated of active tumour-stromal interaction, correlated well with the aggressiveness of the AM tumour. Moreover, it is well acknowledged that the tumour nest tend to infiltrate among cancellous bone trabeculae at the tumour margin, reflective of the osteolytic ability and aggressive behaviour of AM (Zhong *et al.*, 2011). The *in vitro* 3D co-culture model as developed in the present study revealed the heterotypic interaction between two different cell types, AM-1 and KUSA/A1 in the collagen matrix in promoting AM tumour aggressiveness.

6.6 Osteogenic markers expression of 3D cultured osteoblastic cells

Bone-forming mononuclear osteoblasts are derived from undifferentiated mesenchymal precursor cells. There are three major stages of osteoblastogenesis in the osteoblastic cell: proliferation, matrix maturation and mineralization, characterized by the sequential expression of distinctive osteoblast markers. Osteopontin (OPN), bone sialoprotein (BSP) and osteocalcin (OCN) are the most frequently used markers of the osteoblast differentiation process. In general, BSP is the early marker of osteoblast differentiation, while OCN expressed later and concomitantly with mineralization. However, OPN is osteogenic marker expressed in the middle stage of differentiation that peaks twice, once during proliferation and in the later stages of differentiation (Huang *et al.*, 2007). In the present study, the characteristics of cultured KUSA/A1 cells are

mesenchymal origin and their mesenchymal nature are confirmed by strong immunoreactivity for vimentin in contrast to negative cytokeratin expression. Further, the differential expression of osteogenic markers, osteocalcin (OCN), osteopontin (OPN) and bone siaoloprotein (BSP) in KUSA/A1 monoculture indicates their stage of osteogenesis in 3D collagen gel. KUSA/A1 in 3-day culture showed BSP expression but negative OPN expression. In contrast, OCN deposition on the collagen matrix was negative, which may reflect early osteoblastic differentiation of cultured KUSA/A1 in the inducing condition. KUSA/A1 in 3D *in vitro* collagen gel matured over time, showed OPN and OCN deposition on the collagen gel in 14-day culture, which indicated the late stage of osteoblastic differentiation. The mesenchymal nature of KUSA/A1 retained in co-culture construct. However, lower OPN staining intensity and negative OCN deposition on the collagen gel in 14-day culture suggests the reduced osteogenesis ability of KUSA/A1 in co-culture construct. On the other hand, the characteristics of cultured AM-1 cells are epithelial origin and their epithelial nature are confirmed by strong immunoreactivity for cytokeratin in contrast to negative vimentin expression. The epithelial nature of AM-1 and mesenchymal nature of KUSA/A1 retained in co-culture construct. Osteocalcin, a major non-collagenous extracellular protein that play an important role in bone mineral deposition and its expression is restricted to osteoblasts. Surprisingly, OCN also expressed by AM-1 cells cultured in 3D collagen gel in the inducing condition. The heterogenous aberrant osteocalcin expression in AM-1 cultures suggest that AM-1 in collagen matrix in mineralization medium might stimulated osteocalcin promoter activity and that these increased promoter reporter activities corresponded with the endogenous OCN expression in *3D in vitro* cultured AM-1 cells (Gardner *et al.*, 2009).

6.7 Excessive osteoblast proliferation in co-culture construct

The canonical pathway (or Wnt/β-catenin pathway) is especially known to affect the differentiation of osteoblasts. Wnt inhibitors, secreted Frizzled-related proteins (sFRPs)

block the binding of Wnt ligands to the Frizzled (Fz) receptor, act either by binding directly to Wnts or form non-functional complexes by dimerizing with Fz proteins. The sFRPs prevent the nuclear translocation of the transcriptional regulator, β-catenin, resulting in the inactivation of the canonical Wnt signalling pathway and the subsequent inhibition of osteoblastic differentiation.

The relative ratio of AM-1 cell and KUSA/A1 cell in the 3D *in vitro* co-culture construct suggested the excessive proliferation of KUSA/A1 in the presence of AM-1, which is in consistent with the study conducted by Sathi *et al.* (2009) demonstrated that KUSA/A1 cells cultured in conditioned medium of AM-1 showed high cell proliferation. In the present study, it suggests that the heterotypic cellular interaction between KUSA/A1 and AM-1 as a consequence of physical contact through the expression of cytokines in AM-1 that served as an important factor responsible for suppressed osteoblastogenesis in KUSA/A1. Sathi *et al.* (2009) reported that depletion of sFRP-2 in conditioned medium of AM-1 rescued the KUSA/A1-mediated matrix mineralization. Further, sFRP-2 was reported to inhibit apoptosis in the mammary tumour (Lee *et al.*, 2004). Collectively, the relative abundance of KUSA/A1 in the co-culture construct indicates the excessive proliferation of KUSA/A1 in the presence of AM-1. The intercellular interaction between KUSA/A1 and AM-1 potentially activated the expression of cytokine, for instance, sFRP-2 that acts in both autocrine and paracrine manner blocking the Wnt/β-catenin pathway, halted osteoblast differentiation into mature osteoblasts and reduced apoptosis, leading KUSA/A1 cells to continue to proliferate excessively without differentiation. Taken together, the present study emphasizes the relevance of intercellular interaction between osteoblast and AM tumour cell in ameloblastoma towards the tumorigenesis.

6.8 Limitations

6.8.1 3D gel substrate

Collagen-containing scaffolds were superior compared to the hydrogel in supporting the survival and characterization of the cultured cells. In addition, collagen is the major organic component of bone matrix and therefore collagen scaffold could effectively function as a suitable scaffold in a bone environment. However, the rigidity of the collagen gel has a great effect on the cell motility across the gel. Therefore, the concentration of collagen needs to undertake to ensure the motility of cells in the collagen gel for direct physical contact with one another and the subsequent cell-to-cell interactions.

6.8.2 Cell seeding densities

In the present study, initial experiments with varying KUSA/A1 cell seeding densities were undertaken. The outcome of the work clearly indicated that different cell seeding densities performed distinctively in the 3D *in vitro* model. However, it is laborious and difficult to determine the optimal seeding density into the 3D collagen gel as developed. In a co-culture system, the population ratio and the evenly distribution of cells within the scaffold are the key challenges. It is crucial to ensure the even distribution of cells throughout the 3D collagen gel at the time of set up to accurately model the intercellular interaction between the co-cultured cells. Therefore, further work is required to optimize the cell seeding density for the developed 3D *in vitro* model with optimal tumour-osteoblast heterotypic cellular communication without gel shrinkage.

6.8.3 Penetration of medium into gels

The exposed surface area of the culture substrate possibly modulated the diffusion of culture medium in the vicinity of the cultured cells in 3D collagen gel. The cellular behaviour and morphology of cells in different exposed surface area were compared and a larger surface area is corresponding to the physiological relevance of the cultured cell

to their *in vivo* counterparts. Further work requires to undertake the exposed surface are of culture substrate to ensure the optimization of the penetration of culture medium within the collagen scaffold for the growth of cultured cells.

6.8.4 Interspecies differences

Findings in the present study have intrinsic limitations. This preliminary study is influenced by the identities of the cell types being studied, and other pairs of human-mouse ameloblastoma-osteoblast cell populations might exhibit greater or lesser differences than the pairs of cells in the present work. These interspecies differences may compromise or confound attempts at relating the cellular interaction between ameloblastoma tumour cells and osteoblastic cells. Despite of interspecies effects, the potential significance of these findings is indicated by the observations that the osteogenesis ability of osteoblastic cells used here may be key concerning to the aggressiveness of ameloblastoma tumour cells. In order to increase the physiological relevance of the present study to the *in vivo* ameloblastoma tumour microenvironment, an improved version of the *in vitro* 3D AM co-culture model with eliminated interspecies differences is required to address the biologically appropriate cell-to-cell interactions and to examine the stimulatory effects of these interactions on the osteogenesis ability of osteoblastic cells and ameloblastoma growth and progression, which would have a significant prognostic and therapeutic benefit.

6.9 Future studies

The present work describes the development of a 3D *in vitro* culture model of AM. Collagen, an abundant extracellular matrix protein in the bone and hence it served as the basis for the culture model in the present study. This 3D *in vitro* culture model of AM enables the characterization of tumour-stromal interaction in AM towards the tumorigenesis. In addition, KUSA/A1 cells in the collagen gel provided a model closely reflect the osteoblastic differentiation of the osteoblastic cell.

The present study provides indications of AM towards the destruction of bone remodelling as we have shown a reduced mineralized matrix and the presence of cellular nesting in the AM co-culture. Nonetheless, further studies are necessary in order to pin-point a specific cytokines or growth factors interplay of AM tumour cell and osteoblast interactions. Additionally, the levels of gene expression related to the osteoblastic differentiation, bone remodelling, invasiveness and/or aggressive of AM in the co-cultures are also needed to implicate the role of tumour-stromal interaction in AM tumour growth and progression. Nevertheless, the incorporation of the developed AM-1 co-cultures into mouse calvaria is important to validate the physiological relevance of the findings discovered via the 3D *in vitro* model in a relevant *in vivo* model, taking into account the intercellular interactions of the additional host cell types in the tumour microenvironment, endocrine effect of growth factors and cytokines, immune reaction and specific physiological conditions that able to influence the tumour-stromal interactions in the AM.

CHAPTER 7: CONCLUSION

The present study reveals for the first time, the intercellular communication between ameloblastoma tumour cell and osteoblast. Topographic closeness as observed in the co-culture model indicates the presence of heterotypic cell-cell interaction between tumour cell and osteoblast.

Amongst the *in vitro* 3D co-culture model developed, only AM-1/KUSA-A1 co-culture model demonstrated an optimal cell growth and cell-cell communication that found absence in other models. Furthermore, ameloblastoma tumour cells in this model are morphologically and behaviourally mimicking AM *in vivo*, indicated the suitability of AM-1/KUSA-A1 co-culture model as the best *in vitro* 3D co-culture model in reflecting the ameloblastoma-stromal interactions in ameloblastoma disease.

Intercellular communication between ameloblastoma tumour cell and stroma creates a local microenvironment that has a promotive effect on tumour survival and tumour cell growth but growth inhibitory effect on osteoblasts. These ameloblastoma-osteoblast interactions also induce morphodifferentiation of ameloblastoma tumour cells and contribution to the deregulation osteoclastogenesis and thus the subsequent altered local bone metabolism. A working model can be proposed to demonstrate the intercellular interaction between ameloblastoma tumour cells and osteoblast and the outcome of this interaction on morphological and behavioural changes of participating cells (Figure 7.1).

In conclusion, the present study successfully established an *in vitro* 3D co-culture system to stimulate an amelobastoma disease model. This model provides insights into the tumour-osteoblast interactions and the contribution of these interactions on tumoral growth and bone turnover of this enigmatic neoplasm.

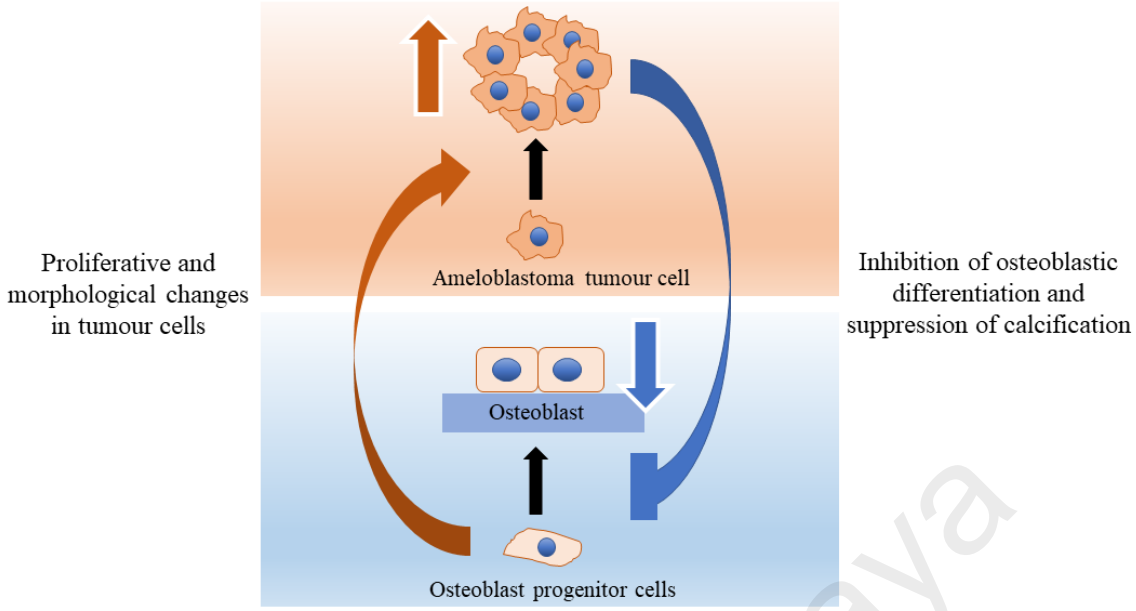

Figure 7.1: A proposed model of ameloblastoma-osteoblast interaction.

Schematic representation of the cellular interaction between AM tumour cells and pre-osteoblastic cells and the subsequent outcome of the interaction on morphological and behavioural changes.

REFERENCES

Adebayo, E. T., Ajike, S. O., & Adekeye, E. O. (2005). A review of 318 odontogenic tumors in Kaduna, Nigeria. *J Oral Maxillofac Surg, 63*(6), 811-819. doi:10.1016/j.joms.2004.03.022

Allegra, C. J., Jessup, J. M., Somerfield, M. R., Hamilton, S. R., Hammond, E. H., Hayes, D. F., . . . Schilsky, R. L. (2009). American Society of Clinical Oncology Provisional Clinical Opinion: Testing for KRAS Gene Mutations in Patients With Metastatic Colorectal Carcinoma to Predict Response to Anti–Epidermal Growth Factor Receptor Monoclonal Antibody Therapy. *J Clin Oncol, 27*(12), 2091-2096. doi:10.1200/jco.2009.21.9170

Altman, D. G., & Bland, J. M. (2009). Parametric v non-parametric methods for data analysis. *Bmj, 338*, a3167. doi:10.1136/bmj.a3167

Alturkistani, H. A., Tashkandi, F. M., & Mohammedsaleh, Z. M. (2016). Histological Stains: A Literature Review and Case Study. *Global Journal of Health Science, 8*(3), 72-79. doi:10.5539/gjhs.v8n3p72

Andrade, F. R., Sousa, D. P., Mendonca, E. F., Silva, T. A., Lara, V. S., & Batista, A. C. (2008). Expression of bone resorption regulators (RANK, RANKL, and OPG) in odontogenic tumors. *Oral Surg Oral Med Oral Pathol Oral Radiol Endod, 106*(4), 548-555. doi:10.1016/j.tripleo.2008.05.042

Angadi, P. V. (2011). Head and Neck: Odontogenic tumor: Ameloblastoma. *Atlas Genet Cytogenet Oncol Haematol, 15*(2), 223-229.

Angelucci, C., Lama, G., Proietti, G., Fabbri, C., Masetti, R., Sica, G., & Maulucci, G. (2011). Breast cancer cells and fibroblasts in co-culture: reciprocal influences on cell adhesion, membrane fluidity and migration. *Ital J Anat Embryo, 116*(2), 12. doi:10.13128/IJAE-9962

Antoni, D., Burckel, H., Josset, E., & Noel, G. (2015). Three-dimensional cell culture: a breakthrough in vivo. *Int J Mol Sci, 16*(3), 5517-5527. doi:10.3390/ijms16035517

Arotiba, J. T., Ogunbiyi, J. O., & Obiechina, A. E. (1997). Odontogenic tumours: a 15-year review from Ibadan, Nigeria. *Br J Oral Maxillofac Surg, 35*(5), 363-367. doi:http://dx.doi.org/10.1016/S0266-4356(97)90411-3

Aubin, J. E. (2001). Regulation of osteoblast formation and function. *Rev Endocr Metab Disord, 2*(1), 81-94.

Ayoub, M. S., Elmalahy, M. H., & Elshafei, M. M. (2011). Expression of human papilloma virus and epstein barrvirus in benign and malignant ameloblastoma. *Int J Acad Res, 3*(2), 23-37.

Baker, B. M., & Chen, C. S. (2012). Deconstructing the third dimension: how 3D culture microenvironments alter cellular cues. *J Cell Sci, 125*(Pt 13), 3015-3024. doi:10.1242/jcs.079509

Bokhari, M., Carnachan, R. J., Cameron, N. R., & Przyborski, S. A. (2007). Culture of HepG2 liver cells on three dimensional polystyrene scaffolds enhances cell structure and function during toxicological challenge. *J Anat, 211*(4), 567-576. doi:10.1111/j.1469-7580.2007.00778.x

Boyce, B. F., & Xing, L. (2007a). Biology of RANK, RANKL, and osteoprotegerin. *Arthritis Res Ther, 9*(Suppl 1), S1-S1. doi:10.1186/ar2165

Boyce, B. F., & Xing, L. (2007b). The RANKL/RANK/OPG pathway. *Curr Osteoporos Rep, 5*(3), 98-104.

Bratthauer, G. L. (1995). The Peroxidase-Antiperoxidase (PAP) Method. In L. C. Javois (Ed.), *Immunocytochemical Methods and Protocols* (pp. 165-173). Totowa, NJ: Humana Press.

Bratthauer, G. L. (2010). The avidin-biotin complex (ABC) method and other avidin-biotin binding methods. *Methods Mol Biol, 588*, 257-270. doi:10.1007/978-1-59745-324-0_26

Celli, J. P. (2012). Stromal interactions as regulators of tumor growth and therapeutic response: A potential target for photodynamic therapy? *Israel journal of chemistry, 52*(8-9), 757-766. doi:10.1002/ijch.201200013

Chantravekin, Y., & Koontongkaew, S. (2014). Effects of ameloblastoma-associated fibroblasts on the proliferation and invasion of tumor cells. *J Cancer Res Ther, 10*(4), 1082-1087. doi:10.4103/0973-1482.138005

Chellaiah, M. A., Kizer, N., Biswas, R., Alvarez, U., Strauss-Schoenberger, J., Rifas, L., . . . Hruska, K. A. (2003). Osteopontin deficiency produces osteoclast dysfunction due to reduced CD44 surface expression. *Mol Biol Cell, 14*(1), 173-189. doi:10.1091/mbc.E02-06-0354

Chen, J., McKee, M. D., Nanci, A., & Sodek, J. (1994). Bone sialoprotein mRNA expression and ultrastructural localization in fetal porcine calvarial bone: comparisons with osteopontin. *Histochem J, 26*(1), 67-78. doi:10.1007/bf00209251

Chen, J., Shapiro, H. S., & Sodek, J. (1992). Developmental expression of bone sialoprotein mRNA in rat mineralized connective tissues. *J Bone Miner Res, 7*(8), 987-997. doi:10.1002/jbmr.5650070816

Chen, X., Cho, D.-B., & Yang, P.-C. (2010). Double staining immunohistochemistry. *North American Journal of Medical Sciences, 2*(5), 241-245. doi:10.4297/najms.2010.2241

Chuang, F. H., Hsue, S. S., Wu, C. W., & Chen, Y. K. (2009). Immunohistochemical expression of RANKL, RANK, and OPG in human oral squamous cell carcinoma. *J Oral Pathol Med, 38*(10), 753-758. doi:10.1111/j.1600-0714.2009.00793.x

Cichon, M. A., Gainullin, V. G., Zhang, Y., & Radisky, D. C. (2012). Growth of lung cancer cells in three-dimensional microenvironments reveals key features of tumor malignancy. *Integr Biol (Camb), 4*(4), 440-448. doi:10.1039/c1ib00090j

da Silva, T. A., Batista, A. C., Mendonca, E. F., Leles, C. R., Fukada, S., & Cunha, F. Q. (2008). Comparative expression of RANK, RANKL, and OPG in keratocystic odontogenic tumors, ameloblastomas, and dentigerous cysts. *Oral Surg Oral Med Oral Pathol Oral Radiol Endod, 105*(3), 333-341. doi:10.1016/j.tripleo.2007.06.009

de Matos, F. R., de Moraes, M., das Neves Silva, E. B., Galvao, H. C., & de Almeida Freitas, R. (2013). Immunohistochemical detection of receptor activator nuclear kappaB ligand and osteoprotegerin in odontogenic cysts and tumors. *J Oral Maxillofac Surg, 71*(11), 1886-1892. doi:10.1016/j.joms.2013.05.023

De Wever, O., & Mareel, M. (2003). Role of tissue stroma in cancer cell invasion. *J Pathol, 200*(4), 429-447. doi:10.1002/path.1398

Del Fattore, A., Teti, A. M., & Rucci, N. (2012). Bone cells and the mechanisms of bone remodelling. *Frontiers in bioscience, 4*, 2302-2321.

Duong, H. S., Le, A. D., Zhang, Q., & Messadi, D. V. (2005). A novel 3-dimensional culture system as an in vitro model for studying oral cancer cell invasion. *Int J Exp Pathol, 86*(6), 365-374. doi:10.1111/j.0959-9673.2005.00441.x

Easton, D. F., Ford, D., & Bishop, D. T. (1995). Breast and ovarian cancer incidence in BRCA1-mutation carriers. Breast Cancer Linkage Consortium. *Am J Hum Genet, 56*(1), 265-271.

Edmondson, R., Broglie, J. J., Adcock, A. F., & Yang, L. (2014). Three-Dimensional Cell Culture Systems and Their Applications in Drug Discovery and Cell-Based Biosensors. *Assay Drug Dev Technol, 12*(4), 207-218. doi:10.1089/adt.2014.573

El-Jawhari, J. J., Sanjurjo-Rodriguez, C., Jones, E., & Giannoudis, P. V. (2016). Collagen-containing scaffolds enhance attachment and proliferation of non-cultured bone marrow multipotential stromal cells. *J Orthop Res, 34*(4), 597-606. doi:10.1002/jor.23070

Eriksson, T. M., Day, R. M., Fedele, S., & Salih, V. M. (2016). The regulation of bone turnover in ameloblastoma using an organotypic in vitro co-culture model. *J Tissue Eng, 7*, 2041731416669629. doi:10.1177/2041731416669629

Fawcett, T. (2013). Matrices for Cell Culture - How to develop healthy attachment. What are the differences, advantages/disadvantages to 3-D matrices? . Retrieved from http://cellculturedish.com/ask-the-expert/matrices-for-cell-culture-how-to-develop-healthy-attachment/

Ferrera, D., Poggi, S., Biassoni, C., Dickson, G. R., Astigiano, S., Barbieri, O., . . . Manduca, P. (2002). Three-dimensional cultures of normal human osteoblasts: proliferation and differentiation potential in vitro and upon ectopic implantation in nude mice. *Bone, 30*(5), 718-725. doi:https://doi.org/10.1016/S8756-3282(02)00691-9

Fischbach, C., Kong, H. J., Hsiong, S. X., Evangelista, M. B., Yuen, W., & Mooney, D. J. (2009). Cancer cell angiogenic capability is regulated by 3D culture and integrin engagement. *Proc Natl Acad Sci U S A, 106*(2), 399-404. doi:10.1073/pnas.0808932106

Fong, E. L., Wan, X., Yang, J., Morgado, M., Mikos, A. G., Harrington, D. A., . . . Farach-Carson, M. C. (2016). A 3D in vitro model of patient-derived prostate cancer xenograft for controlled interrogation of in vivo tumor-stromal interactions. *Biomaterials, 77*, 164-172. doi:10.1016/j.biomaterials.2015.10.059

Fridman, A. L., & Tainsky, M. A. (2008). Critical pathways in cellular senescence and immortalization revealed by gene expression profiling. *Oncogene, 27*(46), 5975-5987. doi:http://www.nature.com/onc/journal/v27/n46/suppinfo/onc2008213s1.html

Fuchigami, T., Kibe, T., Koyama, H., Kishida, S., Iijima, M., Nishizawa, Y., . . . Kishida, M. (2014). Regulation of IL-6 and IL-8 production by reciprocal cell-to-cell interactions between tumor cells and stromal fibroblasts through IL-1alpha in ameloblastoma. *Biochem Biophys Res Commun, 451*(4), 491-496. doi:10.1016/j.bbrc.2014.07.137

Fukumoto, S., Kiba, T., Hall, B., Iehara, N., Nakamura, T., Longenecker, G., . . . Yamada, Y. (2004). Ameloblastin is a cell adhesion molecule required for maintaining the differentiation state of ameloblasts. *J Cell Biol, 167*(5), 973-983. doi:10.1083/jcb.200409077

Gardner, D. G., & Corio, R. L. (1984). Plexiform unicystic ameloblastoma. A variant of ameloblastoma with a low-recurrence rate after enucleation. *Cancer, 53*(8), 1730-1735.

Gardner, T. A., Lee, S. J., Lee, S. D., Li, X., Shirakawa, T., Kwon, D. D., . . . Jung, C. (2009). Differential expression of osteocalcin during the metastatic progression of prostate cancer. *Oncol Rep, 21*(4), 903-908.

Garg, K., Chandra, S., Raj, V., Fareed, W., & Zafar, M. (2015). Molecular and genetic aspects of odontogenic tumors: a review. *Iran J Basic Med Sci, 18*(6), 529-536.

Gordon, J. A., Tye, C. E., Sampaio, A. V., Underhill, T. M., Hunter, G. K., & Goldberg, H. A. (2007). Bone sialoprotein expression enhances osteoblast differentiation and matrix mineralization in vitro. *Bone, 41*(3), 462-473. doi:10.1016/j.bone.2007.04.191

Güler, N., Şençift, K., & Demirkol, Ö. (2012). Conservative Management of Keratocystic Odontogenic Tumors of Jaws. *Sci World J, 2012*, 680397. doi:10.1100/2012/680397

Günhan, Ö., Erseven, G., Ruacan, Ş., Celasun, B., Aydintug, Y., Ergun, E., & Demiriz, M. (1990). Odontogenic tumours. A series of 409 cases. *Aust Dent J, 35*(6), 518-522. doi:10.1111/j.1834-7819.1990.tb04683.x

Harada, H., Mitsuyasu, T., Nakamura, N., Higuchi, Y., Toyoshima, K., Taniguchi, A., & Yasumoto, S. (1998). Establishment of ameloblastoma cell line, AM-1. *J Oral Pathol Med, 27*(5), 207-212.

Härmä, V., Virtanen, J., Mäkelä, R., Happonen, A., Mpindi, J.-P., Knuuttila, M., . . . Nees, M. (2010). A Comprehensive Panel of Three-Dimensional Models for Studies of Prostate Cancer Growth, Invasion and Drug Responses. *PLOS ONE, 5*(5), e10431. doi:10.1371/journal.pone.0010431

Huang, F., Shen, Q., & Zhao, J. (2013). Growth and differentiation of neural stem cells in a three-dimensional collagen gel scaffold. *Neural Regen Res, 8*(4), 313-319. doi:10.3969/j.issn.1673-5374.2013.04.003

Huang, W., Yang, S., Shao, J., & Li, Y.-P. (2007). Signaling and transcriptional regulation in osteoblast commitment and differentiation. *Front Biosci, 12*, 3068-3092.

Hulka, B. S. (1990). Overview of biological markers. In B. S. Hulka, J. D. Griffith, & T. C. Wilcosky (Eds.), *Biological markers in epidemiology* (pp. 3–15). New York: Oxford University Press.

Hwang, J. H., Byun, M. R., Kim, A. R., Kim, K. M., Cho, H. J., Lee, Y. H., . . . Hong, J. H. (2015). Extracellular Matrix Stiffness Regulates Osteogenic Differentiation through MAPK Activation. *PLoS One, 10*(8), e0135519. doi:10.1371/journal.pone.0135519

Isomura, E. T., Okura, M., Ishimoto, S., Yamada, C., Ono, Y., Kishino, M., & Kogo, M. (2009). Case report of extragingival peripheral ameloblastoma in buccal mucosa. *Oral Surg Oral Med Oral Pathol Oral Radiol Endod, 108*(4), 577-579. doi:10.1016/j.tripleo.2009.06.023

Johnson, N. R., Gannon, O. M., Savage, N. W., & Batstone, M. D. (2014). Frequency of odontogenic cysts and tumors: a systematic review. *J Investig Clin Dent, 5*(1), 9-14. doi:10.1111/jicd.12044

Kasamatsu, T., Kitano, Y., & Ohbayashi, H. (2010). [Application of polymer detection systems of Histofine MOUSESTAIN, Mouse MAX-PO and rat MAX-PO for mouse and rat frozen tissue sections]. *Rinsho Byori, 58*(12), 1181-1187.

Kawashima, N., Shindo, K., Sakamoto, K., Kondo, H., Umezawa, A., Kasugai, S., . . . Katsube, K.-i. (2005). Molecular and cell biological properties of mouse osteogenic mesenchymal progenitor cells, Kusa. *J Bone Miner Metab, 23*(2), 123-133. doi:10.1007/s00774-004-0550-y

Kayamori, K., Sakamoto, K., Nakashima, T., Takayanagi, H., Morita, K., Omura, K., . . . Yamaguchi, A. (2010). Roles of interleukin-6 and parathyroid hormone-related peptide in osteoclast formation associated with oral cancers: significance of interleukin-6 synthesized by stromal cells in response to cancer cells. *Am J Pathol, 176*(2), 968-980. doi:10.2353/ajpath.2010.090299

Khaitan, D., Chandna, S., Arya, M. B., & Dwarakanath, B. S. (2006). Establishment and characterization of multicellular spheroids from a human glioma cell line; Implications for tumor therapy. *Journal of Translational Medicine, 4*, 12-12. doi:10.1186/1479-5876-4-12

Khosla, S. (2001). Minireview: the OPG/RANKL/RANK system. *Endocrinology, 142*(12), 5050-5055. doi:10.1210/endo.142.12.8536

Kim, Y., & Othmer, H. G. (2013). A hybrid model of tumor-stromal interactions in breast cancer. *Bull Math Biol, 75*(8), 1304-1350. doi:10.1007/s11538-012-9787-0

Klimkiewicz, K., Weglarczyk, K., Collet, G., Paprocka, M., Guichard, A., Sarna, M., . . . Kieda, C. (2017). A 3D model of tumour angiogenic microenvironment to monitor hypoxia effects on cell interactions and cancer stem cell selection. *Cancer Lett, 396*, 10-20. doi:https://doi.org/10.1016/j.canlet.2017.03.006

Knight, E., & Przyborski, S. (2014). Method for Simple and Routine Three-Dimensional Cell Culture. In J. Haycock, A. Ahluwalia, & J. M. Wilkinson (Eds.), *Cellular In Vitro Testing - Methods and Protocols* (pp. 149-162). USA: Pan Stanford Publishing Pte. Ltd.

Kodama, H.-a., Amagai, Y., Sudo, H., Kasai, S., & Yamamoto, S. (1981). Establishment of a clonal osteogenic cell line from newborn mouse calvaria. *Jpn J Oral Biol, 23*(4), 899-901. doi:10.2330/joralbiosci1965.23.899

Kohli, S. S., & Kohli, V. S. (2011). Role of RANKL–RANK/osteoprotegerin molecular complex in bone remodeling and its immunopathologic implications. *Indian J Endocrinol Metab, 15*(3), 175-181. doi:10.4103/2230-8210.83401

Kumamoto, H., & Ooya, K. (2004). Expression of parathyroid hormone-related protein (PTHrP), osteoclast differentiation factor (ODF)/receptor activator of nuclear factor-kappaB ligand (RANKL) and osteoclastogenesis inhibitory factor (OCIF)/osteoprotegerin (OPG) in ameloblastomas. *J Oral Pathol Med, 33*(1), 46-52.

Kumamoto, H., & Ooya, K. (2005). Immunohistochemical detection of beta-catenin and adenomatous polyposis coli in ameloblastomas. *J Oral Pathol Med, 34*(7), 401-406. doi:10.1111/j.1600-0714.2005.00328.x

Ladeinde, A. L., Ajayi, O. F., Ogunlewe, M. O., Adeyemo, W. L., Arotiba, G. T., Bamgbose, B. O., & Akinwande, J. A. (2005). Odontogenic tumors: a review of 319 cases in a Nigerian teaching hospital. *Oral Surg Oral Med Oral Pathol Oral Radiol Endod, 99*(2), 191-195. doi:10.1016/j.tripleo.2004.08.031

Larsson, A., & Almeren, H. (1978). Ameloblastoma of the jaws. An analysis of a consecutive series of all cases reported to the Swedish Cancer Registry during 1958--1971. *Acta Pathol Microbiol Scand A, 86a*(5), 337-349.

Lau, S. L., & Samman, N. (2006). Recurrence related to treatment modalities of unicystic ameloblastoma: a systematic review. *Int J Oral Maxillofac Surg, 35*(8), 681-690. doi:10.1016/j.ijom.2006.02.016

Lee, J.-L., Lin, C.-T., Chueh, L.-L., & Chang, C.-J. (2004). Autocrine/paracrine secreted Frizzled-related protein 2 induces cellular resistance to apoptosis: a possible mechanism of mammary tumorigenesis. *J Biol Chem, 279*(15), 14602-14609. doi:10.1074/jbc.M309008200

Li, T., Wu, Y., Yu, S., & Yu, G. (2002). Clinicopathological features of unicystic ameloblastoma with special reference to its recurrence. *Zhonghua Kou Qiang Yi Xue Za Zhi, 37*(3), 210-212.

Li, Y., Backesjo, C. M., Haldosen, L. A., & Lindgren, U. (2008). IL-6 receptor expression and IL-6 effects change during osteoblast differentiation. *Cytokine, 43*(2), 165-173. doi:10.1016/j.cyto.2008.05.007

Lian, N., Wang, W., Li, L., Elefteriou, F., & Yang, X. (2009). Vimentin inhibits ATF4-mediated osteocalcin transcription and osteoblast differentiation. *J Biol Chem, 284*(44), 30518-30525. doi:10.1074/jbc.M109.052373

Lin, R. Z., & Chang, H. Y. (2008). Recent advances in three-dimensional multicellular spheroid culture for biomedical research. *Biotechnol J, 3*(9-10), 1172-1184. doi:10.1002/biot.200700228

Lin, S. C., Lieu, C. M., Hahn, L. J., & Kwan, H. W. (1987). Peripheral ameloblastoma with metastasis. *Int J Oral Maxillofac Surg, 16*(2), 202-204.

Liu, X.-q., Kiefl, R., Roskopf, C., Tian, F., & Huber, R. M. (2016). Interactions among Lung Cancer Cells, Fibroblasts, and Macrophages in 3D Co-Cultures and the Impact on MMP-1 and VEGF Expression. *PLOS ONE, 11*(5), e0156268. doi:10.1371/journal.pone.0156268

Locker, G. Y., Hamilton, S., Harris, J., Jessup, J. M., Kemeny, N., Macdonald, J. S., . . . Jr, R. C. B. (2006). ASCO 2006 Update of Recommendations for the Use of Tumor Markers in Gastrointestinal Cancer. *J Clin Oncol, 24*(33), 5313-5327. doi:10.1200/jco.2006.08.2644

Lu, Y., Xuan, M., Takata, T., Wang, C., He, Z., Zhou, Z., . . . Nikai, H. (1998). Odontogenic tumors. A demographic study of 759 cases in a Chinese population. *Oral Surg Oral Med Oral Pathol Oral Radiol Endod, 86*(6), 707-714.

Luis-Ravelo, D., Antón, I., Vicent, S., Hernández, I., Valencia, K., Zandueta, C., . . . Lecanda, F. (2011). Tumor-stromal interactions of the bone microenvironment: in vitro findings and potential in vivo relevance in metastatic lung cancer models. *Clinical & experimental metastasis, 28*(8), 779-791. doi:10.1007/s10585-011-9409-5

Lundberg, A. S., Hahn, W. C., Gupta, P., & Weinberg, R. A. (2000). Genes involved in senescence and immortalization. *Curr Opin Cell Biol, 12*(6), 705-709.

Luo, H. Y., & Li, T. J. (2009). Odontogenic tumors: a study of 1309 cases in a Chinese population. *Oral Oncol, 45*(8), 706-711. doi:10.1016/j.oraloncology.2008.11.001

Martina, J. D., Simmons, C., & Jukic, D. M. (2011). High-definition hematoxylin and eosin staining in a transition to digital pathology. *Journal of Pathology Informatics, 2*, 45. doi:10.4103/2153-3539.86284

Mathieu, P. S., & Loboa, E. G. (2012). Cytoskeletal and Focal Adhesion Influences on Mesenchymal Stem Cell Shape, Mechanical Properties, and Differentiation Down Osteogenic, Adipogenic, and Chondrogenic Pathways. *Tissue Eng Part B Rev, 18*(6), 436-444. doi:10.1089/ten.teb.2012.0014

Matthews, B. G., Naot, D., Callon, K. E., Musson, D. S., Locklin, R., Hulley, P. A., . . . Cornish, J. (2014). Enhanced osteoblastogenesis in three-dimensional collagen gels. *BoneKEy Rep, 3*. doi:10.1038/bonekey.2014.55

Meghj, S., Sandy, J. R., & Harris, M. (1998). Bone remodelling - cellular and biochemical aspects. In M. Harris, M. Edgar, & S. Meghji (Eds.), *Clinical Oral Science* (pp. 85-94). Oxford, Boston: Wright.

Nakanishi, Y., Ochiai, A., Kato, H., Tachimori, Y., Igaki, H., & Hirohashi, S. (2001). Clinicopathological significance of tumor nest configuration in patients with esophageal squamous cell carcinoma. *Cancer, 91*(6), 1114-1120.

Nalabolu, G. R. K., Mohiddin, A., Hiremath, S. K. S., Manyam, R., Bharath, T. S., & Raju, P. R. (2017). Epidemiological study of odontogenic tumours: An institutional experience. *J Infect Public Health, 10*(3), 324-330. doi:https://doi.org/10.1016/j.jiph.2016.05.014

Naylor, S. (2003). Biomarkers: current perspectives and future prospects. *Expert Rev Mol Diagn, 3*(5), 525-529. doi:10.1586/14737159.3.5.525

Nurhayu Ab Rahman. (2014). Oral and maxillofacial pathologic lesion: Retrospective studies on prevalence and sociodemographic features. *Arch Orofac Sci, 9*(2), 65-75.

Otsuka, E., Yamaguchi, A., Hirose, S., & Hagiwara, H. (1999). Characterization of osteoblastic differentiation of stromal cell line ST2 that is induced by ascorbic acid. *Am J Physiol, 277*(1), C132-C138.

Ottewell, P. D. (2016). The role of osteoblasts in bone metastasis. *Journal of Bone Oncology, 5*(3), 124-127. doi:10.1016/j.jbo.2016.03.007

Pal, S. K., Sakamoto, K., Aragaki, T., Akashi, T., & Yamaguchi, A. (2013). The expression profiles of acidic epithelial keratins in ameloblastoma. *Oral Surg Oral Med Oral Pathol Oral Radiol, 115*(4), 523-531. doi:10.1016/j.oooo.2013.01.017

Peschon, J. J., Behringer, R. R., Cate, R. L., Harwood, K. A., Idzerda, R. L., Brinster, R. L., & Palmiter, R. D. (1992). Directed expression of an oncogene to Sertoli cells in transgenic mice using mullerian inhibiting substance regulatory sequences. *Mol Endocrinol, 6*(9), 1403-1411. doi:10.1210/mend.6.9.1331774

Philipsen, H. P., Reichart, P. A., Slootweg, P. J., & Slater, L. J. (2005). Neoplasms and tumour-like lesions arising from the odontogenic apparatus and maxillofacial skeleton: Introduction. In L. Barnes, J. W. Eveson, P. A. Reichart, & D. Sidransky (Eds.), *World Health Organization Classification of Tumours. Pathology and Genetics of Tumours of the Head and Neck* (3rd ed., pp. 285–286). Lyon, France: IARC.

Pogrel, M. A., & Montes, D. M. (2009). Is there a role for enucleation in the management of ameloblastoma? *Int J Oral Maxillofac Surg, 38*(8), 807-812. doi:10.1016/j.ijom.2009.02.018

Pogrel, M. A., Schmidt, B. L., & Robertson, C. G. (2006). Clinical Pathology: Odontogenic and Nonodontogenic Tumors of the Jaws. In P. W. Booth, S. A. Schendel, & J. E. Hausamen (Eds.), *Maxillofacial Surgery* (Vol. 2nd, pp. 490–534). Churchill Livingstone: Edinburgh, UK.

Prideaux, M., Wijenayaka, A. R., Kumarasinghe, D. D., Ormsby, R. T., Evdokiou, A., Findlay, D. M., & Atkins, G. J. (2014). SaOS2 Osteosarcoma cells as an in vitro model for studying the transition of human osteoblasts to osteocytes. *Calcif Tissue Int, 95*(2), 183-193. doi:10.1007/s00223-014-9879-y

Proff, P., & Romer, P. (2009). The molecular mechanism behind bone remodelling: a review. *Clin Oral Investig, 13*(4), 355-362. doi:10.1007/s00784-009-0268-2

Puchtler, H., Meloan, S. N., & Terry, M. S. (1969). On the history and mechanism of alizarin and alizarin red S stains for calcium. *J Histochem Cytochem, 17*(2), 110-124. doi:10.1177/17.2.110

Qian, Y., & Huang, H. Z. (2010). The role of RANKL and MMP-9 in the bone resorption caused by ameloblastoma. *J Oral Pathol Med, 39*(8), 592-598. doi:10.1111/j.1600-0714.2009.00882.x

Ramanathan, K., Chelvanayagam, P. I., Ng, K. H., & Ramanathan, J. (1982). Ameloblastomas--a clinicopathologic study of 133 cases in peninsular Malaysia. *Med J Malaysia, 37*(1), 18-24.

Reichart, P. A., Philipsen, H. P., & Sonner, S. (1995). Ameloblastoma: biological profile of 3677 cases. *Eur J Cancer B Oral Oncol, 31b*(2), 86-99.

Richards, J. B., Zheng, H. F., & Spector, T. D. (2012). Genetics of osteoporosis from genome-wide association studies: advances and challenges. *Nat Rev Genet, 13*(8), 576-588. doi:10.1038/nrg3228

Riffle, S., Pandey, R. N., Albert, M., & Hegde, R. S. (2017). Linking hypoxia, DNA damage and proliferation in multicellular tumor spheroids. *BMC Cancer, 17*, 338. doi:10.1186/s12885-017-3319-0

Rittling, S. R., Matsumoto, H. N., McKee, M. D., Nanci, A., An, X. R., Novick, K. E., . . . Denhardt, D. T. (1998). Mice lacking osteopontin show normal development and bone structure but display altered osteoclast formation in vitro. *J Bone Miner Res, 13*(7), 1101-1111. doi:10.1359/jbmr.1998.13.7.1101

Rizzardi, A. E., Johnson, A. T., Vogel, R. I., Pambuccian, S. E., Henriksen, J., Skubitz, A. P., . . . Schmechel, S. C. (2012). Quantitative comparison of immunohistochemical staining measured by digital image analysis versus pathologist visual scoring. *Diagn Pathol, 7*, 42. doi:10.1186/1746-1596-7-42

Sand, L., Jalouli, J., Larsson, P.-A., Magnusson, B., & Hirsch, J.-M. (2000). Presence of human papilloma viruses in intraosseous ameloblastoma. *J Oral Maxillofac Surg, 58*(10), 1129-1134. doi:http://dx.doi.org/10.1053/joms.2000.9573

Sandra, F., Hendarmin, L., Kukita, T., Nakao, Y., Nakamura, N., & Nakamura, S. (2005). Ameloblastoma induces osteoclastogenesis: a possible role of ameloblastoma in expanding in the bone. *Oral Oncol, 41*(6), 637-644. doi:10.1016/j.oraloncology.2005.02.008

Sandra, F., Hendarmin, L., & Nakamura, S. (2006). Osteoprotegerin (OPG) binds with tumor necrosis factor-related apoptosis-inducing ligand (TRAIL): suppression of TRAIL-induced apoptosis in ameloblastomas. *Oral Oncol, 42*(4), 415-420. doi:10.1016/j.oraloncology.2005.09.009

Sandros, J., Heikinheimo, K., Happonen, R. P., & Stenman, G. (1991). Expression of p21RAS in odontogenic tumors. *Apmis, 99*(1), 15-20.

Santos Tde, S., Piva, M. R., Andrade, E. S., Vajgel, A., Vasconcelos, R. J., & Martins-Filho, P. R. (2014). Ameloblastoma in the Northeast region of Brazil: A review of 112 cases. *J Oral Maxillofac Pathol, 18*(Suppl 1), S66-71. doi:10.4103/0973-029x.141368

Sathi, G. A., Inoue, M., Harada, H., Rodriguez, A. P., Tamamura, R., Tsujigiwa, H., . . . Nagatsuka, H. (2009). Secreted frizzled related protein (sFRP)-2 inhibits bone formation and promotes cell proliferation in ameloblastoma. *Oral Oncol, 45*(10), 856-860. doi:10.1016/j.oraloncology.2009.02.001

Sathi, G. A., Tsujigiwa, H., Ito, S., Siar, C. H., Katase, N., Tamamura, R., . . . Nagatsuka, H. (2012). Osteogenic genes related to the canonic WNT pathway are down-regulated in ameloblastoma. *Oral Surg Oral Med Oral Pathol Oral Radiol, 114*(6), 771-777. doi:10.1016/j.oooo.2012.08.453

Schneider, C. A., Rasband, W. S., & Eliceiri, K. W. (2012). NIH Image to ImageJ: 25 years of image analysis. *Nat Methods, 9*(7), 671-675.

Sears, R., Nuckolls, F., Haura, E., Taya, Y., Tamai, K., & Nevins, J. R. (2000). Multiple Ras-dependent phosphorylation pathways regulate Myc protein stability. *Genes Dev, 14*(19), 2501-2514.

Sellmyer, M. A., Bronsart, L., Imoto, H., Contag, C. H., Wandless, T. J., & Prescher, J. A. (2013). Visualizing cellular interactions with a generalized proximity reporter. *Proc Natl Acad Sci U S A, 110*(21), 8567-8572. doi:10.1073/pnas.1218336110

Siar, C. H., Lau, S. H., & Ng, K. H. (2012). Ameloblastoma of the jaws: a retrospective analysis of 340 cases in a Malaysian population. *J Oral Maxillofac Surg, 70*(3), 608-615. doi:10.1016/j.joms.2011.02.039

Siar, C. H., & Ng, K. H. (1993). Ameloblastoma in Malaysia--a 25-year review. *Ann Acad Med Singapore, 22*(6), 856-860.

Siar, C. H., & Ng, K. H. (2014). Differential expression of transcription factors Snail, Slug, SIP1, and Twist in ameloblastoma. *J Oral Pathol Med, 43*(1), 45-52. doi:10.1111/jop.12065

Siar, C. H., Tsujigiwa, H., Ishak, I., Hussin, N. M., Nagatsuka, H., & Ng, K. H. (2015). RANK, RANKL, and OPG in recurrent solid/multicystic ameloblastoma: their distribution patterns and biologic significance. *Oral Surg Oral Med Oral Pathol Oral Radiol, 119*(1), 83-91. doi:10.1016/j.oooo.2014.09.017

Stewart, S. A., & Weinberg, R. A. (2002). Senescence: does it all happen at the ends? *Oncogene, 21*(4), 627-630. doi:10.1038/sj/onc/1205062

Tapscott, S. J., Bennett, G. S., Toyama, Y., Kleinbart, F., & Holtzer, H. (1981). Intermediate filament proteins in the developing chick spinal cord. *Dev Biol, 86*(1), 40-54. doi:http://dx.doi.org/10.1016/0012-1606(81)90313-4

Tay, J. Y., Bay, B. H., Yeo, J. F., Harris, M., Meghji, S., & Dheen, S. T. (2004). Identification of RANKL in osteolytic lesions of the facial skeleton. *J Dent Res, 83*(4), 349-353. doi:10.1177/154405910408300415

Tekkesin, M. S., Mutlu, S., & Olgac, V. (2011). The Role of RANK/RANKL/OPG Signalling Pathways in Osteoclastogenesis in Odontogenic Keratocysts, Radicular Cysts, and Ameloblastomas. *Head and Neck Pathology, 5*(3), 248-253. doi:10.1007/s12105-011-0271-1

Truong, D., Puleo, J., Llave, A., Mouneimne, G., Kamm, R. D., & Nikkhah, M. (2016). Breast Cancer Cell Invasion into a Three Dimensional Tumor-Stroma Microenvironment. *Sci Rep, 6*, 34094. doi:10.1038/srep34094

Ulrike, K., Michaela, K., Andrea Maria, G., Thomas, R., Christian, T., Johannes, D., & Peter, R. (2001). A New Rapid Immunohistochemical Staining Technique Using the EnVision Antibody Complex. *Journal of Histochemistry & Cytochemistry, 49*(5), 623-630. doi:10.1177/002215540104900509

Umezawa, A., Maruyama, T., Segawa, K., Shadduck, R. K., Waheed, A., & Hata, J.-I. (1992). Multipotent marrow stromal cell line is able to induce hematopoiesis in vivo. *J Cell Physio 151*(1), 197-205. doi:10.1002/jcp.1041510125

Vanoven, B. J., Parker, N. P., & Petruzzelli, G. J. (2008). Peripheral ameloblastoma of the maxilla: a case report and literature review. *Am J Otolaryngol, 29*(5), 357-360. doi:10.1016/j.amjoto.2007.10.002

Vered, M., Muller, S., & Heikinheimo, K. (2017). Ameloblastoma. In A. K. El-Naggar, J. K. C. Chan, J. R. Grandis, T. Takata, & P. J. Slootweg (Eds.), *World Health Organization Classification of Head and Neck Tumours* (Vol. 4th, pp. 215–218). Lyon IARC.

Vinci, M., Gowan, S., Boxall, F., Patterson, L., Zimmermann, M., Court, W., . . . Eccles, S. A. (2012). Advances in establishment and analysis of three-dimensional tumor spheroid-based functional assays for target validation and drug evaluation. *BMC Biol, 10*, 29. doi:10.1186/1741-7007-10-29

Wang, X., Sun, L., Maffini, M. V., Soto, A., Sonnenschein, C., & Kaplan, D. L. (2010). A complex 3D human tissue culture system based on mammary stromal cells and silk scaffolds for modeling breast morphogenesis and function. *Biomaterials, 31*(14), 3920-3929. doi:10.1016/j.biomaterials.2010.01.118

Wendler, F., Stamp, G. W., & Giamas, G. (2016). Tumor-Stromal Cell Communication: Small Vesicles Signal Big Changes. *Trends Cancer, 2*, 326-329. doi:10.1016/j.trecan.2016.05.007

Whitlock, C. A., Tidmarsh, G. F., Muller-Sieburg, C., & Weissman, I. L. (1987). Bone marrow stromal cell lines with lymphopoietic activity express high levels of a pre-B neoplasia-associated molecule. *Cell, 48*(6), 1009-1021. doi:10.1016/0092-8674(87)90709-4

Woo, S. M., Rosser, J., Dusevich, V., Kalajzic, I., & Bonewald, L. F. (2011). Cell line IDG-SW3 replicates osteoblast-to-late-osteocyte differentiation in vitro and accelerates bone formation in vivo. *J Bone Miner Res, 26*(11), 2634-2646. doi:10.1002/jbmr.465

Wu, P. C., & Chan, K. W. (1985). A survey of tumours of the jawbones in Hong Kong Chinese: 1963-1982. *Br J Oral Maxillofac Surg, 23*(2), 92-102.

Yoon, H. J., Jo, B. C., Shin, W. J., Cho, Y. A., Lee, J. I., Hong, S. P., & Hong, S. D. (2011). Comparative immunohistochemical study of ameloblastoma and ameloblastic carcinoma. *Oral Surg Oral Med Oral Pathol Oral Radiol Endod, 112*(6), 767-776. doi:10.1016/j.tripleo.2011.06.036

Zhang, S., Gelain, F., & Zhao, X. (2005). Designer self-assembling peptide nanofiber scaffolds for 3D tissue cell cultures. *Seminars in Cancer Biology, 15*(5), 413-420. doi:https://doi.org/10.1016/j.semcancer.2005.05.007

Zhong, Y., Guo, W., Wang, L., & Chen, X. (2011). Molecular markers of tumor invasiveness in ameloblastoma: An update. *Ann Maxillofac Surg, 1*(2), 145-149. doi:10.4103/2231-0746.92780